Regioselective acylation of 2-methoxynaphthalene catalyzed by a C-H superacid and chemistry of mercaptoazulenes

BY

Alexander Sergeevich Vorushilov©

Submitted to the Department of Chemistry
and the Faculty of the Graduate School of the University of Kansas
In partial fulfillment of the requirements for the degree of
Doctor of Philosophy

Dr. Mikhail V. Barybin – Chairperson

_____
Dr. Cindy L. Berrie

_____
Dr. Daryle H. Busch

_____
Dr. Timothy A. Jackson

_____
Dr. Aaron M. Scurto

Date Defended 10-26-2010

The Dissertation Committee for Alexander Vorushilov certifies that this is the approved Version of the following dissertation:

Regioselective acylation of 2-methoxynaphthalene catalyzed by a C-H superacid and chemistry of mercaptoazulenes

_____
Dr. Mikhail V. Barybin – Chairperson

_____
Dr. Cindy L. Berrie

_____
Dr. Daryle H. Busch

_____
Dr. Timothy A. Jackson

_____
Dr. Aaron M. Scurto

Date Approved: 12-17-2010

Abstract

This Thesis work consists of three Chapters. The first two chapters describe the synthesis and catalytic application of carbon-based superacids and attempts of their immobilization on inorganic supports. Pentafluorophenyl(*bis*)triflyl methane was synthesized in two steps from pentafluorobenzyl bromide. Due to the strong electron withdrawing nature of the trifluoromethylsulfonyl and pentafluorophenyl groups, the methyne hydrogen atom is exceptionally labile. The *para*-fluorine atom in the above superacid is labile enough to be substituted by oxygen nucleopiles (hydroxyl and propyloxy). Both the "parent" and 4-substituted acids catalyze highly regioselective acylation of 2-methoxynaphthalene (2-MON) by acetic anhydride. This acylation reaction affords highly valuable 6-methoxy-2-acetonaphthone (2,6-AMN) along with a small amount of 7-methoxy-1-acetonaphthone (1,7-AMN) as opposed to the classic Friedel-Crafts acylation that employs strong Lewis acids such as aluminum trichloride and produces mainly the *ortho*-acylation product 1,2-AMN. The mechanistic studies described herein suggest that the acylation reaction leading to the formation of the thermodynamically preferred 2,6-AMN is a two step process that involves acylation of 1-position of 2-MON followed by the acyl group transfer to the 6-position of the ring. All of the reaction products – 1,2-AMN, 2,6-AMN, 1,7-AMN and diacetyl-methoxynaphthalene – were isolated or independently synthesized and their structures were confirmed by spectroscopic and mass-spectral methods. The diacylation product was determined to be 1,7-diacetyl-2-methoxynaphthalene, not the 2-acetylaceto-6-methoxynaph-thalene that was previously proposed to be the diacylated species.

The acylation of 2-MON was found to be sensitive to the concentration of the catalyst. Lower catalyst loadings (*ca.* 1 mol %) led to selective formation of 1,2-AMN, while a loading

greater than 9 mol % afforded selectively 2,6-AMN and 1,7-AMN 8:1 molar ratio, respectively. The outcome of the reaction was also found to depend dramatically on the solvent medium. Indeed, employing nitromethane as a solvent produced 2,6- and 1,7-AMN, while running the reaction in hexanes resulted in selective formation of 1,2-AMN with a nearly 100% conversion. Only trace amounts of 2,6-AMN were detected when the reaction was conducted in ethyl acetate. Systematic theoretical studies have supported these observations – the relative energies of formation of the acylated products, as well as the relative energies of the corresponding σ-complex intermediates in nitromethane and hydrocarbons indicate the advantage of 2,6- and 1,7-AMN isomers over the kinetically preferred 1,2-AMN. However, the energy gap in hydrocarbons was too large for the transacylation to proceed.

The pentafluoro(bis)triflyl methane and its *para*-hydroxy derivative were physisorbed on silicon oxide in attempts to immobilize the catalyst on an inorganic support. Both of the silicas have catalyzed acylation of 2-MON with high regioselectivity. The product distribution suggests that the acylation process occurs inside of the pores or on the surface of the silica. However, the catalyst leaches out of the support, making this, method not industrially feasible. The studies of the physisorbed CH acid's catalystic activity supports the hypothesis that once permanently tethered to an insoluble inorganic support, the CH acid would remain a highly active catalyst. A few unsuccessful attempts to chemically bind the catalyst and its derivatives to silicon oxide network have been made.

The third Chapter of this Thesis describes synthesis and characterization of a series of mercaptoazulenes, their coordination chemistry and self assembly on Au(111) surfaces. 1,3-Diethoxycarbonyl-2-mercaptoazulene and 1,3-diethoxycarbonyl-6-mercaptoazulene were synthesized from the corresponding haloazulenes in good yields. 1,3-Diethoxycarbonyl-2-

mercaptoazulene was decarboxylated to afford 2-mercaptoazulene and 1,3-dicyano-2-mercaptoazulene was synthesized to complete the series. Diethyl 2- and 6-mercaptoazulene-1,3-dicarboxylates react with the dinuclear complex $[Au_2(dcpm)]Cl_2$ (dcpm = bis(dicyclohexylphosphino) methane) to give the corresponding bis(thiolate)-digold complexes. Both gold complexes as well as two of the mercaptoazulenes were characterized by XRD. The di-gold motifs in the complexes of 2- and 6-azulenyl thiolates feature strong aurophilic interactions; although the relative orientation of the azulene rings in these species is quite different from the analogous isocyanoazulene complex.

All of the mercaptoazulenes have formed air- and moisture stable monolayers on Au(111) films. Characterization of some azulenyl thiolate films was greatly facilitated by incorporation of ancillary nitrile “spectroscopic” handles, a novel approach in the surface chemistry of organic thiols, to the best of our knowledge.

Abbreviations used in this Thesis

1,2-AMN – 2-methoxy-1-acetonaphthone

1,7-AMN – 7-methoxy-1-acetonaphthone

2,6-AMN – 6-methoxy-2-acetonaphthone

CH-acid – 2,3,4,5,6-pentafluorophenylbis(trifluoromethylsulfonyl)methane

dcpm - bis(dicyclohexylphosphino)methane

DFT – Density Functional Theory

dppm – bis(diphenylphosphino)methane

ILs – Ionic liquids

LED – Light emitting diode

LMCT – ligand to metal charge transfer

LMMCT – ligand to metal-metal bond charge transfer

PTA – phosphotungistic acid

SAM – self-assembled monolayer

XRD – X-ray diffraction

Acknowledgments.

First, I would like to thank my advisor, who has been helpful and supportive throughout my graduate career. Without his great teaching and mentoring abilities, none of this would have happened. His bright mind and persistence in achieving the best result possible in the chemistry lab and outside of it have helped me shape my views on science and life, making me stronger as a chemist and a person. I will certainly miss the atmosphere of your research group, but I will remember all of the bright, azulene-colored years of graduate school. Thank you, Misha. I would like to thank all the faculty of the Department of Chemistry who were always willing to help. Specifically, I would like to thank my committee members – Dr. Timothy Jackson, Dr. Cindy Berrie, Dr. Daryle Busch and Dr. Aaron Scurto for all their help. Thank you all for your time and patience.

Special thanks go to Dr Randall Robinson whose great passion for chemistry and outstanding teaching abilities have inspired me along the way. Randy's advice was priceless and he has taught me countless little tricks that have dramatically improved my synthetic skills. My deepest gratitude to Drs. Tom Holovics and Stephan Deplazes, who have been great lab mates, colleagues and friends and have made my first years at KU so much easier.

My collaborators, who have influenced my research over these years, thank you all for the bright ideas and valuable time. Dr. Bala Subramaniam, Dr. Daryle Busch and Dr. Daryle Fahey, who have introduced me to a more practical view on the molecules. Drs. K. Gong and S. Sarsani who have been great team mates at the CEBC solid acid project. Dr. Ward Thompson and Dr. K. Mitchell-Koch deserve warmest thanks for their theoretical work that has allowed us to better understand the nature of the acylation reaction.

I thank Dr. Cindy Berrie and Brad Neal for their work on the surface chemistry of azulenyl thiols. Dr. Berrie's collaboration has drastically expanded the limits of the research conducted in Barybin's group making this team truly unique and exciting to fork for. Dr. Victor Day for his help with X-ray diffraction experiments; Dr. D. Vandervelde, Dr. J. Douglas and S. Neuenswander for their help within the NMR facility, thank you all.

I am grateful to all former and present members of the Barybin group – John Meyers for all the energy he brought to the group, Andy Spaeth his sense of humor, Brad Neal for the different point of view on chemistry, Kolbe Scheetz for being himself, David McGinnis, Yumiko Tomotsogu and Tiffany Maher for shaping the group in what it is today. It was a great ride that I will never forget.

All the great people that I have met in Kansas who have made these years so great in terms of chemistry and times outside of the lab – the Yakovlevs, Danich and Sergei, Noah, Josh, Matt, Toby and many other, I cherish your friendship and appreciate everything you gave me. Thank you all.

Finally, I thank my family for everything you did and keep doing for me. My wife Alena for her love and support that have helped me get to where I am now. I love you very much. My mom Nonna and my dad Sergei for all they did for me - providing me love and advice, for all the 2^{nd} grade Math and Science problems I couldn't solve on my own. You have provided me the foundation and encouragement for my advancement in education and life and I am very thankful for that. All of my extended family for looking after me and supporting all of my best efforts deserves only best words of gratitude. And last but not least, all the people who have crossed paths with me on my chemistry quest – my high school chemistry teachers, my first research

group in Zelinsky Institute for Organic Chemistry in Moscow, my friends in other universities and industry. Thank you all very much.

Table of Contents

List of Tables

Chapter I

Chapter III

Appendix H

Table of Contents

Chapter III

List of Tables

Chapter I

Chapter III

Appendix K

List of Figures

Chapter I

Chapter II

Chapter III

List of Schemes

Chapter I

Chapter II

Chapter III

Chapter I

Regioselective acylation of 2-methoxynaphthalene

by pentafluorophenylbis(triflyl)methane and its derivatives

1.1 Introduction

Regioselective Friedel-Crafts acylation and alkylation of aromatic molecules has been an area of intense chemical research for many years. Industrial importance of these reactions and difficulties in separation of regioisomers of important intermediates (e.g., 6-methoxy-2-acetonapthone, 3-substituted indoles, 2- and 4-acetylbenzoic acids[1-4]), as well as high cost of catalysts[5-7] and reaction media or large environmental impact of the process[8,9] have kept the interest high . Traditionally, highly concentrated inorganic acids (sulfuric[10,11], phosphoric[12,13] of hydrofluoric[14-16]), strong low molecular weight Lewis acids (aluminum[17] or boron trihalides[18]) or combination of the above[19,20] were used to facilitate these processes. However, these methods have a few fundamental flaws, such as formation of acid soluble oils[21], high corrosiveness of the catalysts[22,23] and residual amounts of catalysts dissolved in the final product[24,25]. For instance, alkylation of isobutene – one of the most important processes employed in gasoline synthesis requires using up to 70-100 kg of H_2SO_4 per ton of alkylate[26]. The process is biphasic and requires substantial energy input in regeneration efforts, as well as strict safety precautions due to potential evolution of SO_2 and H_2S[27].

As an example, **Scheme 1.1** illustrates the industrial process for acylation of isobutylbenzene, where the target compound is 4-isobutylacetophenone, a precursor for Ibuprophen (2-(4-(2-methylpropyl)- phenyl)propanoic acid)[15], whereas 2-isobutylacetophenone is an undesired biproduct. The process was developed by BHC Company and won the 1997 US Presidential Green Chemistry Challenge Award.

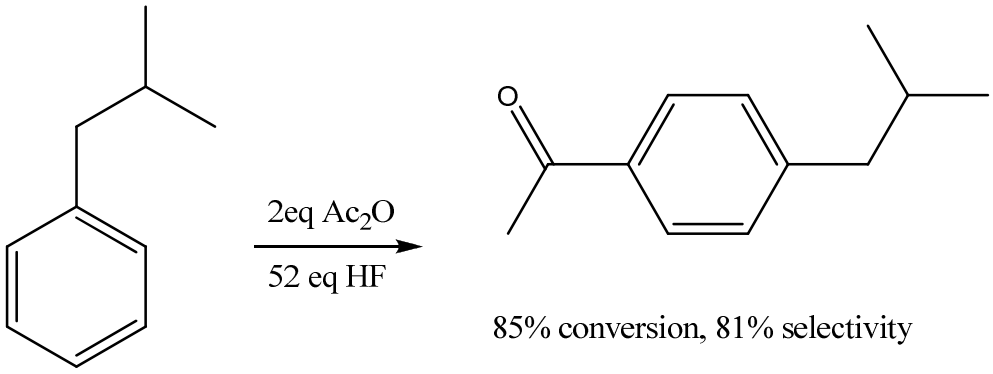

Scheme 1.1 Acylation of Isobutylbenzene[15].

However, this process employs large excess of hydrofluoric acid, which is very toxic, and generates acid soluble oils that deactivate the catalyst. Nevertheless, using the original Friedel-Crafts conditions for this transformation involves greater than a stoichiometric amount of strong Lewis acids, such as $AlCl_3$, and thereby leads to substantial amounts of corrosive waste, while showing relatively poor selectivity[28] .

Another approach to Bronsted acid-catalyzed acylation and alkylation reactions is the use of zeolites as solid acid catalysts. Over 130 known types of alumosilicates[29] provide a wide selection of pore diameters, surface areas and acidity, thus offering a great potential for highly selective catalysis. For example, in the approach for solid acid catalyzed acylation of 2-methoxynaphthalene, selectivity towards the desired 6-methoxy-2-acetonaphthone in the zeolite B (polymorph C) was shown to be higher than in zeolite ITQ-17 (code BEC)[7]. Both of the zeolites exhibit similar Bronsted acidity and were used to catalyze acylation reactions under identical conditions. The experimental data have indicated reaction dependence not only on the acidity, but also on the diffusion coefficient, which is related to the channel size (6.2×6.6 Å and 6.2×7.2 Å for ITQ-17 and Beta respectively). Even though both of these zeolites provided good conversions (65% in both cases) and selectivity (58% and 75% for Beta and ITQ-17

respectively), this method has little practical value due to zeolite pore clogging and the use of one molar excess of the more expensive reagent (the required 2-MON/Ac_2O ratio is 2:1). Further theoretical studies of the structure-reactivity relationships of mesoporous alumosilicates indicated that the formation of 2 major isomers (6-methoxy-2-acetonaphthone (2,6-AMN) and 2-methoxy-1-acetonaphthone (1,2-AMN)) correlates with the pore size / molecule size ratio of the zeolites with ISV-type exhibiting the highest selectivity towards the 2,6-AMN (Tables **1.1** and **1.2**)[30]. The rigidity of the networked structure, however, makes it possible to regenerate and reuse the catalyst without destruction of the core.

Table 1.1 Zeolite pore and simulation box diameters

Zeolite	**Symmetry**	**Unit cell composition**	**Pore diameter (Å)**	**Simulation box**
MOR	Orthorhombic	[SiO2]48	6.5x7.0	2x2x6
LTL	Hexagonal	[SiO2]36	7.1	2x2x6
BEA	Tetragonal	[SiO2]64	7.6x6.1	6x1.6x1
ISV	Tetragonal	[SiO2]64	6.3x6.1	6x1.6x1

Table 1.2 Naphthalenes structural dimensions

Molecule	**Dimensions**		
	a (Å)	*b* (Å)	*c* (Å)
2-MON	10	6	2.8

1,2-AMN	10.3	8.1	4.1
2,6-AMN	12.3	6.2	2.8

Ionic liquids (ILs) catalysis has grown into an area of intense investigations in the past 30 years. Even though ILs had been known since late 19th century[31] and room temperature ILs had first been described in 1914[32], they were not considered attractive for industrial applications due to their kinetic instability with regard to air and water. It was not until 1992 when Wilkes and Zaworotko reported the preparation and characterization of a range of ILs that could be used on the bench without being handled in an inert atmosphere[33]. Numerous processes have been patented and some commercialized since then by the chemical companies, such as BASF[34], Chevron[35], PetroChina[36] and others[37]. In **Scheme 1.2**, the process for the synthesis of 4-hydroxy-phenylbutanoic acid by Ely Lilly is shown. At 180 °C, pyridinium hydrochloride acts as both the solvent and the catalyst for the hydrolysis process, yielding the target product that constitues an intermediate in a HDL control drug LY518674[38].

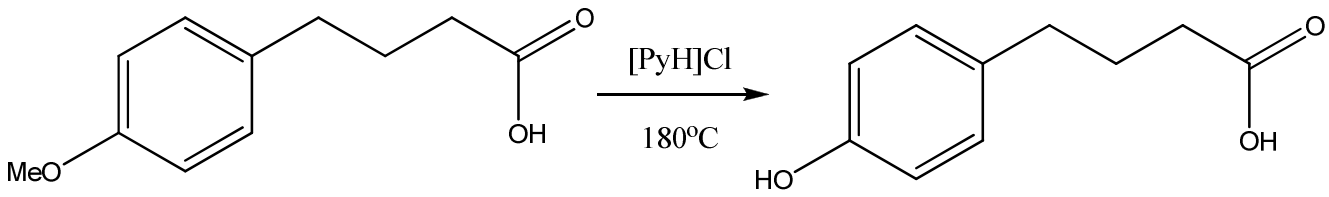

Scheme 1.2 Hydrolysis of 4-methoxyphenylbutanoic acid[38].

ILs are also used as supporting media for strong Lewis acids. For example, Gd(III) trifluoromethanesulfonate (triflate) has shown very promising activity towards acylation of

aromatic alcohols and amines with acetic anhydride in 1-butyl-3-methylimidalolium tetrafluoroborate and hexafluorophosphate while offering great recyclability and high conversions. The high density and ionic nature of the media make separation of the product easy and the IL containing the catalyst may be reused[39].

Some of the most attractive features of ionic liquids are tunable density and viscosity that can vary from 0.8 to 3.3 g/l and 22-40000 cP respectively, as well as low volatility and vapor pressure at STP[40].

Heteropolyacids were examined as acylation and alkylation catalysts in both molecular and supported forms[41-43]. Keggin type phosphotungistic acid (PTA, $H_3PW_{12}O_{40}$) was found to promote Friedel-Crafts acylation of substituted benzenes with crotonic acid[41,43] and benzoylation of benzene[42]. Being a mild Bronsted acid, PTA can be used as a source of protons or doped with cesium ($Cs_{3-x}H_xPW_{12}O_{40}$) to form a Lewis acid. Numerous advantages of PTA (high temperature tolerance, solubility in water and surface area, to name a few) make it attractive for greener process engineering. **Scheme 1.3** shows how PTA is used for separation of isobutylene and 1- and 2-butenes by selective hydrolysis of isobutylene. It is followed by dehydration of *tert*-butanol, a starting material for methacrylic acid synthesis[44]. Other research in this field involved substituting PTA for Phosphomolibdic, silicotungistic and silicomolibdic acids that provided a range of pK_as[45].

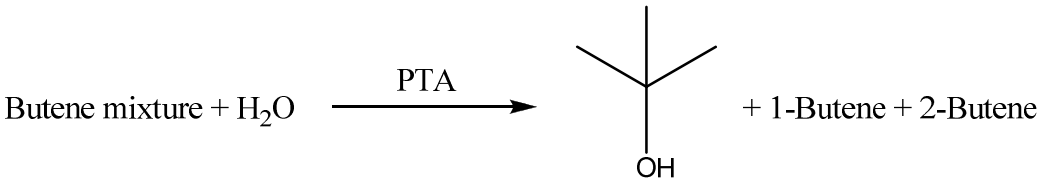

Scheme 1.3 Selective hydrolysis of butylenes catalyzed by PTA[44].

The acids described above, however, have numerous disadvantages, such as low solubility in organic media, high molecular weight and/or pK_a. Organic superacids remain a target in many industrial and academic process investigations. The term "superacid" was first suggested by Hall and Conant in 1927 and defined as the acid with the Hammett acidity function (H_0) below that of sulfuric acid[46]. The first superacids to be tested for their catalytic properties were trifluoromethanesulfonic[47] and fluorosulfonic acids[48]. Triflic acid, for example, was successfully employed for transalkylation of benzene by diethylbenzene[49]. However, high corrosiveness and cost of the catalyst have prevented a broader range of its use. Nevertheless, organic Bronsted acids and their transition metal salts remain attractive targets for synthetic and catalytic purposes due to not only their H_0 function, but also high solubility in organic media and low nucleophilicity of the conjugate base. Other organosulfonic acids such as toluenesulfonic, 4- and 2-nitrosulfonic and fluorophenylsulfonic have been employed as well[50].

Chiral phosphoric acids are known to catalyze asymmetric reactions, such as stereoselective Mannich type aminoketonation (by R- or S-BINOL phosphoric esters) of aroylaldehydes by aromatic amines and cyclohexanones[51], as well as Pictet-Spengler ring closure[52]. Lanthanide and actinide metals are very well known for their Lewis acidity and pairing the cation to a highly soluble organic counter ion has been studied. For instance, scandium triflate (0.1-2.5 mol %) has shown excellent activity toward acylation of alcohols in acetonitrile at ambient temperatures. Acylation of menthol with 0.1 mol % of the catalyst afforded a 95% yield of the target compound in acetonitrile over 15 minutes compared to a 75% conversion in 55 minutes if 300 mol% of dimethylaminopyridine in triethylamine was used[53]. Other lanthanide metal salts of triflic acid that have been investigated include those of Gd, Yb, Ce, and Sm[54,55].

Carbon and nitrogen based Bronsted acids have been extensively studied due to the low nucleophilicity of their conjugate bases and high solubility in organic solvents. *Bis*-triflylmethylsulfonyl methane and *bis*-trifluoromethylsulfonyl amide are among the strongest Bronsted acids available[56,57]. Their derivatives have been applied in different processes, such as electrolytes in batteries[58,59], fluorinating agents[60], and Lewis acid catalysts[61]. However, the core reason for the high interest in these compounds is their Bronsted acidity. *Bis*-triflylmethylsulfonyl methane was first synthesized in 1957[62] and is a very strong acid with the pK_a value of 1.0 in methylisobutyl ketone[56]. Being one of the strongest carbon-based acids, this compound was utilized, for example, as a catalyst in olefin polymerization[63]. However, the combination of the strong acidity of the compound and its high cost made it a less than ideal target for wide investigations. Some of the related compounds have exhibited superacidity and, thus, higher activity in catalysis. Methyne based acids provide stronger acidity due to an additional electron withdrawing group in their structure. In 1987, Turowsky and Seppelt successfully synthesized tris((trifluoromethyl)sulphonyl)methane and structurally resolved its potassium salt[64]. Due to the electron withdrawing power of the triflyl groups, the CS_3 skeleton of the anion is nearly planar that suggests a high degree of delocalization of the electron pair. The acidity of this compound was later determined by comparison of its gas phase Gibbs energy of dissociation with the corresponding ΔG values for sulfuric and nitric acids. The ΔG values for tris((trifluoromethyl)sulphonyl)methane, H_2SO_4, and HNO_3 are 289.0, 302.2, and 317.8 kcal/mol respectively[65].

Carboranes are one of the strongest carbon based Bronsted acid classes isolated to date[66]. For example, $H(C_7H_{15}B_{11}Cl_6)$, is known to protonate arenes, such as benzene and alkyl benzenes, at ambient temperatures to form stable arenium carborates[67], whereas fluorosulfonic acid only

protonates benzene to some extent in solution[68]. The arenium salts were stable enough to be isolated and structurally characterized by single crystal XRD, which indicates that the counterion has a remarkably low basicity (**Figure 1.1**).

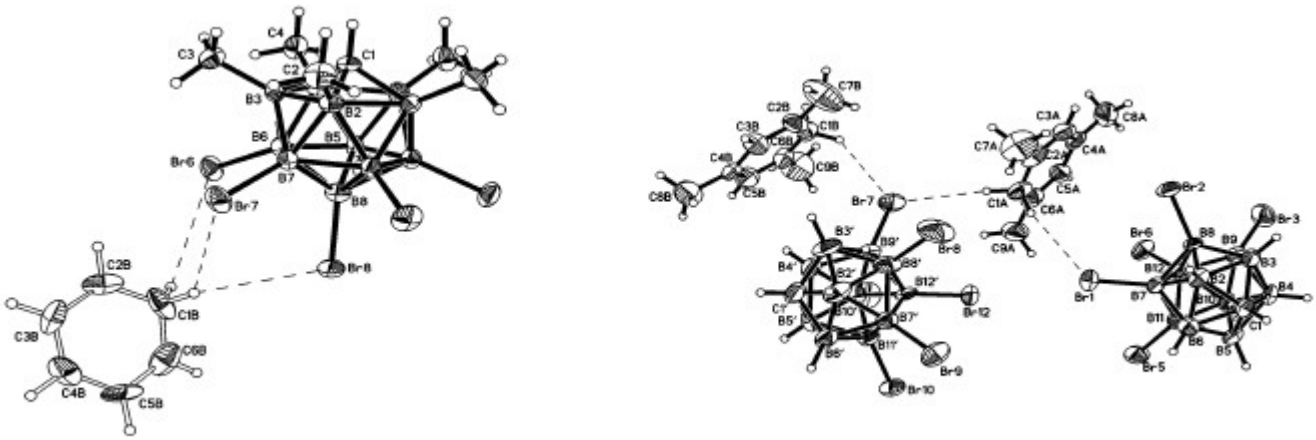

Figure 1.1 Thermal ellipsoid (50%) plots of the structures involving benzenium (left) and toluenium (right) cations[67].

Unlike the Bronsted acids enhanced by addition of strong Lewis acids (e.g., HSO_4F/SbF_5 - "magic acid")[69], the carborane-based acids do not interfere with the protonation process via supplying oxidizing equivalents or nucleophilic halide ions. Though such acids are only stable under an inert atmosphere, their use may help clarify some of the mechanistic aspects of the protonation of weakly basic molecules. An interesting approach to the synthesis of neutral materials with extraordinary low affinity for a proton was discovered by Rewicki and coworkers some 30 years ago[70]. It was found that fluoradene exhibits unusually low pKa's for a hydrocarbon in DMSO (10.5). A theoretical study suggested that some of the cyano-substituted fluoradenes may have the gas phase acidity as low as -20 and below, if they can be synthetically accessed. The results are supportive of large conjugated aromatic systems' low proton affinities,

which, in principle, opens a new area for weakly coorditating anions and superacids research. Another general idea of the search for organic superacids is based on introducing perfluorinated organic blocks to the structure that will not only act as strong EWGs, but also provide lipophilicity that would reduce hygroscopicity and enhance solubility of the compound in non-polar solvents. This strategy has produced a number of strong acids with strong affinity for organic solvents. Yamamoto *et. al*. have synthesized a very strong Bronsted acid - pentafluoromethylbis(triflyl)methane in 2001 and have demonstrated its modification and catalytic activity towards Friedel-Crafts acylation and other processes[71]. This carbon based acid has a pK_a value of 1.5 in glacial acetic acid (compared to the value of 7.5 for H_2SO_4) as determined by the ^1H NMR measurement of a proton chemical shift by the Schantl's method[72]. This very low pK_a value places the compound in the category of superacids.

1.2 Work Described in Chapter One

The syntheses and characterization of several carbon-based superacids are described in the following sections of Chapter I. Pentafluorophenylbis(triflyl)methane as well as its *para*-substituted derivatives were prepared by an improved version of the synthesis originally reported by Yamamoto and coworkers[71]. The catalytic activities of these strong CH acids toward acylation of 2-methoxynaphthalene were evaluated. Detailed studies of the reaction kinetics, thermodynamics, as well as investigation of the solvent effects are described. The CH acid catalyzes the acylation of 2-MON in nitromethane to mostly yield the desired 2,6-AMN, an intermediate in (*S*)-naproxen synthesis, with only small amounts of 1,7-AMN as a side product. However, changing the solvent medium from nitromethane to hexanes and ethyl acetate resulted

in selective acylation of the 1-position of the naphthalene ring and exclusive formation of 1,2-AMN. The acylation reaction was also found to depend significantly on the catalyst loading: decreasing the catalyst concentration from 10 to 1 mol% resulted in a selective conversion of 2-MON to 1,2-AMN instead of the expected 2,6-AMN. 2,6-AMN was also synthesized from the 1,2-AMN isomer that has acted as the source of acetyl group. The reaction mechanism was reevaluated and certain thermodynamic and kinetic aspects were addressed computationally in collaboration with Prof. Ward Thompson and Dr. Katie Mitchell-Koch.

1.3 Experimental Section

1.3.1 General Methods and Procedures

Unless specified otherwise, the procedures were performed in air. When inert atmosphere conditions were required, 99.5% argon purified by passage through columns of activated BASF catalyst and molecular sieves was used. All connections involving the gas purification system were made of glass, metal or other materials impermeable to air. For air-free procedures, standard Schlenk techniques were employed using a double-manifold vacuum line. Solvents, including deuterated solvents were freed of impurities by usual procedures and stored under argon. NMR samples were analyzed on Bruker DRX-400 and Bruker Avance 500 Spectrometers. ^{1}H and ^{13}C chemical shifts are given with reference to residual solvent resonances relative to $SiMe_4$. Melting points are uncorrected and were determined for samples in sealed capillary tubes. GC-MS spectra were recorded on a Quattro Micro triple quadrupole mass analyzer with the sample introduction via an Agilent 6890N gas chromatograph.

1.3.2. Synthesis of 2,3,4,5,6-pentafluorophenyltriflyl methane

A solution of 2,3,4,5,6-pentafluorophenyl benzyl bromide (2.80 g, 10.7 mmol), sodium trifluoromethyl-sulfinate (2.5 g, 16 mmol) and tetrabutylammonium iodide (0.42 g, 1.1 mmol) in 25 mL of dry propionitrile was refluxed for 48 hrs under argon atmosphere. The resulting solution was stripped from the solvent under vacuum and the residue was sublimed in vacuum to yield 75% (2.5 g, 8.0 mmol) of 2,3,4,5,6-pentafluorophenyltriflyl methane as white crystals. M.P. = 106-108 °C. ^{1}H NMR (400 MHz, 25 °C, $CDCl_3$): δ 4.65 (s, 2H) ppm. ^{19}F NMR (376 MHz, 25 °C, $CDCl_3$): δ -77.06 (t), -138.47 (d), -148.24 (t), 159.3 (m) ppm. $^{13}C\{^{1}H\}$ NMR (101 MHz, 25 °C, $CDCl_3$): δ 44.28 ppm.

1.3.3. Synthesis of 2,3,4,5,6-pentafluorophenyl(bis)triflyl methane

This reaction was conducted under the inert atmosphere of argon. A solution of 2,3,4,5,6-pentafluorophenyltriflyl methane (8.30 g, 26.5 mmol) was dissolved in 160 mL of air and moisture free diethyl ether and the solution was cooled to -78 °C using dry ice/acetone bath. To this chilled solution, 32.5 mL of *t*-BuLi (1.7 M in pentane, 55.3 mmol) was added drop-wise and reaction was stirred for one hour. Then, 3.6 mL of triflic anhydride (28.9 mmol) was added and the mixture was allowed to warm to room temperature overnight with stirring. The reaction mixture was quenched with 20 mL of 10% aqueous H_2SO_4, the organic layer was collected, and the solvent was evaporated from the organic fraction *in vacuo*. The resulting oil was dissolved in 300 mL of 0.5 M aqueous NaOH and extracted with 200 mL of hexanes. The aqueous layer was acidified with concentrated H_2SO_4 to pH < 1 and extracted with hexanes (5×100 mL). The organic extracts were combined and dried over anhydrous Na_2SO_4, then concentrated to about 50 mL and cooled to -18 °C in a freezer. After 18 hours microcrystals were collected, dried, and

sublimed under reduced pressure to yield the product (6.50 g, 14.6 mmol) in a 55% yield as white crystals. M.P. = 84 – 86 °C (Lit 86-87 °C)[73]. ^{1}H NMR (400 MHz, 25 °C, $CDCl_3$): δ 6.2 (s, 1H) ppm. ^{19}F(376 MHz, 25 °C, $CDCl_3$): δ -74.0 (d), -126.8 (m), -139.5(t), 141.8 (m), 156.1 (m), 157.1 (m) ppm.

1.3.4. Synthesis of 2,3,5,6-tetrafluoro-4-hydroxyphenyl(bis)triflyl methane.

A solution of 2,3,4,5,6-tetrafluorophenyl(bis)triflyl methane (0.225 g, 0.504 mmol) and KOH (0.17 g, 3.0 mmol) in 13 mL of t-BuOH was refluxed for 3.5 hours. The reaction mixture was then cooled to room temperature, diluted with 40 mL of diethyl ether and washed with 100 mL of 10% aqeous HCl. The aqueous layer was separated and extracted with diethyl ether (2×50 ccm) and the combined organic extracts were dried over anhydrous $MgSO_4$. Triethylamine (2.00 mL, 14.3 mmol) was added to the solution and the solvent was removed on a rotary evaporator to yield 0.303 g (0.5 mmol) of ligh brown crystals of the triethylammonium salt of 2,3,5,6-terafluoromethyl(bis)triflyl methane in 100% yield. The acid was stored as the salt and reconstituted by addition of a strong mineral acid followed by extraction with hexanes before use. ^{1}H NMR (400 MHz, 25 °C, $CDCl_3$): δ 0.65 (t, 3H), 2.52 (q, 2H), 4.24 (s, broad) ppm. ^{19}F(376 MHz, 25 °C, $CDCl_3$): δ -82.0 (s), -144.6 (d), -171.1(d) ppm.

1.3.5. Synthesis of 2,3,5,6-tetrafluoro-4-propyloxyphenyl(bis)triflyl methane.

Sodium hydride (60% suspension in oil, 0.37 g, 9.3 mmol) was washed with hexanes, dried in vacuum, and placed under argon. Then it was suspended in 10 mL of dry pyridine and cooled to 0 °C. To this NaH suspension, n-propanol (0.40 g, 6.5 mmol) in 2 mL of pyridine was added and the reaction mixturewas stirred for one hour at 0^{o}C. 2,3,4,5,6-Pentafluorophenyl-(bis)triflyl methane (1.0 g, 2.2 mmol) dissolved in 15 mL of pyridine was added to the reaction

and the mixture was heated in an oil bath (71 °C) overnight with stirring. Then, the reaction was quenched with ice-water mixture, acidified with concentrated H_2SO_4 until the pH was below 1 and extracted with diethyl ether (3×50 mL). The combined organic extracts were dried over anhydrous Na_2SO_4 and the solvent was removed *in vacuo*. The resulting dark oil was extracted with boiling hexanes (2×50 mL). The extracts were stripped from on a rotary evaporator and then dried in vacuum to yield 2,3,5,6-pentafluorophenyl-4-propoxy(bis)triflyl methane (0.850 g, 1.75 mmol) as a light yellow oilin a 79.5% yield. ^{1}H NMR (400 MHz, 25 °C, $CDCl_3$): δ 6.2 (s, 1H), 4.41 (t, 2H), 1.86 (m, 2H), 1.07 (t, 3H) ppm. ^{19}F(376 MHz, 25 °C, $CDCl_3$): δ -74.2 (s), -129.8 (m), -142.3(m), 153.5 (m), 154.6 (m) ppm. $^{13}C\{^{1}H\}$ NMR (101 MHz, 25 °C, $CDCl_3$): δ 124.18, 120.90, 117.62, 114.34, 93.7, 76.99, 70.96, 23.28, 9.90 ppm.

1.3.6a. General Procedure for Acylation of 2-Methoxynaphthalene.

Unless specified otherwise, all reactions were carried out in air atmosphere. All GC/MS data were collected on a Quattro Micro triple quadrupole mass analyzer with sample introduction via a Agilent 6890N gas chromatograph. A solution of acetic anhydride (1 eq), 2-methoxy-naphthalene (1 eq) and the catalyst (0.1 eq) in nitromethane (5 mL per gram of the substrate) was refluxed for 24 hrs. The reaction progress was monitored by GC and the concentrations of the products were obtained by integration of corresponding GC peaks. The GC response factor was determined by chromatographing an equimolar mixture of 2-Methoxynaphthalene and 6-methoxy-2-acetonaphthone.

1.3.6b. Acylation of 2-Methoxynaphthalene with the 2,3,4,5,6,-pentafluorophenyl-(bis)triflyl methane.

2-methoxynaphthalene (1.5 g, 9.5 mmol), acetic anhydride (1.0 g, 9.8 mmol) and the catalyst (0.215 g, 0.47 mmol) were refluxed in 8 mL of nitromethane. After 24 hours, the reaction mixture was cooled and separated on a silica gel column eluted with a hexanes-ethyl acetate mixture (1:1). From the first band, 0.420 g (2.65 mmol) of 2-MON was recovered. The second band yielded 0.310 g (1.55 mmol) g of 2-methoxy-1-acetonaphthone and 6-methoxy-2-acetonapthone. The third band provided 0.016 g (0.066 mmol) of 1,6-diacetyl-2-methoxynaphthalene. The identity of these compounds was confirmed by GC/MS and ^{1}H NMR means. ^{1}H NMR (400 MHz, 25 °C, $CDCl_3$): 1,6-acetyl-2-methoxynaphthalene: δ 8.42 (s, 1H), 8.02 (d, 2H), 7.81 (d, 1H), 7.35 (d, 1H), 4.01 (s, 3H), 2.69 (s, 3H), 2.65 (s, 3H) ppm. 2-Methoxynaphthalene: δ 7.77 (m, 3H), 8.02 (d, 2H), 7.46 (m, 1H), 7.36 (m, 1H), 7.18 (m, 2H), 3.93 (s, 3H) ppm.

1.3.6c. Acylation of 2-Methoxynaphthalene with the "CH" acid.

1.3.6.c1 Acylation of 2-MON catalyzed by 2,3,4,5,6-pentafluorophenyl(bis)triflyl methane in nitromethane.

A solution of 2-MON (1.5 g, 9.5 mmol), acetic anhydride (1.0 mL, 10 mmol), and pentafluoro(bis)triflyl methane (0.440 g, 0.986 mmol) was refluxed for 24 hours in 10 mL of nitromethane. The reaction progress was monitored at 10, 20, 60, 120, 360 and 1440 minutes by GC/MS to determine changes in the concentrations of the four key compounds (2-Methoxynaphthalene, 2-methoxy-1-acetonaphthone, 7-methoxy-1-acetonaphthone, 6-methoxy-2acetonaphthone – 2-MON, 1,2-AMN, 1,7-AMN 2,6-AMN, respectively).

Compound	5 min	10	30 min	90 min	120 min	545 min	1440 min
2-MON	33.8%	41.2%	42.9%	44.6%	47.6%	47.3%	48.3%
1,2-AMN	23%	13%	6.8%	2.5%	1.75%	0%	0%
2,6-AMN	24.2%	33.8%	41.8%	47.5%	46%	47.7%	49.8%
1,7-AMN	4.5%	4.9%	3.5%	3.3%	3.3%	4.1%	1.8%
1,2,6-DiAMN	14.1%	6.2%	4.9%	1.9%	1.2%	0.2%	0%

1.3.6.c2 Acylation of 2-MON catalyzed by 2,3,5,6-tetrafluoro-4-propoxyphenyl(bis)triflyl methane in nitromethane.

A solution of 2-MON (0.775 g, 4.90 mmol), acetic anhydride (0.50 mL, 5.3 mmol) and 4-propyloxytetrafluoro(bis)triflyl methane (0.200 g, 0.411 mmol) was refluxed for 25 hours in 10 mL of nitromethane. The reaction progress was monitored at 10, 20, 60, 120 and 1500 minutes to determine changes in the concentrations of the four key compounds (2-Methoxynaphthalene, 2-methoxy-1-acetonaphthone, 7-methoxy-1-acetonaphthone, 6-methoxy-2acetonaphthone – 2-MON, 1,2-AMN, 1,7-AMN 2,6-AMN, respectively).

Compound	10 min	20 min	60 min	120 min	1500 min
2-MON	35.1	37.0	40.7	43.3	51.7
1,2-AMN	43.3	26.3	13.8	6.3	0
2,6-AMN	15.1	25.6	34.9	42.2	44.2
1,7-AMN	2.1	3.3	3.8	4.0	4.0
1,2,6-DiAMN	4.2	7.6	6.6	3.9	0

1.3.6.c3 Acylation of 2-MON catalyzed by 2,3,4,5,6-pentafluorophenyl(bis)triflyl methane in hexanes.

A solution containing 2,3,4,5,6-pentafluorophenyl(bis)triflyl methane (0.132 g, 0.296 mmol), 2-MON (0.50 g, 3.2 mmol), and acetic anhydride (0.33 mL, 3.5 mmol) in 5 mL of hexanes was heated with stirring at 110 °C in 5 in a pressure vial for 25 hours. The reaction mixture was then diluted with hexanes, washed with 10% aqueous NaOH solution and water, and dried over Na_2SO_4. The solvent was removed to yield 2-methoxy-1-acetonaphtone (0.63 g, 3.2 mmol). ^{1}H NMR (400 MHz, 25 °C, $CDCl_3$): δ 7.89-7.78 (m, 3H), 7.52 (m, 1H), 7.38 (m, 1H), 7.28-7.17 (m, 1H), 3.95 (s, 3H), 2.69 (s, 3H), 1.07 (t, 3H) ppm. MS (EI): m/z = 200.2.

1.3.6.c4 Acylation of 2-MON catalyzed by 2,3,4,5,6-pentafluorophenyl(bis)triflyl methane in nitromethane.

A solution of 2-MON (1.55 g, 9.80 mmol), acetic anhydride (1.00 mL, 10.6 mmol), and pentafluoro(bis)triflyl methane (0.050 g, 0.103 mmol) in 10 mL of nitromethane was heated at 100 °C for 24 hours in a glass vial. The reaction was then stopped and analyzed by GC/MS means. 2-Methoxy-1-acetonaphthone formed in a 73% yield.

1.3.6.c5 Acylation of 2-MON catalyzed by 2,3,4,5,6-pentafluorophenyl(bis)triflyl methane in ethyl acetate.

A solution of 2-MON (0.50 g, 3.2 mmol), acetic anhydride (0.35 mL, 3.7 mmol), and pentafluoro(bis)triflyl methane (0.050 g, 0.103 mmol) in 5 mL of ethyl acetate was heated at 110 °C for 20 hours in a glass vial. The reaction mixture then analyzed by GC/MS. 2-Methoxy-1-acetonaphthone was produced in a 64% yield.

1.3.6.c6 Acylation of 2-MON catalyzed by 2,3, 5,6-tetrafluoro-4-propyloxyphenyl(bis)triflyl methane in hexanes.

A solution of 2-MON (1.56 g, 9.86 mmol), acetic anhydride (2.0 mL, 21 mmol), and 2,3,5,6-tetrafluoro-4-propyloxyphenyl(bis)triflyl methane (0.120 mg, 0.247 mmol) in 5 mL of hexanes was heated at 110 °C for 20 hours in a glass vial. The reaction was then stopped and analyzed by GC/MS. The yield of 2-methoxy-1-acetonaphthone was quantitative by GC/MS.

1.3.7. Synthesis of 1,6-diacetyl-2-methoxynaphthalene.

The procedure of Jacques *et. al.*[74] was used with minor adjustments. Dry nitrobenzene (100 mL) and 26.7 g of aluminum trichloride (0.200 mol) were placed in a round bottom flask under inert atmosphere. Then 14 mL of acetyl chloride (0.20 mol) was added drop-wise with stirring. To this mixture, 2-MON (30 g, 0.19 mol) was added and the reaction was allowed to stir

for 70 hours at room temperature followed by 80 minutes at 60 °C. The mixture was then cooled to room temperature and cautiously quenched with aqueous HCl/ice mixture. The resulting solution was diluted with 50 mL of chloroform. The organic layer was washed with dilute aqueous HCl, then with saturated aqueous $NaHCO_3$, and water. The organic phase was dried over $MgSO_4$ overnight and the solvent was removed *in vacuo*. The main products (2-methoxy-1-acetonaphthone and 6-methoxy-2-acetonaphthone) were removed by vacuum distillation (0.01 torr, 108 °C) and the residue was chromatographed on silica gel using diethyl ether eluent. The ether solution was concentrated to 100 mL and allowed to crystallize at -18 °C overnight to yield 2,6-diacetyl-2-hydroxynaphthalene (0.4 g, 1.75 mmol), M/z = 228 by GCMS. The crystals were then dissolved in an acetone/water mixture (5/1 mL) containing 1.00 g of KOH (17.9 mmol) and the solution was stirred for one hour. Dimethyl sulfate (1 mL, 6 mmol) was added to the reaction mixture over a period of one hour. After stirring for 4 hours at room temperature, the mixture was diluted with water and extracted with diethyl ether. The organic phase was dried over $MgSO_4$ and then chromatographed on silica gel (eluent – $CHCl_3/Et_2O$, 4:1) to yield 8 mg of 1,6-diacetyl-2-methoxynaphthalene.

^{1}H NMR (400 MHz, 25 °C, $CDCl_3$): δ 8.42 (d, J = 1.7Hz, 1H), 8.02 (m, 2H), 7.81 (d, J = 9 Hz, 1H) 7.35 (d, J = 9.1 Hz, 1H), 4.01 (s, 3H), 2.70 (s, 3H), 2.66 (s, 3H) ppm. $^{13}C\{^1H\}$ NMR (101 MHz, 25 °C, $CDCl_3$): δ 204.63, 197.81, 156.23, 133.53, 132.94, 130.59, 127.89, 125.98, 125.24, 124.30, 113.55, 77.55, 77.23, 76.91, 56.53, 32.85, 26.80 ppm.

1.3.8 Reacylation of 2-methoxy-1-acetonaphthone catalyzed by pentafluoro-(bis)triflyl methane.

2-Methoxy-1-acetonaphthone (0.362 mg, 1.81 mmol), pentafluorophenyl(bis)triflyl methane (0.082 g, (0.18 mmol), and glacial acetic acid (0.25 mL, 4.4 mmol) were heated in a pressure vial at 110 °C for 4 hours. The reaction progress was monitored by GC/MS at 15, 45, 120 and 240 minutes.

Compound	15	45	120	240
2-MON	46.6%	43%	46.5	46.5
1,2-AMN	18%	10%	4.4%	0
1,7-AMN	6	6	5.4	4.8
2,6-AMN	41.5%	42.7	49.2	50
1,2,6-DiAMN	0	5.9	3.4	0

1.3.9 Recovery of pentafluorophenyl(bis)triflyl methane from an acylation reaction mixture.

A solution of 2-MON (1.5 g, 9.5 mmol), acetic anhydride (1.0 mL, 10 mmol), and pentafluoro(bis)triflyl methane (0.400 g, 0.897 mmol) in 10 mL of nitromethane was refluxed for 24 hours. The reaction mixture was cooled down to room temperature and concentrated to 2 mL. It was then diluted with 50 mL of hexanes and extracted thrice with 25 mL of 10% aqueous KOH. The combined aqueous extracts were acidified with concentrated HCl until the pH<1 and the resulting solution was extracted with 2×25 mL of diethyl ether. The etherial extracts were

combined and dried over Na_2SO_4. The solvent was removed *in vacuo* to yield 12.5% of the recovered pentafluorophenyl(bis)triflyl methane (0.050 g, 0.112 mmol).

1.3.10. Computational work.

All computational work was performed by Dr. K. Mitchell-Koch and Prof. W. Thompson at the University of Kansas[75]. The relative free energies of 2,6-AMN, 1,2-AMN and 1,7-AMN as well as the energies of the reaction intermediates were calculated using Density Functional Theory (DFT) theory and employing Gaussian 98 and 2003 programs[76,77]. Computations were performed using Becke's three parameter hybrid exchange functional with the LYP correlation functional. The standard 6-31G valence split set was applied in all cases. Solvation energies were calculated using Polarized Continuum Model, atomic charges were obtained from Natural Bond Orbital (NBO) program[78].

1.4 Results and Discussion

The improved synthesis of pentafluoro(bis)triflyl methane ("CH acid") can be performed on a large scale and affords good yields of the product. Functionalization of this compound was successful and the derivatives of the catalyst showed activities towards the acylation of 2-MON that are similar to that of the parent acid. The outcome of the acylation reaction was found to greatly depend on the concentration of the catalyst as well as the nature of the solvent medium. Varying the nature of the reaction medium and/or catalyst loading allowed tuning the product distribution form exclusive formation of the kinetically preferred isomer to a very selective production of the particularly desirable 6-methoxy-2-acetonaphthone.

For the synthesis of the CH acid reported herein, the original procedure of Yamamoto *et al.*[71] was substantially modified. The nucleophilic substitution of bromine in pentafluorobenzyl

bromide by sodium trifluoromethane sulfinate followed by deprotonation of the acidic methylene group by *t*-BuLi and capture of the resulting anion with triflic anhydride yielded the desired product. Substitution of the original column chromatographic isolation/purification procedure by sublimation of the crude product produced a very dry catalyst and dramatically reduced the amount of solvent used in the synthesis (**Scheme 1.4)**. The final product is crystalline and stable at ambient temperature. However, it proved to be extremely hygroscopic and is best stored at -18 °C in a tightly sealed container.

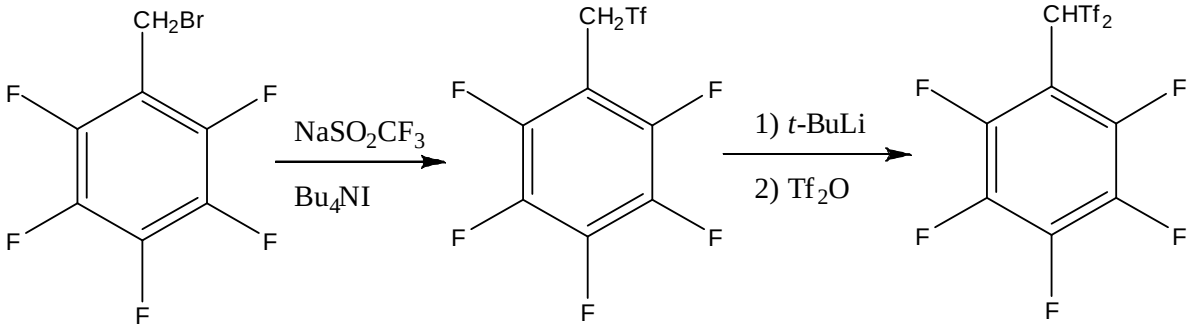

Scheme 1.4 Synthesis of pentafluorophenyl(bis)triflyl methane

The CH acid catalyst is very soluble in most organic solvents. However, extraction of organic solutions of the acid with aqueous bases results in complete migration of the deprotonated acid to the inorganic phase. The *para*-fluorine substituent at the aromatic ring appears to be quite labile. The authors of the original synthesis have found that it can be substituted by aryllithium and perfuoroalkoxy nucleophiles[79]. In this Thesis work, two derivatives of the CH acid were synthesized by reacting it with nucleophiles – hydroxide and propyloxy anions to produce 4-hydroxytetrafluorophenyl(bis)triflyl and 4-propyloxytetrafluoro-phenyl(bis)triflyl methanes, respectively, in reasonable yields. The acid and its derivatives have been previously used for acetalization of benzaldehydes, acylation of anisole, as well as a number of other processes[71]. We have found that the compound can catalyze acylation of 2-

methoxynaphthalene with high regioselectivity.

1.4.1 Investigation of the mechanism of the acylation of 2-MON

The CH acid was tested as a catalyst in regioselective Friedel-Crafts acylation of 2-methoxynaphthalene, a key inter-mediate in synthesis of (s)-naproxene. The conventional route of this acylation employs excess $AlCl_3$ in nitrobenzene or BF_3/HF, as well as acetyl chloride as an acylating reagent and, strictly speaking, the process cannot be called catalytic[80]. A broad variety of catalysts has been explored to promote this reaction. A theoretical study of the acylation process has suggested 7 possible products[7] (**Scheme 1.5**). In addition to the expected products – 1,2-, 2,6-, 1,7-acetylmethoxynaphthalenes - the researchers have also proposed formation of hydroxy-, acetylhydroxy- and alkylnaphthalenes.

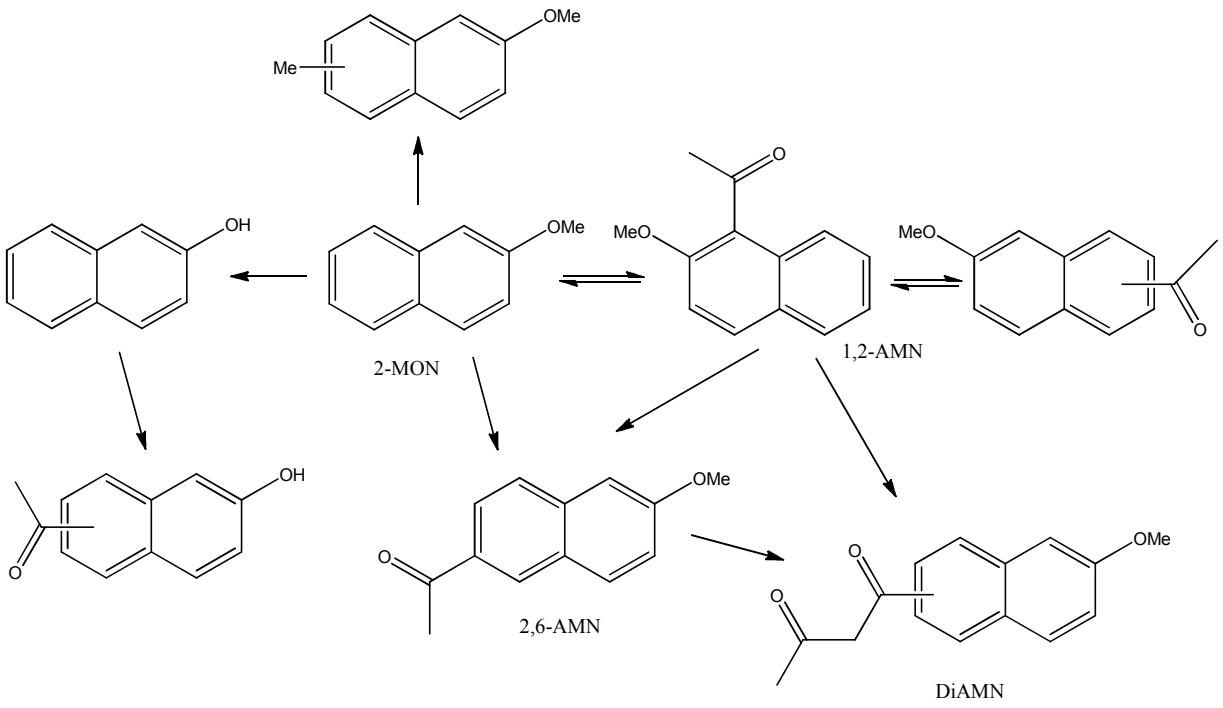

Scheme 1.5 Proposed pathways of acylation of 2-methoxynaphthalene promoted

by a Bronsted acid[7].

When 9 mol% of the CH acid was refluxed with an equimolar mixture of 2-MON and acetic anhydride in nitromethane, 62% of the substrate was found to be converted after 10 minutes. Careful peak area integration in the GC analysis of the reaction mixture indicated the formation of 2-methoxy-1-acetonaphthone as the dominant product. The reaction was allowed to continue to proceed for a total 24 hours and it was found that the distribution of the products kept gradually changing, until reaching equilibrium after about 20 hours reaction time under the given conditions. In addition to major isomeric products – 2,6-AMN and 1,2-AMN - formation of 7-methoxy-1-acetonaphthone (1,7-AMN) was observed as well. Upon quenching, the reaction mixture was separated by chromatographic means and the structures of all isolated products were confirmed by ^{1}H NMR and GC/MS. However, one of the products, the formation of which was clearly seen on the GC chromatogram at the beginning of the reaction, completely disappeared by the time the system reached equilibrium and, therefore, could not be isolated. A mass-spectrum of this GC fraction showed a strong peak with m/z = 241.1 that suggests a diacylated product. Corma *et.al*. have proposed that the second acylation may be happening not at the aromatic ring, but on the first added acetyl group that has a potential for enolizing in strongly acidic solutions[7], forming 2-acetylaceto-6-methoxynaphthalene. The other possible product of the acylation is 1,6-diacetyl-2-methoxynaphthalene and was previously proposed by Hoskins and coworkers[81]. In order to determine the true nature of this product, 1,6-diacetyl-2-methoxynaphthalene was independently synthesized in this Thesis work by acylation of 2-MON with excess of acetyl chloride and aluminum trichloride followed by alkylating the resulting 1,6-diacetyl-2-hydroxynaphthalene with dimethyl sulfate. The chemical structure of 1,6-diacetyl-2-methoxynaphthalene was unumbigously identified by ^{1}H and ^{13}C NMR and its mass spectrum

and GC retention time matched those of the above transient product in question.

As discussed above, the acylation of 2-MON catalized by the CH acid needs 20 hours to reach equilibrium. According to GC analysis, in the first minutes of the process, the majority of the substrate is converted to 1,2-acetylmethoxynaphthalene (**Figure 1.2**). However, the concentration of this product decreases with time until complete disintegration when the equilibrium is reached. The retention times for the acylation products are 5.37, 6.81, 6.99, 7.45, 8.69 s for 2-MON, 1,2-AMN, 1,7-AMN, 2,6-AMN and 1,2,7-DiAMN, respectively.

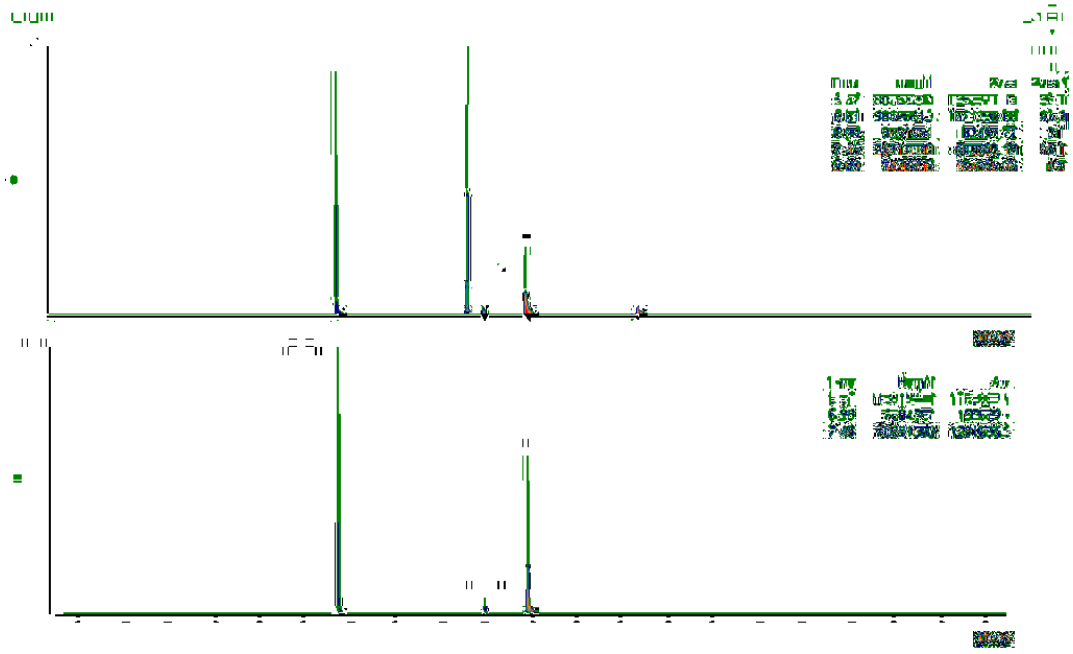

Figure 1.2 GC trace of the acylation of 2-MON at 10 and 1440 minutes (top and bottom trace respectively).

It was previously suggested[7] that 1,2-AMN undergoes transacylation with 2-MON and deacylation in order to form 2,6-AMN and 2-MON respectively. We have introduced 1,2-AMN to the standard acylation reaction conditions (equimolar amounts of the substrate and acetic acid, 15 mol% of the catalyst in refluxing nitromethane) and within 20 minutes formation of

substantial amounts of the transacylated product, 2,6-MON, was noted (**Scheme 1.6**) along with the rapid disappearance of the 1,2-AMN trace in the gas chromatogram.

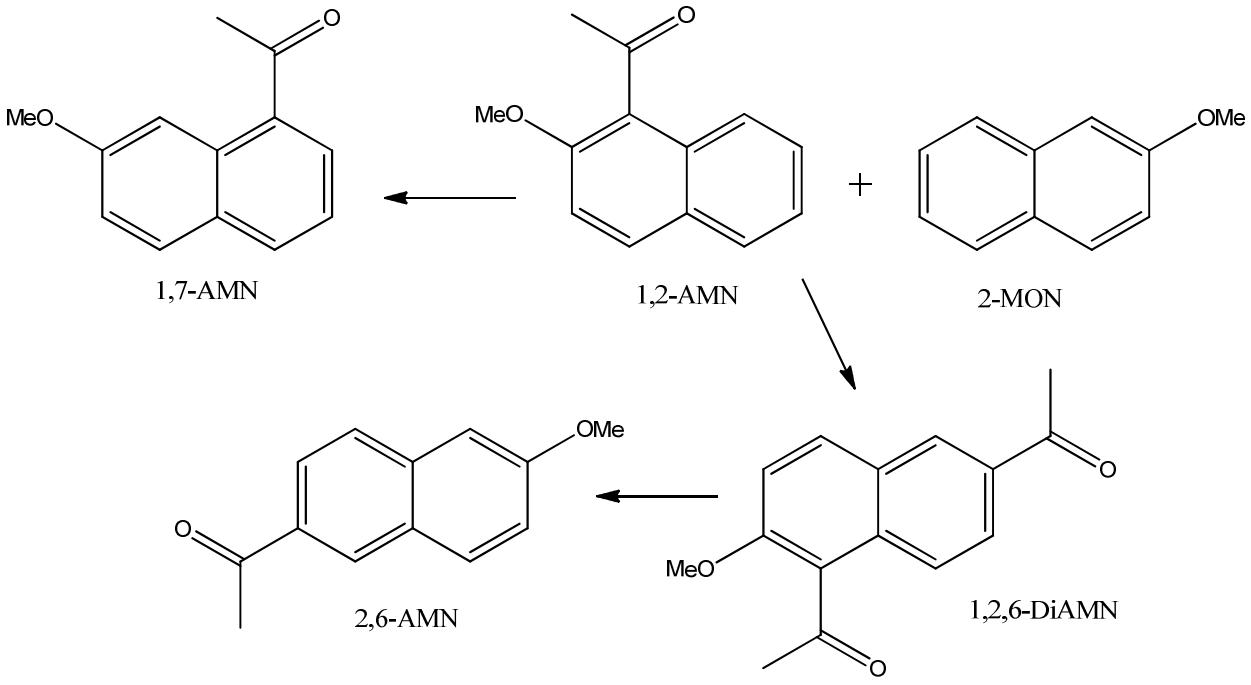

Scheme 1.6 Transacylation of 1,2-AMN promoted by a CH acid

The reaction reached the equilibrium point after 20 hours and the final product ratio (1,7-AMN to 2,6-AMN) was similar to that observed for a typical acylation of 2-MON with acetic anhydride (1:10), as was the product concentration change with time (**Figure 1.3**). The formation of 1,7-AMN and 2,6-AMN compounds in this experiment suggests that the acylation of 2-MON at the 6- position likely occurs *via* protonation of 1,2-AMN followed by nucleophilic attack of the reactive intermediate by the 6- carbon atom of 2-MON.

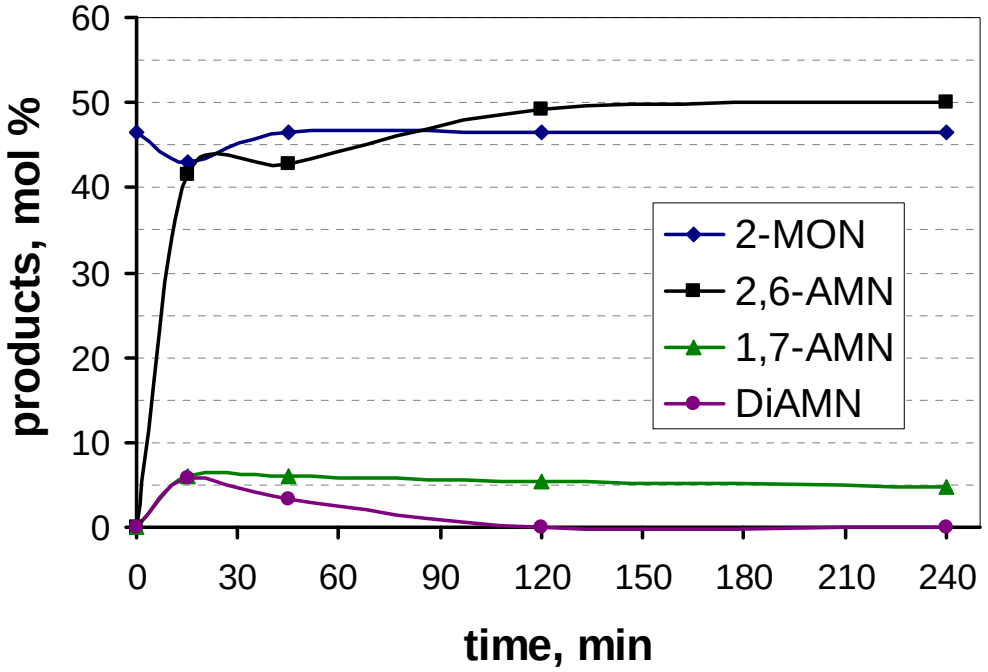

Figure 1.3. Dynamics of transacylation of 1,2-AMN.

It was logical to suggest that 1,2-MON is the kinetically preferred product, while the target 2,6-MON is thermodynamically preferred. While we observed the reaction progress, we have assumed that the time needed for the mixture to reach an equilibrium point should depend on the concentration of the catalyst. However, a 1 mol% catalyst loading has unexpectedly resulted in a regioselective acylation of a kinetically preferred 1- position (73% conversion by GC). At these concentrations the reaction needs less than 2 hours to stop progressing, but adding more catalyst (another 9 mol %, 10 mol % total loading) has redirected the reaction towards formation of the desired 2,6-AMN and the previously formed 1,2-AMN was completely transformed into the starting material and the thermodynamically preferred isomer resulting in a 2.1 to 1 ratio of 2-MON to 2,6-AMN. It is interesting to mention that while the conversion of 2-MON has remained lower than the one with the original procedure, the ratio of 1,7- to 2,6-AMN was the same (1:8). (The theoretical study of this phenomenon will be discussed further in this Chapter). After the activity of the parent compound was studied in detail, its derivatives were synthesized and applied in the acylation synthesis in order to find the effect the *para* subsituent

would have on the activity of the catalyst. Acylation of the substrate with *p*-Propoxytetrafluorophenyl(bis)triflyl methane at the same conditions has resulted in a 45% conversion of the starting material, yielding 40% 2,6-AMN and 4% 1,2-AMN, which shows that the electron donating alkyloxy group has very little effect on the catalytic activity.

The reaction dynamics were very close to those of pentafluorophenyl(bis)triflyl methane with the reaction reaching equilibrium after about 22 hours. The fact that the reaction is approaching equilibrium at given conditions indicates that the catalyst enables the reverse reaction.

The product formation over time suggests that at first, the kinetically preferred 1,2-AMN is formed, that then transacylates the starting material forming 2,6-AMN and 1,7-AMN (**Figure 1.4**).

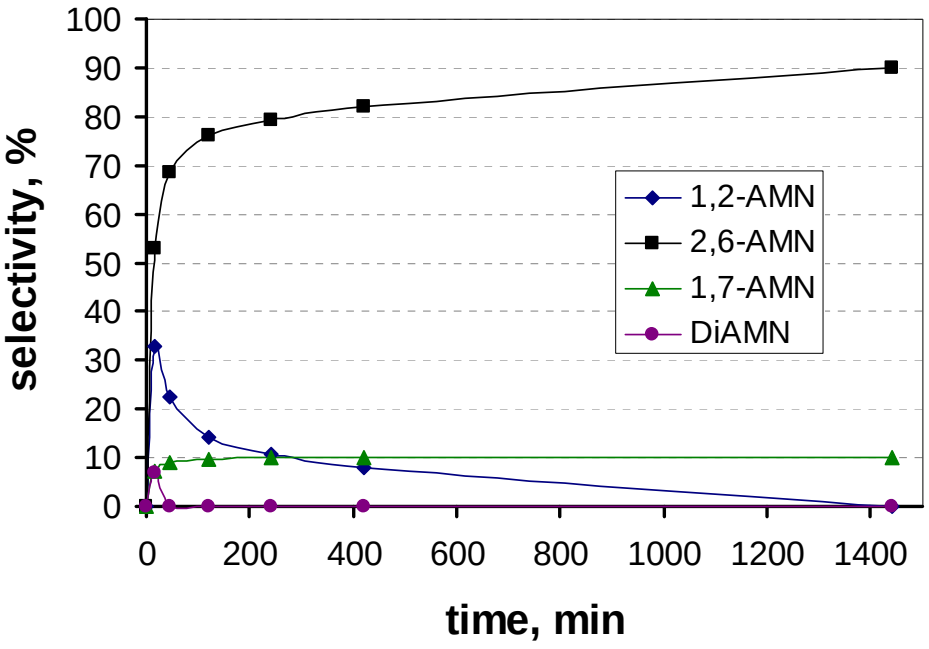

Figure 1.4. Concentrations of acylation products over time.

The difference of dipole moments of the 2 products (1,2-AMN and 2,6-AMN) is obvious, thus, it was suggested that the polarity of the media will have an impact on the product distribution. Conducting the synthesis in hexanes (110^0C, pressure vial) has resulted in 100% conversion of the starting material into the kinetically preferred product even with reduced catalyst loading (2.5-10 mol %) and using ethyl acetate as reaction media yielded 75% of 1,2-AMN selectively (traces of 2,6-AMN were detected), substituting the catalyst for p-Propoxy homologue has resulted in the same product formation.

It was not clear if the solvent acted as a proton source in order to support the transalkylation reaction. In order to investigate this hypothesis, the reaction was conducted in deuterated nitromethane. The isotope distribution (200.1:201.1 mass peaks) in the mass spectrum was found to have very little difference with the mass spectrum of the 2,6-MON that was synthesized in CH_3NO_2 (1:7 and 1:5 for nitromethane and nitromethane-d_3 respectively), which indicates that the solvent does not act as a source of labile protons.

The proposed mechanism of the reaction is shown in **Scheme 1.6**. As it is observed on **Figure 1.3**, both kinetic and thermodynamic products are formed from the starting material. However, the 1,2-AMN transacylates 2-MON to form one of 2 thermodynamically preferred products -1,7-AMN and 2,6-AMN. At the same time, it was observed that the first acylation does not fully suppress nucleophilicity of the substrate and second acylation can occur, but the presence of the resulting 1,2,7-DAMN is only observed with the high concentrations of 1,2-AMN indicating that the diacylated methoxynaphthalene is likely acting as an acetyl carrier for the transacylation reaction.

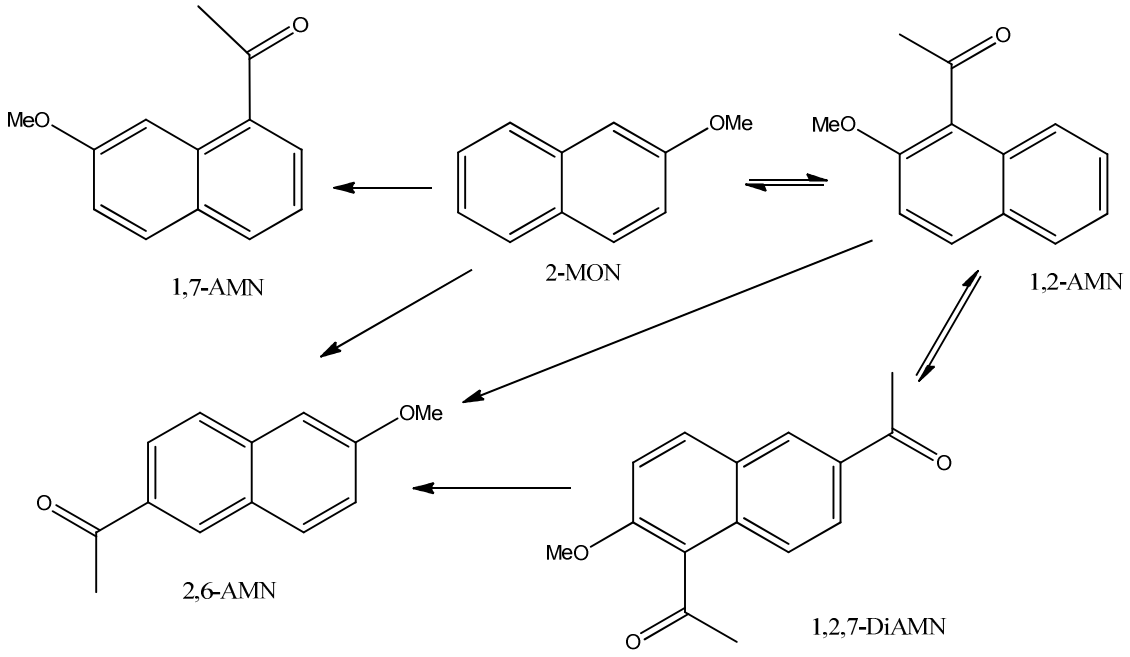

Scheme 1.7 Processes observed in the acylation of 2-MON process (2-MON (9.5 mmol), acetic anhydride (10 mmol) and CH acid (0.99 mmol) in nitromethane (10 mL)).

The goal of the project – a greener acylation process with recyclable catalyst was reached by extraction of the acid from the reaction mixture. Both of the catalysts have exhibited kinetic and thermodynamic stability in the reaction conditions and were possible to extract from the reaction mixture with basic aqueous solutions. The deprotonated acid was possible to reconstitute by acidifying the aqueous solution with strong mineral acids followed by extraction by organic solvent, even though the yields were mediocre. However, this points at a possibility of reusing the catalyst.

1.4.2 Theoretical explanation of kinetic and thermodynamic aspects of the process

The isomer distribution and formation rates were indicating that the thermodynamically preferred products are 1,7- and 2,6-AMNs. This was explained by a DFT calculation of the relative energies of formation of AMNs at 373K in nitromethane (**Table 1.3**)[75]. The energy of

formation of the main product was found to be lower than the ΔG^0 of 1,2- and 1,-7 AMN.

Table 1.3 Relative energies of formation and concentrations at equilibrium (standard conditions).

Acylation product	Relative energy of formation kcal/mol	Expected concentrations at equilibrium	Observed concentrations at equilibrium
1,2-AMN	4.9	0.1%	0%
2,6-AMN	0	97.6%	90%
1,7-AMN	2.8	2.3%	10%

From the free energy differences, yields were calculated assuming the reaction goes to equilibrium. Theoretical calculations are in good correlation with the experimental yields of the regioisomers - 0%, 90% and 10% for 1,2-, 2,6- and 1,7-AMN respectively. The kinetic preference for the *ortho* acylation can be explained by the difference of charges of carbon atoms. While the 1- position of the ring has a relative charge of 0.31, 6- and 7- carbon atoms have charges of 0.25 and 0.23 respectively. The difference in electron density on these carbon atoms ultimately leads to the stability of transition σ-complexes which are shown in **Table 1.4**[75].

Table 1.4 Relative energies of transition σ-complexes calculated by B3LYP/6-31G*.

σ-complex	Relative energy in heptanes (kcal/mol)	Relative energy in nitromethane (kcal/mol)
$[1,2\text{-AMN}]^+$	0	0

$[1,7\text{-AMN}]^+$	6.21	5.09
$[2,6\text{-AMN}]^+$	7.34	6.06

The kinetically preferred 1,2-AMN is shown to be the most stable in both hexanes and nitromethane, which is in line with the experimental data. The 2,6-AMN is the least stable in both systems, but the difference in relative energies drops 1.28 kcal/mol from heptanes to nitromethane. This difference may be enough that the 2,6-intermediate may not be kinetically accessible in hexanes. The other explanation may be the reversibility of the acylation process in nitromethane that makes the synthesis of 2,6-AMN a two step process that occurs via the 1,2-AMN that then transacylates the remaining 2-MON to form the thermodynamically preferred product.

The activity of the *para*-functionalized acid, that had very little difference with activity of the parent compound towards the acylation of 2-MON in given conditions, was studied by comparison of *ab initio* calculated gas phase acidities of the pentafluorophenyl(bis)triflyl methane and 4-(4-vilylphenyl)tetra-fluorophenyl(bis) triflyl methane to ΔH_{acid} of strong mineral acids. Substitution of *para*-fluorine with styryl function did affect the acidity as expected - the ΔH_{acid} has decreased from 307 to 295 kcal/mol. However, when compared to nitric and hydrobromic acids (323 and 321 kcal/mol respectively), the carbon acid has a significantly higher acidity. This data has supported the idea of immobilization of the catalyst by introducing a polymeric functional group in the *para* position of the phenyl ring.

1.5 Conclusions and future work

In this chapter synthesis, modification and catalytic activity of pentafluorophenyl(bis)triflyl methane has been described. The compound and its derivatives have catalyzed he acylation of 2-methoxynaphthalene by acetic anydride and were proven robust enough to be extracted from the reaction mixture and reused without any loss of activity. The acylation reaction was found to be dependent on the concentration of the catalyst, temperature and media. Further investigation of the solvent effect on reaction equilibrium may be needed in order to achieve better control over the product formation. All of the reaction products were isolated and their structures were confirmed by NMR and mass spectrometry. The mechanism of the acylation reaction was studied in detail and reevaluated. It was found to be a two step process involving formation of a kinetically preferred product followed by an intermolecular transacylation reaction. The kinetically preferred product acts as a source of acetyl cation if introduced to the reaction conditions. Some of the products of acylation and alkylation that were previously proposed were not found to form in present reaction conditions. Furthermore, identity of the diacylation product 1,6-acetyl-2-methoxynaphthalene was confirmed by ^{1}H and ^{13}C NMR of the compound that was independently synthesized and a compound extracted from the reaction mixture. The future direction of research on this subject should involve chemical modification of the catalyst in order to increase its lipophilicity and ease of separation from aqueous media. Preliminary studies have shown that the CH acid can promote esterification of fatty acids to produce biodiesel and the catalyst can be regenerated and reused. However, more studies on the structure-activity dependence are needed. Attempts to immobilize the catalyst on insoluble support media are discussed in the following Chapter.

1.6 References

(1) Yadav, J. S.; Subba Reddy, B. V.; Murthy, C. V. S. R.; Mahesh Kumar, G.; Madan, C. *Synthesis* **2001**, 783.

(2) Suárez, A. G. *Tetrahedron Lett.* **1999**, *40*, 3523.

(3) Lloyd, D. H.; Nichols, D. E. *J. Org. Chem.* **1986**, *51*, 4294.

(4) Gooßen, L. J.; Ghosh, K. *Eur. J. Org. Chem.* **2002**, *2002*, 3254

(5) Yamamoto, H.; Payette, J. N. *Synfacts* **2008**, *2008*, 0717.

(6) Chen, Y.; Lu, Y.; Li, G.; Liu, Y. *Organic Letters* **2009**, *11*, 3838.

(7) Botella, P.; Corma, A.; Navarro, M. T.; Rey, F.; Sastre, G. J. *J. Catal.* **2003**, *217*, 406.

(8) Sartori, G.; Maggi, R. *Chem. Rev.* **2006**, *106*, 1077.

(9) Davenport, K. G.; Linstid Iii, C. H. US Patent 4593125, 1986.

(10) Feller, A.; Lercher, J. A. *Adv. Catal.* **2004**, *48*, 229.

(11) Malone, M. F.; Huss, R. S.; Doherty, M. F. **2003**, *37*, 5325.

(12) Ergloff, G.; Weinert, P. C. *Proc. World Pet. Congr* **1951**, *IV*, 210.

(13) De Clerk, A.; Pujado, P. R. *Ind. Eng. Chem. Res* **2004**, *43*, 7449.

(14) Kantam, M. L.; Sateesh, M.; Choudary, B. M.; Ranganath, K. V. S.; Raghavan, K. V. Process for Alkylation of Naphthyl Ethers. U.S. Patent 6320082, 2001.

(15) Elango, V.; Murphy, M. A.; Smith, B. L.; Davenport, K. G.; Mott, G. N.; Zey, E. G.; Moss, G. L. U.S. Patent 4 981 995, 1991.

(16) Olson, A. C. *Ind. Chem. Ing.* **1960**, *52*, 833.

(17) Olah, G. A. *Friedel-Crafts and related reactions*; Interscience: New York, 1963; Vol. 1.

(18) Olah, G. A.; Wang, Q.; Surya Prakash, G. K. *Catal. Lett.* **1991**, *13*, 55.

(19) Smith, G. P.; Dworkin, A. S.; Pagni, R. M.; Zingg, S. P. *J. Am. Chem. Soc.* **1989**, *111*, 525.

(20) Zhao, Z.-K.; Qiao, W.-H.; Li, Z.-S.; Wang, G.-R.; Cheng, L.-B. *J. Mol. Cat. A-Chem.* **2004**, *222*, 207.

(21) Berenblyum, A. S.; Ovsyannikova, L. V.; Katsman, E. A.; Zavilla, J.; Hommeltoft, S. I.; Karasev, Y. Z. *App. Cat. A-Gen.* **2002**, *232*, 51.

(22) Hashim, H. H.; Valerioti, W. L. *Mater. Perfomance* **1993**, *32*, 50.

(23) Meyer, D. W.; Chapin, L. E.; Muir, R. F. *Chem. Eng. Prog.* **1983**, *79*, 59.

(24) Matthews, C. W.; Batman, E. S.; King, J. F. Aluminum Phenoxide Catalyst Removal. U.S. Patent 4929770, 1990.

(25) Bakshi, A. S. Sulfuric Acid Alkylation Process. U. S. Patent 7652187, 2010.

(26) Albright, L. F. *Ind. Eng. Chem. Res* **2002**, *41*, 5627.

(27) Laursen, J. K.; Karavanov, A. N. *Chem. Pet. Eng.* **2006**, *42*, 1573.

(28) *Kirk-Othmer Encyclopedia of Chemical Technology*; 5th ed. 1997; Vol. 24, p 38.

(29) Baerlocher, C.; Meier, W. M.; Olson, D. H. *Atlas of Zeolite Framework Types*; 5 ed.; Elseiver, 2001.

(30) Patil, S. P.; Yadav, G. D. *Comput. Biol. Chem.* **2003**, *23*, 393.

(31) Gabriel, S.; Weiner, J. *Ber.* **1888**, *21*, 2669.

(32) Walden, P. *Bull. Acad. Sci. St. Perersburg* **1914**, 405.

(33) Wilkes, J. S.; Zaworotko, M. J. *J. Chem. Soc., Chem. Comm.* **1992**, 965.

(34) Ryan, T. A.; Ryan, C.; Seddon, E. A.; Seddon, K. R. *Phosgene and Related*

Carbonyl Halides; Elsevier: Amsterdam, 1996.

(35) Timken, H. K. C.; Elomari, S.; Trumbull, S.; Cleverton, R. Integrated Alkylation Process using Ionic Liquid Catalysts. U.S. Patent 2006131209, 2006.

(36) Liu, Z. C.; Zhang, R.; Xu, X. M.; Xia, R. G. *Oil Gas J.* **2006**, *104*, 52.

(37) Plechkova, N. V.; Seddon, K. R. *Chem. Soc. Rev* **2008**, *37*, 123.

(38) Schmidt, R. C.; Beck, C. A.; Cronin, J. S.; Staszak, M. A. *Org. Process Res. Dev.* **2004**, *8*, 670.

(39) Alleti, R.; Oh, W. S.; Perambuduru, M.; Afrasiabi, Z.; Sinn, E.; Reddy, V. P. *Green Chem.* **2005**, 203.

(40) *CRC Handbook of Chemistry and Physics*; 73 ed.; CRC Press: Boca Raton, 1992.

(41) De Castro, C.; Primo, J.; Corma, A. *J. Mol. Cat. A-Chem* **1998**, *134*, 215.

(42) Izumi, Y.; Ogawa, M.; Nohara, W.; Urabe, K. *Chemistry Letters* **1992**, *21*, 1987.

(43) De Castro, C.; Corma, A.; Primo, J. *J. Mol. Cat. A-Chem* **2002**, *177*, 273.

(44) Misono, M.; Nojiri, N. *Appl. Catal.* **1990**, *64*, 1.

(45) Ivakin, A. A.; Kurbatova, L. D.; Kapustina, L. A. *Zh. Neorg. Khim.* **1978**, *23*, 2545.

(46) Hall, N. F.; Conant, J. B. *J. Am. Chem. Soc.* **1927**, *49*, 3047.

(47) Howells, R. D.; Mccown, J. D. *Chem. Rev.* **1977**, *77*, 69.

(48) Olah, G. A.; Farooq, O.; Husain, A.; Ding, N.; Trivedi, N. J.; Olah, J. A. *Catal. Lett.* **1991**, *10*, 239.

(49) Al-Kinany, M. C.; Al-Khowaiter, S. H. *Stud. Surc. Sci. Catal.* **1999**, *122*, 375.

(50) Akiyama, T. *Chem. Rev.* **2007**, *107*, 5744.

(51) Guo, Q.-X.; Liu, H.; Guo, C.; Luo, S.-W.; Gu, Y.; Gong, L.-Z. *J. Am. Chem. Soc.*

2007, *129*, 3790.

(52) Seayad, J.; Seayad, A. M.; List, B. *J. Am. Chem. Soc.* **2006**, *128*, 1086.

(53) Ishihara, K.; Kubota, M.; Kurihara, H.; Yamamoto, H. *J. Org. Chem.* **1996**, *61*, 4560.

(54) Yoon, H.-J.; Lee, S.-M.; Kim, J.-H.; Cho, H.-J.; Lee, Y.-S. *J. Appl. Chem.* **2007**, *11*, 425.

(55) Fortuna, C. G.; Musumarra, G.; Nardi, M.; Procopio, A.; Sindona, G.; Scire, S. *J. Chemometrics* **2006**, *20*, 418.

(56) Koshar, R. J.; Mitsch, R. A. *J. Org. Chem.* **1973**, *38*, 3358.

(57) Foropoulos, J.; Desmarteau, D. D. *Inorg. Chem.* **1983**, *23*, 3720.

(58) Macfarlane, D. R.; Huang, J.; Forsyth, M. *Nature* **1999**, *402*, 792.

(59) Saffarian, H.; Ross, P.; Behr, F. E.; Gard, G. L. *J. Electrochem. Soc.* **1990**, *137*, 1345.

(60) Singh, S.; Desmarteau, D. D.; Zuberi, S. S.; Witz, M.; Huang, H. N. *J. Am. Chem. Soc.* **1987**, *109*, 7194.

(61) Mikami, K.; Kotera, O.; Motayama, Y.; Sakaguchi, H.; Maruta, M. *Synlett.* **1996**, 171.

(62) Gramstad, T.; Haszeldine, R. N. *J. Chem. Soc.* **1957**, 4069.

(63) Hall, H. K.; Atsumi, M. *Polym. Bull.* **1988**, *19*, 319.

(64) Turowsky, L.; Seppelt, K. *Inorg. Chem.* **1988**, *27*, 2135.

(65) Koppel, I. A.; Taft, R. W.; Anvia, F.; Zhu, S.-Z.; Hu, L.-Q.; Sung, K.-S.; Desmarteau, D. D.; Yagupolski, L. M.; Yagupolski, Y. L.; Ignat'ev, N. V.; Kondratenko, N. V.; Volkonskii, A. Y. *J. Am. Chem. Soc.* **1994**, *116*, 3047.

(66) Juhatz, M.; Hoffmann, S.; Stoyanov, E.; Kim, K.-C.; Reed, C. A. *Angew. Chem. Int. Ed.* **2004**, *43*, 5352.

(67) Reed, C. A.; Kim, K.-C.; Stoyanov, E. S.; Stasko, D.; Tham, F. S.; Mueller, L. J.; Boyd, P. D. *J. Am. Chem. Soc.* **2003**, *125*, 1796.

(68) Brouwer, D. M.; Mackor, E. L.; Maclean, C.; Wiley Interscience: New York, 1970; Vol. 1.

(69) Olah, G. A.; Prakash, G. K. S.; Sommer, J. *Superacids*; Wiley: New York, 1985.

(70) Dietrich, H.; Bladauski, D.; Grosse, M.; Roth, K.; Rewicki, D. *Chem. Ber.* **1975**, *108*, 1807.

(71) Ishihara, K.; Hasegawa, A.; Yamamoto, H. *Angew. Chem. Int. Ed.* **2001**, *40*, 4077.

(72) Rode, B. M.; Engelbrecht, A.; Schantl, J. Z. *J. Prakt. Chem.* **1973**, *7*, 1.

(73) Hasegawa, A.; Ishikawa, T.; Ishihara, K.; Yamamoto, H. *Bull. Chem. Soc. Jpn.* **2005**, *78*, 1401.

(74) Arsenijevic, L.; Arsenijevic, V.; Horeau, A.; Jacques, J. *Org. Synth* **1973**, *53*, 5.

(75) Mitchell-Koch, K. R., University of Kansas, 2008.

(76) Frisch, M.; Trucks, G.; Schlegel, H.; Scuseria, G.; Robb, M.; Cheeseman, J.; Zakrzewski, V.; J.A. Montgomery, J.; Stratmann, R.; Burant, J.; Dapprich, S.; Millam, J.; Daniels, A.; Kudin, K. N.; Strain, M.; Farkas, O.; Tomasi, J.; Barone, V.; Cossi, M.; Cammi, R.; Mennucci, B.; Pomelli, C.; Adamo, C.; Clifford, S.; Ochterski, J.; Petersson, G.; Ayala, P.; Cui, Q.; Morokuma, K.; Salvador, P.; Dannenberg, J.; Malick, D.; Rabuck, A.; Raghavachari, K.; Foresman, J.; Cioslowski, J.; Ortiz, J.; Baboul, A.; Stefanov, B.; Liu, G.; Liashenko, A.; Piskorz, P.; Komaromi, I.; Gomperts, R.; Martin, R.; Fox, D.;

Keith, T.; Al-Laham, M.; Peng, C.; Nanayakkara, A.; Challacombe, M.; Gill, P.; Johnson, B.; Chen, W.; Wong, M.; Andres, J.; Gonzalez, C.; Head-Gordon, M.; Replogle, E.; Pople, J.; Gaussian 98 (revision A.11) ed.; Gaussian, Inc.: Pittsburgh, PA, 2001.

(77) Frischand, M.; Trucksand, G.; Schlegel, H.; Scuseria, G.; Robb, M.; Cheeseman, J.; J.A. Montgomery, J.; Vreven, T.; Kudin, K.; Burant, J.; Millam, J.; Iyengar, S.; Tomasi, J.; Barone, V.; Mennucci, B.; Cossi, M.; Scalmani, G.; Rega, N.; Petersson, G.; Nakatsuji, H.; Hada, M.; Ehara, M.; Toyota, K.; Fukuda, R.; Hasegawa, J.; Ishida, M.; Nakajima, T.; Honda, Y.; Kitao, O.; Nakai, H.; Klene, M.; Li, X.; Knox, J.; Hratchian, H.; Cross, J.; Bakken, V.; Adamo, C.; Jaramillo, J.; Gomperts, R.; Stratmann, R.; Yazyev, O.; Austin, A.; Cammi, R.; Pomelli, C.; Ochterski, J.; Ayala, P.; Morokuma, K.; Voth, G. A.; Salvador, P.; Dannenberg, J.; Zakrzewski, V.; Dapprich, S.; Daniels, A. D.; Strain, M.; Farkas, O.; Malick, D.; Rabuck, A.; Raghavachari, K.; Foresman, J.; Ortiz, J.; Cui, Q.; Baboul, A.; Clifford, S.; Cioslowski, J.; Stefanov, B. B.; Liu, G.; Liashenko, A.; Piskorz, P.; Komaromi, I.; Martin, R.; Fox, D.; Keith, T.; Al-Laham, M.; Peng, C.; Nanayakkara, A.; Challacombe, M.; Gill, P.; Johnson, B.; Chen, W.; Wong, M. W.; Gonzalez, C.; Pople, J. A.; Gaussian 03 (Revision D.01) ed.; Gaussian, Inc.: Wallingford, CT, 2004.

(78) Glendening, E. D.; Reed, A. E.; Carpenter, J. E.; Weinhold, F.; NBO Version 3.1 ed.

(79) Ishihara, K.; Hasegawa, A.; Yamamoto, H. *Synlett.* **2002**, 1299.

(80) Zoeller, J. R.; Sumner, C. E. *J. Org. Chem.* **1990**, *55*, 319.

(81) Girdler, R. B.; Gore, P. H.; Hoskins, J. A. *J. Chem. Soc. C.* **1966**, 181.

Chapter II

Immobilization of the 2,3,4,5,6-pentafluorophenyl(bis)triflyl methane on solid supports.

2.1 Introduction

Heterogeneous catalysis is one of the important topics in industrial process research and design. Containing the catalyst in a solid phase has numerous advantages over a single phase process, such as ease of separation and catalyst handling and loading[1]. However, heterogeneous processes on average have slower reaction rates when compared to their homogeneous counterparts due to lower collision probabilities. There are few general approaches to synthesis of insoluble Bronsted acids for use as catalysts. Immobilization of small acidic molecules on polymeric or network support has been documented for a variety of acids[2].

Numerous Bronsted acids were adsorbed to or contained in inorganic support materials: sulfuric acid absorbed on silica was found to catalyze alcohol acetylation and Friedländer annulation reactions at ambient temperatures[3,4]; toluene sulfonic acid doped silica gel (5% by mass) was applied to catalyze the condensation of o-phenylenediamines and aldehydes to produce benzimidazoles (an important class of pharmacophores)[5]; alumina impregnated with phosphoric acid, a so called "solid phosphoric acid", was characterized as a "solid superacid"[6], an acid with a pKa lower than that of 100% H_2SO_4, and used in propylene oligomerization and other processes[7].

Oxide supports may play other important roles in catalysts' properties, e.g. phosphoric acid is thought to react with the surface hydroxyls of silica to form monomeric and polymeric phosphates[8]. More complex systems containing heteropolyacids as the source of protons were immobilized on these type of supports as well. Phosphotungistic acid promotes alcohol esterification with acetic acid when tied to SiO_2 and ZrO_2[9]. The stability of the Keggin type acid allows calcinations of the solid acid at temperatures as high as 500^oC that ensures water removal[10]. While the vast majority of heteropolyacids studied in this field are Keggin type[11],

other types such as Wells-Dawson[12] and Preyssler[13] structure acids were successfully immobilized on silicon oxides and were shown to catalyze certain H^+-promoted organic reactions. Silica and alumina can serve as very robust and kinetically inert supports for Lewis acids as well. Aluminum trichloride, a widely used acid in chemical synthesis, was tethered to silica to be used to catalyze Mannich type aminoformylation of aromatic ketones[14] and γ-alumina to be used for isobutene polymerization[15]. Unlike the molecular form, both silica- and alumina-acid composites were recycled and reused, thus making the processes environmentally friendlier. A number of *f*-block metal salts were immobilized on oxide supports. Some of the examples include lanthanum sulfate, that catalyzes allylation of carbonyls[16], as well as yttrium and samarium siloxides that promote polymerization of isobutene without significant loss of activity[17] and other processes[18]. Mixed oxides containing tungsten[19], zirconium[20] and niobium[21,22] are also being studied for catalyzing various esterification and alkylation processes.

Polymeric organic materials are widely used in industrial chemistry. Ion exchange resins are among the most promising materials for acidic catalysis. Polymers of various types containing sulfonic acid groups have been synthesized and tested. Dowtex-50 that had been introduced in 1948[23] was one of the first highly acidic ion exchange resins. While its acidity is on par with hydrochloric acid, its stability has allowed its use in numerous reactions that require a source of protons[24]. The acidity of Dowex may be enhanced by utilization of sulfonyl groups to immobilize a Lewis acid[25]. **Scheme 2.1** illustrates the synthesis of the above superacid. The aluminum-sulfur-chloride ratio was found to be 1-2-2 and the metal is evenly distributed throughthe polymer bead.

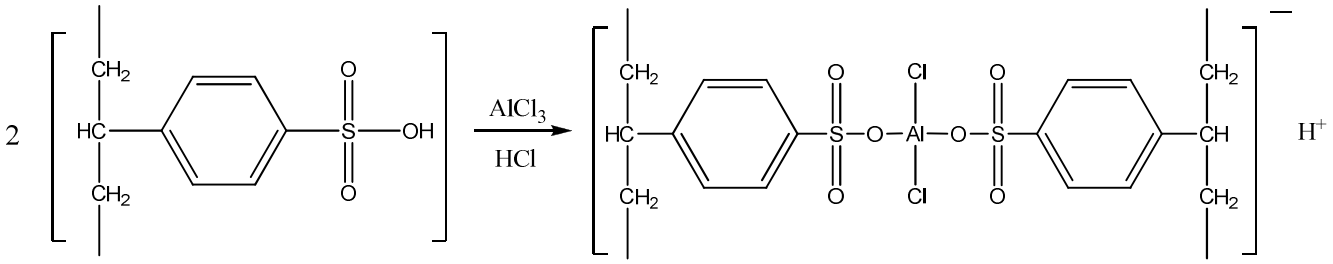

Scheme 2.1 Synthesis of a composite Bronsted-Lewis acid from Dowtex-50 polymer[25].

A number of other resins used to catalyze organic reactions that are widely represented on the market include Amberlyst (Rohm and Haas)[26], Indion-130 and 190 (Indion)[27], Deloxan ASP (Degussa)[28] and Nafion (DuPont)[29]. DuPont's Nafion resins require a closer look within this Introduction due to their unusual properties. Although the Nafion brand resins were originally synthesized for electrochemical purposes[30], the high Hammett acidity function of the resin ($11<H_0<13$), close to that of sulfuric acid, has placed this material among other solid acids[31].

The perfluorinated backbone's electron withdrawing nature enhances the acidity, while providing a robust support for the sulfoxides. Varying concentration of sulfoxide groups and branching through the Nafion family allows a broad range of applications of the resin, such as catalysts[32], membranes[33], and solid electrolytes[34]. However application of the original resin in catalysis was limited due to its low surface area (~0.02 m^2/g), so another modification was needed to improve the accessibility of the material's active sites[35]. In 1996, a group of researchers at DuPont synthesized a Nafion resin/silica nanocomposite (**Figure 2.1**) in order to increase the dispersion of acidic sites on the surface[36]. The resulting material showed an increase in catalytic activity of up to three orders of magnitude in some of the processes[29]. Further research proved the composite to efficiently catalyze a broad variety of reactions from esterification to sulfonation and hydrolysis[37]. Some of the other resins supported on silicon oxide

include Aciplex[38] and Flemion[39].

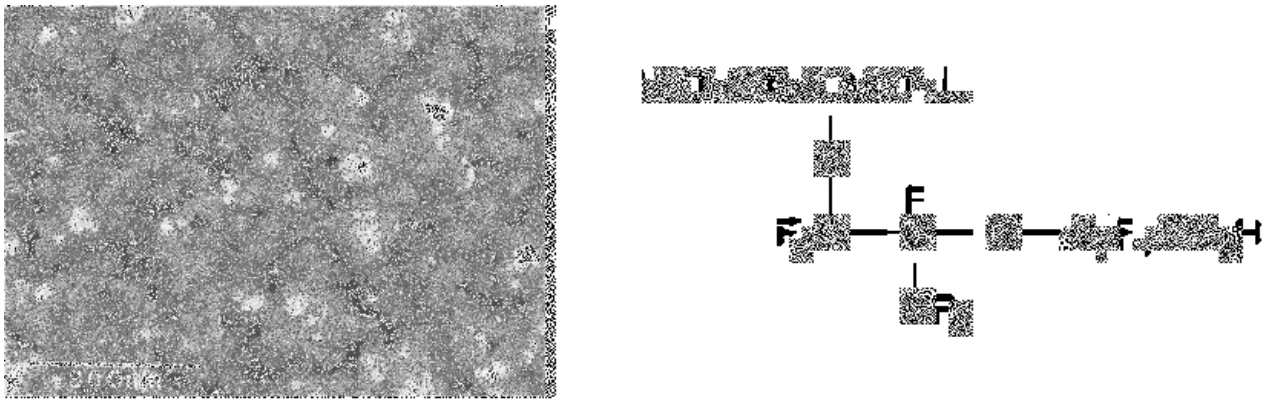

Figure 2.1 Nafion SAC-13 nanocomposite (left, SEM image adapted from Harmer *et. al.*)[36] and Nafion-H resin (right).

Tethering a Bronsted superacid – pentafluorophenyl(bis)triflyl methane to insoluble support was attempted by Yamamoto and coworkers by attaching the core molecule to polystyrene[40]. Although the resulting polystyrene acid was swollen by a number of organic solvents, the researchers were not able to overcome the low acid site density of the material[41].

2.2 Work Described in Chapter Two

Attempts to immobilize the pentafluorophenyl(bis)triflyl methane (CH acid) and 2,3,5,6-tetrafluoro-4-hydroxyphenyl(bis)triflyl methane on silicon oxide are described in the following sections of Chapter II.

The CH acid synthesis and chemical modification were described in Chapter I of this Thesis. Both physisorption and chemisorption of the CH and its hydroxy derivative have proven to be ineffective or failed. Although the acid doped silica catalyzed acylation of 2-MON and displayed high regioselectivity, the low conversion and catalyst deactivation do not make this

process an attractive alternative to existing methods.

2.3 Experimental Section

2.3.1 General methods and procedures

Unless specified otherwise, all procedures were performed in the air, except for those requiring an Ar atmosphere (99.5% purified by passage through columns of activated BASF catalyst and molecular sieves). All connections involving the gas purification system were made of glass, metal or other materials impermeable to air. Standard Schlenk techniques were employed using a double-manifold vacuum line. Solvents, including deuterated solvents were freed of impurities by standard procedures and stored under argon. NMR samples were analyzed on Bruker DRX-400 and Bruker Avance 500 Spectrometers. GC-MS spectra were recorded on a Quattro Micro triple quadrupole mass analyzer with the sample introduction via the Agilent 6890N gas chromatograph. BET analysis of silicon oxide was performed by Dr. R.S.V. Sarsani at the department of Chemical Engineering of the University of Kansas. Elemental analysis was performed by Desert Analytics (now Columbia Analytical Services), Tuscon, Az.

2.3.2 Physisorption of pentafluorophenyl(bis)triflyl methane on silica.

The silica was synthesized by a general procedure of Harmer *et al* [36]. A mixture of 20.4g of $Si(OMe)_4$, 3.3 g of deionized water and 0.3 mL of 0.04M HCl was stirred for 45 minutes. To 50mL of aqueous solution of 2.5 g of pentafluorophenyl(bis)triflyl methane, 25 mL of 0.4 M aqueous NaOH solution was added and the resulting solution was stirred for 15 minutes. The orthosilicate solution was then transferred rapidly to the CH acid solution with vigorous stirring.

The resulting mixture gelled immediately. The gel was kept in an oven at 95 ^{o}C for 2 days, followed by drying at reduced pressure (.01 Torr) overnight. The resulting fine solid was reacidified by washing with a 3M HCl solution, and then four times with deionized water. The resulting material was treated with nitric acid at 75 ^{o}C overnight and washed with large amounts of deionized water. Finally, the product was dried in a vacuum oven for 24 hours at 0.01 Torr and 100 ^{o}C. By fluorine elemental analysis 2.5 wt% of the CH acid was incorporated into the silica framework.

2.3.2a Acylation of 2-MON in presence of the CH-silica.

CH-silica composite (0.4 g), 2-MON (1.5g, 10 mmol) and acetic anhydride (1 mL, 10 mmol) were refluxed in nitromethane for 24 hours. The reaction mixture was cooled and the catalyst was filtered off, washed with diethyl ether and dried. The dark solution was analyzed by GC/MS and was found to produce 2,6-AMN selectively (conversion 6%).

2.3.3 Synthesis of 3-chloropropyl-functionalized silica gel.

Nafion beads (7.43 g) were refluxed in 40 mL of concentrated HCl for 2 hours and then stirred at room temperature for 2 days. The silica was filtered off and washed with 250 mL of deionized H_2O followed by drying under vacuum overnight (55^{o}C, 0.01 Torr). The resulting 7.48 g of fine silica was placed in 100 mL of a toluene solution of 6.8 g (3.7 mmol) of 3-chloropropyltriethoxysilane and the mixture was heated to reflux for 2 hours. The reaction mixture was then dried under vacuum (40^{o}C, 0.07 Torr) overnight to yield 1.3 g of white functionalized silica.

2.3.3a Reaction of 3-chloropropyl-functionalized silica gel with 4-hydroxy-tetrafluorophe-nyl(bis)triflyl methane.

A 0.59 g quantity of a of sodium hydride (60% suspension in mineral oil, 41 mmol) was washed repeatedly with hexanes and dried in vacuum. Dry NaH was placed under argon and 3.8 g of 4-hydroxytetrafluorophenyl(bis)-triflylmethane in 10 mL of pyridine was added to the flask. The reaction mixture was stirred overnight at room temperature. The deprotonated conjugate base of the acid was transferred to 4.0 g of 3-chloropropyl-functionalized silica suspended in 30 mL of pyridine and the mixture was stirred at room temperature for 16 hours, then heated to 60 °C for 4 days. The resulting suspension was centrifuged and the solid was washed with large amounts of deionized water, 5% solution of HCl, and then stirred in 30% aqueous HCl for 4 days. The reconstituted acid was washed with large amounts of deionized water until the washings become neutral followed by acetone. Drying the precipitate under vacuum yielded 2.50 g of fine yellow solid. The material did not exhibit any activity toward acylation of 2-MON under standard conditions.

2.3.4. Physisorption of 4-hydroxytetrafluorophenyl(bis)triflyl methane on silica.

To a flask containing 4.80 g (31.5 mmol) tetramethylorthosilicate, 2.5 g of 4-hydroxytetrafluoro-phenyl (bis)triflyl methane was added and the mixture was vigorously stirred for 10 minutes. Then 0.5 mL of H_2O was added and the gel was stirred for another 2 hours followed by drying in vacuum for 8 hours (0.01 Torr, 40 °C) to yield 5.89 g of a brown solid.

2.3.4a. Acylation of 2-MON in presence of silica 2.3.4.

Silica **2.3.4** (500 mg), 2-MON (750 mg, 4.74 mmol), and acetic anhydride (0.5 mL, 5.3 mmol) were heated at 90 °C in nitromethane under the inert atmosphere of argon for 14 hours. The reaction was cooled down and analyzed by GC. 2,6-AMN was produced selectively with 23.5% conversion of 2-MON.

The silica gel was filtered, washed with diethyl ether and dried under vacuum for 1 hour. The recovered material showed no catalytic activity when subjected to the same reaction conditions.

2.4 Results and Discussion

Although the attempts to tether the CH acid to inorganic supports have failed, the outcome was interesting enough to be described in a separate Chapter.

As described in Chapter 1, the labile nature of the *para*-fluorine of the acid allows modification of the core structure with oxy nucleophiles. These aryl(bis)triflylmethanes did not appear to lose their activity towards the acylation reaction when compared to the parent pentafluorophenyl(bis)triflylmethane thereby supporting the hypothesis that the acid may stay active while tethered to the silicon oxide. The “parent” CH acid’s modification clearly requires a hard nucleophile – as our attempts to tether the acid to a silica support *via* the nucleophilic substitution of the *para*-fluorine have not been successful. On the other hand, this substitution should be possible as we were able to functionalize the CH acid with propyloxy and hydroxy nucleophiles. **Scheme 2.2** summarizes some of the reaction conditions that were applied.

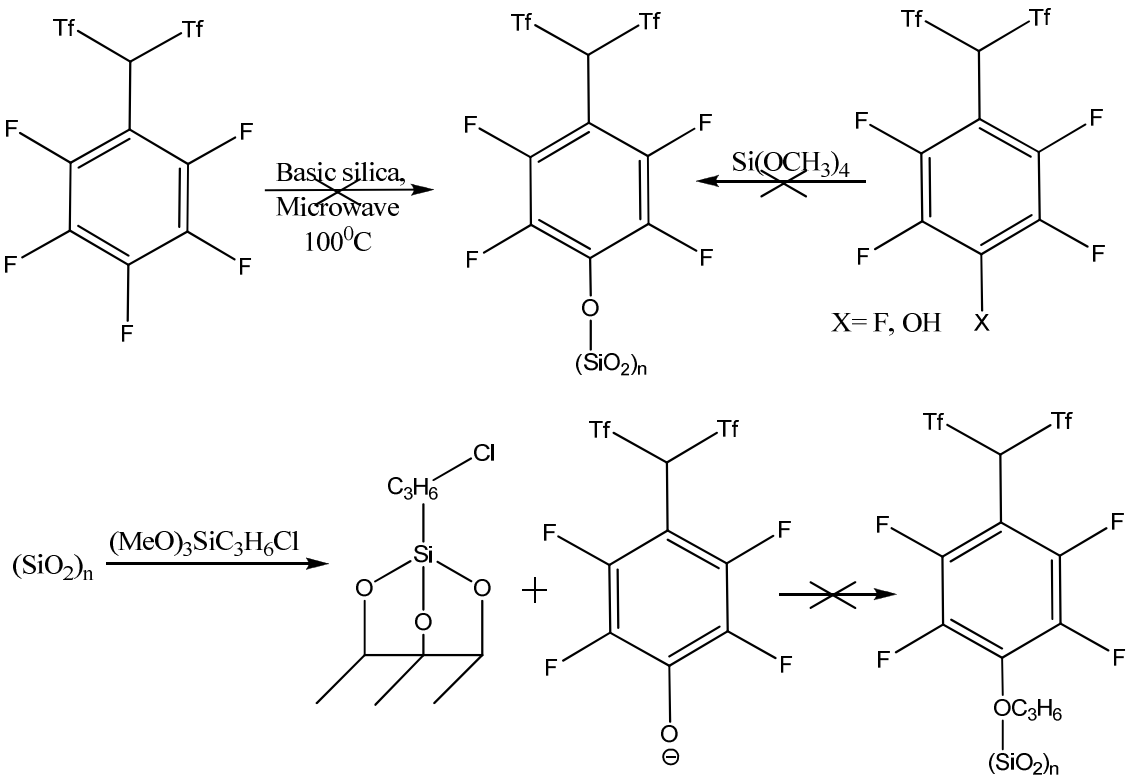

Scheme 2.2 Attempted immobilization of CH acid on insoluble supports.

The first attempt to immobilize the CH acid on silica via adsorption was made through the sol gel technique and resulted in 2.5 wt% incorporation of the CH acid in the silica framework. The resulting material showed some activity towards catalyzing the target reaction. Although the conversion was low (6%), the acylation selectively produced the thermodynamically preferred 2,6-AMN. The catalyst, however, leached out of the substrate pores and could not be reused. Since we had access to the modified *p*-hydroxy CH acid, we attempted the sol gel technique in hope of incorporating the hydroxyl group of the acid into the silicon-oxygen network. The resulting material was capable of catalyzing the acylation of 2-MON, however, the acid was not immobilized on the silica and leached out. The GC traces of the acylation reactions are shown on **Figure 2.2**. Interestingly enough, both of the physisorbed solids showed some catalytic activity and produced the target compound.

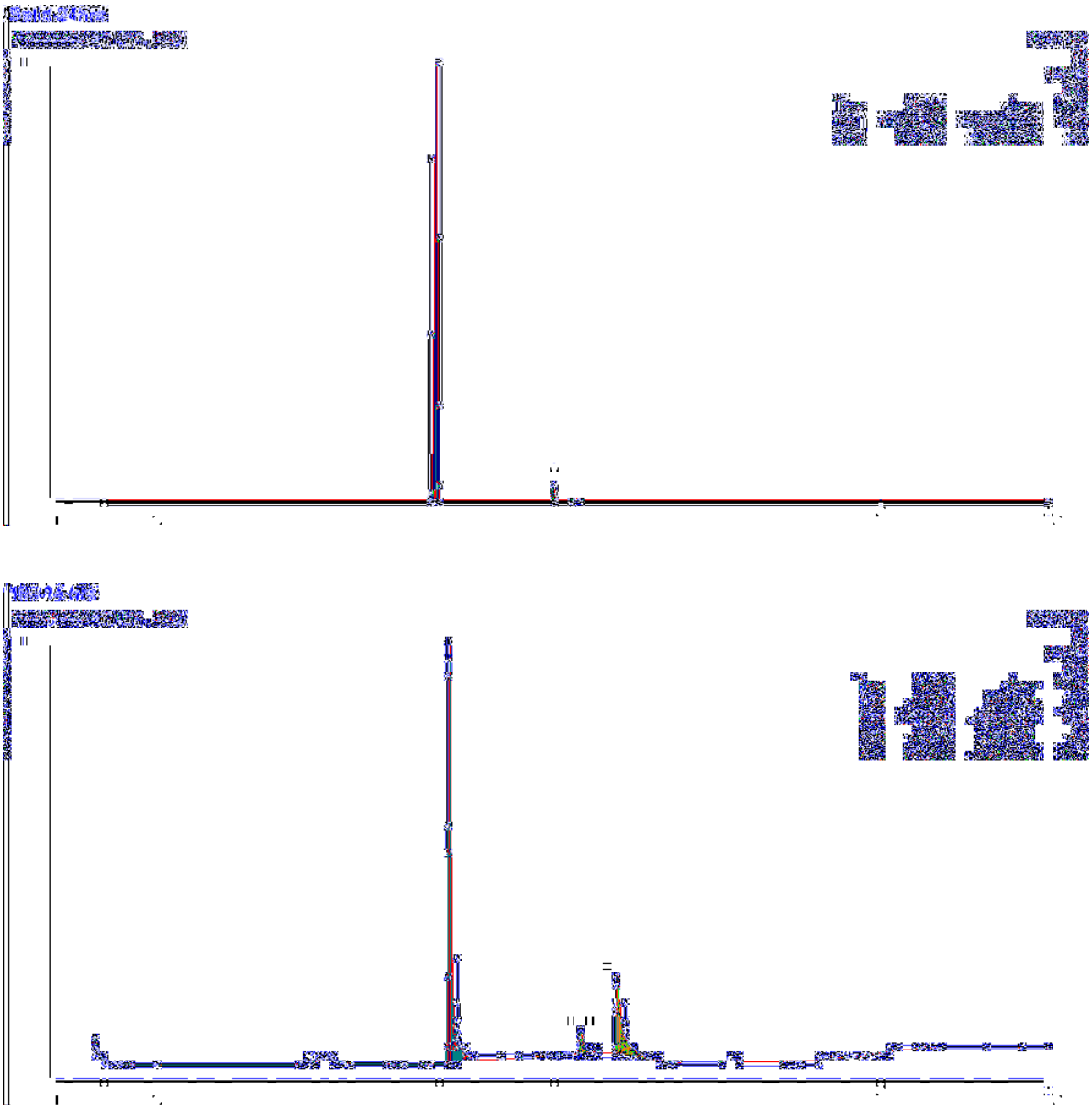

Figure 2.2 GC traces of acylation of 2-MON catalyzed by silicas **2.3.2**(top) and **2.3.4**(bottom)

As seen on a GC trace of acylation of 2-MON with silica 2.3.2, the only product observed is the thermodynamically preferred 2,6-AMN (retention times are 6.94 min on top and 7.73 min on bottom trace). However, a low loading of the catalyst suggests that the acylation process happens on the silica surface. The possibility of the catalysis by leached out CH acid in the

solution phase was ruled out by experiment **1.3.6a** that had shown that the low concentration of the catalyst leads to formation of a kinetically preferred product. These data are in line with the previous observations involving the acid-doped silica[5]. The observed activity of the CH acid-doped silica led to the attempted synthesis of the propyloxy-modified catalyst. While the surface of the silica was successfully coated with 3-chloropropyl groups via attachment of 3-chloropropylorthosilicate, our attempts to use the 4-hydroxy-derivatized CH acid as a nucleophile to permanently attach the acid to the surface have failed and the resulting material showed no catalytic activity. The deprotonated 4-hydroxy group did not exhibit nucleophilic behavior, which is probably due to extensive electron density delocalization along the highly electron-withdrawing perfluoroaryl and triflyl groups.

2.5 Conclusions and future work

The CH acid-doped silica gel displayed some catalytic activity in regard to acylation of 2-MON. The product distribution suggests that the reaction occurs at the surface of the silica or inside of the pores, not in the solution of the acid leached out of the pores. In fact, if the process was indeed occurring in the homogenous solution, selective formation of the kinetically preferred 1,2-AMN would have been observed as in **1.3.6a**. These data point to the potential of tethering the acid or its derivatives to such supports. Unfortunately, the *para*-hydroxy-derivatized CH acid was not nucleophilic enough to get incorporated into the silica during gel formation. Although the actual amount of the catalyst used in both cases was lower than the usual 10-15 mol% that were used in the catalytic activity evaluation described in Chapter I of this Thesis, the lower conversions and the catalyst deactivation make doped silica unattractive for the preparative synthesis of 2,6-AMN.

Future attempts to immobilize the catalyst are necessary in order to overcome the high cost

of the material. For instance, organic supports, such as hydroxyl-containing polymers, may be considered in order to fix the catalyst on the insoluble matrix to make Nafion type resins[36]. Other routes may include syntheses of organosilicon monomers containing the CH acid followed by the sol-gel polymerization of the product.

2.6 References.

(1) Thomas, J. M.; Raja, R. *Top. Catal.* **2006**, *40*, 3.

(2) Liu, P. N.; Xia, F.; Wang, Q. W.; Ren, Y. J.; Chen, J. Q. *Green Chem* **2010**, *12*, 1049.

(3) Shirini, F.; Zolfigol, M. A.; Mohammadi, K. *Bull. Korean Chem. Soc.* **2004**, *25*, 325.

(4) Dabiri, M.; Azimi, S. C.; Bazgir, A. *Monatsh. Chem.* **2007**, *138*, 659.

(5) Chakhabarty, M.; Mukherjee, R.; Karmakar, S.; Harigaya, Y. *Monatsh. Chem.* **2007**, *138*, 1279.

(6) Krzywicki, H.; Marczewski, M. *J. Chem. Soc., Faraday Trans. 1* **1980**, *76*, 1311.

(7) Busca, G.; Ramis, G.; Lorenzelli, V.; Rossi, P. F. *Langmuir* **1989**, *5*, 911.

(8) Nooney, M. G.; Campbell, A.; Murrell, T. S.; Lin, X.-F.; Hossner, L. R.; Chusuei, C. C.; Goodman, D. W. *Langmuir* **1998**, *14*, 2750.

(9) Li, J.-G.; Peng, Y.-Q. *J. Chin. Chem. Soc.* **2010**, *57*, 305.

(10) Brahmkhatri, V.; Patel, A. *Kinet. Catal.* **2010**, *51*, 380.

(11) Romanelli, G. P.; Autino, J. C. *Mini Rev. Org. Chem.* **2009**, *6*, 359.

(12) Bennardi, D.; Ruiz, D.; Romanelli, G. P.; Autino, J. C.; Baronetti, G.; Thomas, H. J. *Lett. Org. Chem.* **2008**, *5*, 607.

(13) Hu, C.; Zhang, Y.; Xu, L.; Peng, G. *Appl. Catal. A. Gen.* **1999**, *177*, 237.

(14) Li, Z.; Ma, X.; Liu, J.; Feng, X.; Tian, G.; Zhu, A. *J. Mol. Catal.* **2007**, *272*, 132.

(15) Cai, T.; He, M. *Catal. Lett.* **2003**, *86*, 17.

(16) Sreekanth, P.; Kim, S.-W.; Hyeon, T.; Kim, B. M. *Adv. Synth. Catal.* **2003**, *345*, 936.

(17) Touchard, V.; Spitz, R.; Boisson, C.; Llauro, M.-F. *Macromol. Rapid Commun.* **2004**, *25*, 1953.

(18) Okuhara, T. *Chem. Rev.* **2002**, *102*, 3641.

(19) Ramu, S.; Lingaiaha, N.; Prabhavati, B. L. A.; Devi, R. B. N.; Prasadb, I.; Suryanauanaa, P. S. *Appl. Catal. A.* **2004**, *276*, 163.

(20) Segawa, K.; Kihara, N.; Yamamoto, H. *J. Mol. Catal.* **1992**, *74*, 213.

(21) Goncalves, J. D. A.; Ramos, A. L. D.; Rocha, L. L. L.; Domingos, A. K.; Monteiro, R. S.; Peres, J. S.; Furtado, N. C.; Taft, C. A.; Aranda, D. a. G. In *J. Phys. Org. Chem.* 2010.

(22) Ushikubo, T.; Iizuka, T.; Hattori, H.; Tanabe, K. *Catal. Today* **1993**, *16*, 291.

(23) Bauman, W. C.; Skidmore, J. R.; Osmun, R. H. *J. Ind. Eng. Chem.* **1948**, *40*, 1350.

(24) Ali, S. H.; Merchant, S. Q. *Ind. Eng. Chem. Res.* **2009**, *48*, 2519.

(25) Fuentes, G. A.; Gates, B. C. *J. Catal.* **1982**, *76*, 440.

(26) Feng, X. L.; Guan, C. J.; Zhao, C. X. *J. Chem. Res., Synop.* **2003**, 744.

(27) Yadav, G. D.; Nalawade, S. P. *Chem. Eng. Sci.* **2003**, *58*, 2573.

(28) Yadav, G. D.; Mujebur-Rahuman, M. S. M. *Org. Process Res. Dev.* **2002**, *6*, 706.

(29) Harmer, M. A.; Sun, Q. *Appl. Catal. A.* **2001**, *221*, 45.

(30) Sondheimer, S. J.; Bunce, N. J.; Fyfe, C. A. *JMS-Rev. Macromol. Chem. Phys.* **1986**, *C26*, 353.

(31) Olah, G. A.; Prakash, G. K. S.; Sommer, J. *Science* **2006**, *13*, 1979.

(32) Olah, G. A.; Iyer, P. S.; Prakash, G. K. S. *Synthesis* **1986**, 513.

(33) Ma, Z. Q.; Cheng, P.; Zhao, T. S. *J. Membr. Sci* **2003**, *215*, 327.

(34) Kannan, R.; Kakade, B. A.; Pillai, V. K. *Angew. Chem. Int. Ed.* **2008**, *47*, 2653.

(35) Sun, Q.; Harmer, M. A.; Farneth, W. E. *Ind. Eng. Chem. Res.* **1997**, *36*, 5541.

(36) Harmer, M. A.; Sun, Q.; Farneth, W. E. *J. Am. Chem. Soc* **1996**, *118*, 7708.

(37) Gelbard, G. *Ind. Eng. Chem. Res.* **2005**, *44*, 8468.

(38) Okuyama, K.; Takata, K.; Odawara, D.; Suzuki, T.; Nakata, S.-I.; Okuhara, T. *Appl. Catal. A.* **1999**, *190*, 253.

(39) Sambandam, S.; Ramani, V. *J. Power Sources* **2007**, *170*, 259.

(40) Ishihara, K.; Hasegawa, A.; Yamamoto, H. *Angew. Chem. Int. Ed.* **2001**, *40*, 4077.

(41) Kokubo, Y.; Hasegawa, A.; Kuwata, S.; Ishihara, K.; Yamamoto, H.; Ikariya, T. *Adv. Synth. Catal.* **2005**, *347*, 220.

Chapter III

2- and 6-azulenylthiols: synthesis, structure, coordination chemistry and self-assembling on Au(111) surface

3.1.1 Introduction to Azulene-based Ligands.

Azulene (bicylcol[5.3.0]decapentaene) was first isolated in 1860s from German chamomile and yarn distillates[1] as derivatives of the parent compound. Azulene is a structural isomer of a naphthalene, although due to electronic inhomogenity of its · -system it has a dipole moment of 1.08D[2] and a lower HOMO-LUMO gap[3] (**Figure 1.1)**. The first synthesis of azulene was performed via a ring expansion of indane and was published in 1936 by P. Plattner[4]. However, due to low yields and explosive nature of diazomethane utilized in the reaction, the azulenes were hard to access until Hafner[5] and Nozoe[6] discovered more convenient and efficient routes to substituted azulenes. Since then azulenes have been used in a variety of applications, such as pharmacology[7,8], cosmetology[9,10], materials (advanced polymers[11,12] and optical materials[13,14]), dyes[15,16] and liquid crystals[17,18].

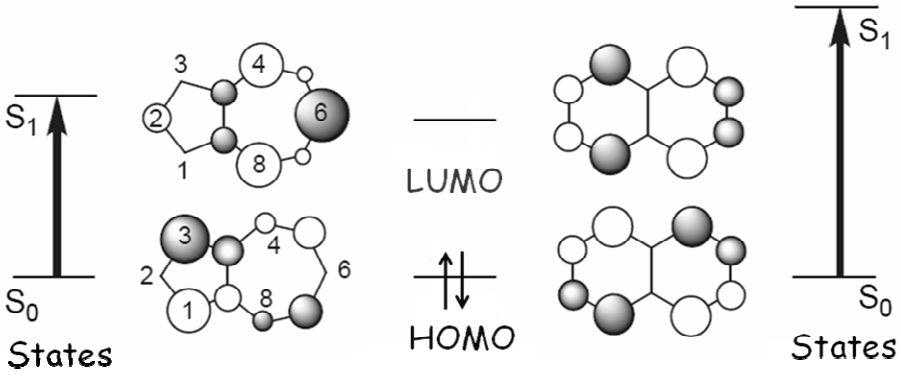

Figure 3.1 HOMO- LUMO gaps of azulene and naphthalene[3].

The interest in azulene chemistry arises in part from the unusual electronic properties of the molecule. It was suggested, based on theoretical considerations, that naphthalene has lower molecular conductivity than the azulene[19]. In addition, the azulenic motif constitutes a natural defect in certain carbon nanotubes that is responsible for high conductivity of such materials[20].

Azulenes have been applied in a variety of electronic applications. For example, 1,3-polyazulene has been shown to be a good conducting material[21] upon protonation with trifluoroacetic acid. The polymer forms a polyazulenyl cation radical, which was observed by EPR. Azulene-thiophene copolymers of poly{1,3-bis[2-(3-alkylthienyl)]azulene} general formula, where the alkyl length ranges from methyl to tetradecyl, have better conductivity than most of the thiophene-arylene copolymers[22,23] and exhibit a chemochromic effect upon protonation with trifluoroacetic acid, while 1,3-azulene – fluorene copolymer is capable of switching color from yellow to green reversibly due to formation of azulenium cation in the solid phase if electrical potential is applied[12]. Azulene derivatized celluloses have been synthesized and found to be promising conductive and fluorescent materials[24]. Low oxidation/reduction barriers and bright coloration of azulenes have made them attractive targets for electrochromic applications. Hexakis(6-octyl-2-azulenyl)benzene and hexakis(6-hexadecyl-2-azulenylethinyl)benzene are great example of a system with tunable reduction properties; insertion of an ethynyl linker between the azulene and the benzene rings results in a 5 step reduction process, whereas the former compound undergoes a single step 6 electron reduction[25].

The HOMO-LUMO gap of azulene can be easily tuned by incorporating electron donating or withdrawing substituents at odd- or even-numbered positions of the azulene providing a range of absorbed wavelengths[26]. (**Figure 3.2**) While adding electron donating groups (EDG) to an odd (1, 3, 5 and 7) position destabilizes the HOMO and LUMO+1, placing electron withdrawing groups (EWG) at the above positions stabilizes these orbitals. Functionalizing even-numbered positions on the azulene ring (2, 4, 6 and 8) with EWGs leads to stabilization of LUMO, while EDGs would destabilize this virtual orbital. Indeed, this is demonstrated by the colors of azulene derivatives covering the full range of wavelengths in the visible from yellow to violet[1,5,6,15,27].

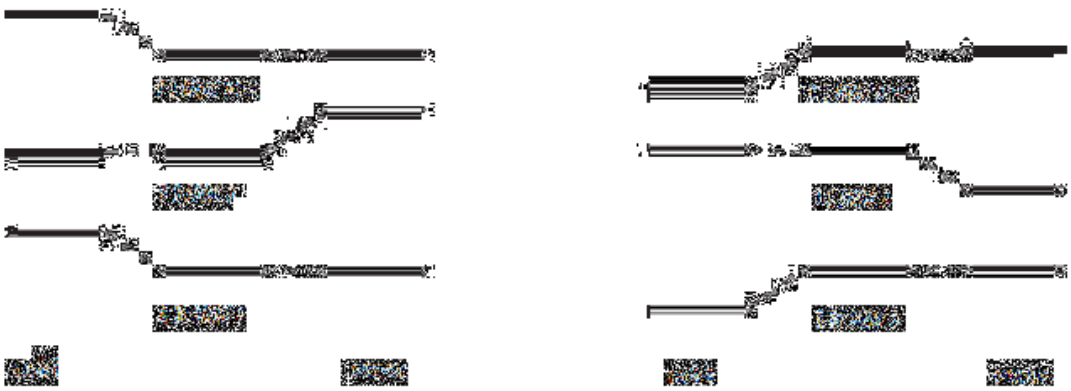

Figure 3.2 The change in HOMO, LUMO and LUMO+1 of azulene with addidion of electron donating (left) and electron withdrawing groups to odd and even positions of azulenes[28]

Azulene's bright coloration and luminescent properties have made it attractive for dye and marker design. For instance, a system involving a porphyrin ring modified with 4-azulenyl moiety consititutes a very promising two photon absorbing pigment[27]. Azulenocyanines are another example of a prospective dye where the azulene backbone lowers the LUMO of tetraazaporphyrin, thereby pushing the absorption in the near IR region. In addition, these compounds exhibit high extinction coefficients making them good potential targets for molecular dyes[29].

A number of studies of azulene in the organometallic context have demonstrated that azulene as a ligand undergoes multihapto complexation (often poorly predictable) which may be accompanied by C-C coupling[30-32] of two azulenic moieties (**Figure 3.3**)

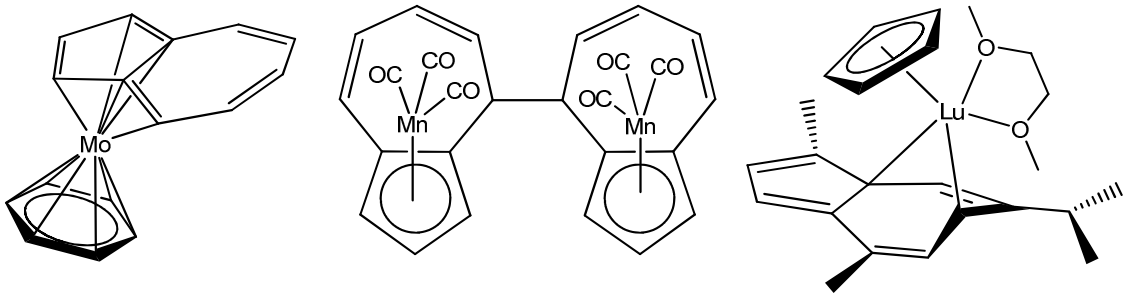

Figure 3.3 Examples of multihapto bounding of azulene to different metal centers

Azulenes directly bound to metals without the loss of aromaticity have also been described. However, these involve embedding the azulenic moiety into a rigid framework such as a porphyrin ring[33].

Using a junction group is another strategy to connect a metal center to an azulene scaffold. Several systems featuring an azulenic moiety bound to a single or multiple metal centers through carboxy[34], oxy[35], isocyano[36] and other linkers are known. 2-Hydroxyazulene-1,3-dicarboxylates were found to form $[Ln(Az)_4]^-$ with lanthanides (Nd^{3+}, Er^{3+}, Yb^{3+}, Tm^{3+})[35]. These complexes provide high quantum yields for luminescence in the near-IR region due to efficient sensitization by the ligands that may be used in biological imaging or LED fabrication. Crown ethers containing azulene moiety were synthesized to potentially serve as ion sensors with the

π-system of the azulene directly interacting with the guest particle[37]. Some of the chromoinophores have shown great selectivity and color sensitivity towards specific cations[37,38]. 1,3-and 5,7-azulenic acid alkylamides are capable of selective binding to anions such as chloride and fluoride, and, as a recent study suggests, are potential building blocks for anion sensors[39].

A number of azulene bridged metal complexes were designed and synthesized[40]; 2,6-azulene-dicarboxylic acid linking two quadruple bound bimetallic Mo or W moieties was described by Chisholm *et al* in 2005[34]. These complexes were described as a class III

(completely delocalized) type of mixed-valence compounds with strong coupling almost exclusively occurring through the π^* orbitals of the bridging azulene.

A potential for application of azulene's electronic inhomogenity in organometallic chemistry was demonstrated by Barybin *et al.* through the synthesis of 5 possible isocyanoazulenes and their complexation with low-valent chromium (**Figure 3.4**).

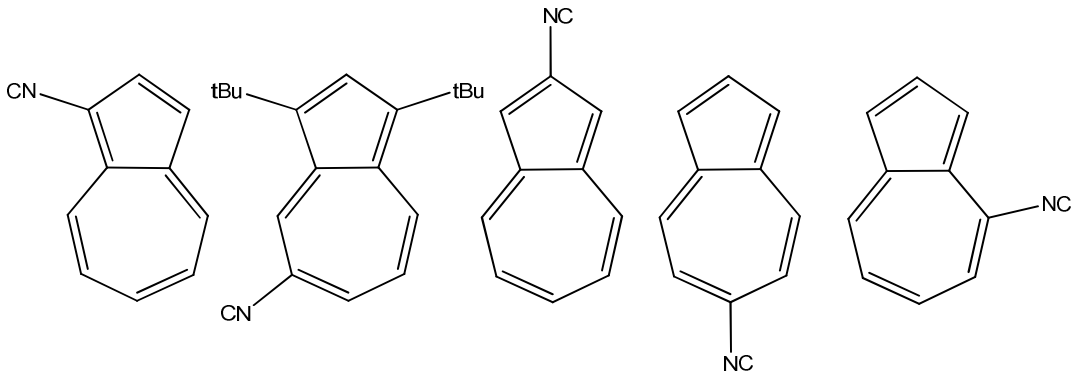

0/+1	-0.98V	-0.87V	-0.69V	-0.49V	-0.44V
+1/+2	-0.42V	-0.29V	-0.16V	-0.03V	+0.02V

Figure 3.4 Drawings of 1-, 5-, 2-, 6-, and 4-isocyanoazulenes and the $E_{1/2}$ potentials for the corresponding $[Cr(CNAz)_6]^{z/z+1}$ complexes (vs. FcH/FcH^+).

The resulting "electrochemical series" of half-wave potentials provides astrategy for fine adjustment of the ligand's donor/acceptor ratio[36].

3.1.2 Introduction to Thiolates.

Thiols are homologues of alcohols with the oxygen substituted for sulfur. Regardless of the similarities, the two related classes of ligands have different applications in organometallic chemistry. In geochemistry, sulfur and oxygen's different affinities to different metals were classified in the first half of 20th century by Goldschmidt in his Classification of the Metals work[41]. Lithophiles, such as alkali, early transition and lanthanide metals form very stable compounds with

oxygen, while siderophiles (Ag, Fe, Ir etc) and chalcophiles (Zn, Ag, Cu etc) have higher affinity to sulfur. Thiolates play important role in some of biological processes. Coenzyme A, for instance, reacts with acetic acid to form a thioester and acts as an acyl carrier in biosynthesis of various phytochemicals[42]. Many iron-containing porphyrins have donor thiolate ligands in an axial position. It is thought that the thiolate ligation promotes hydrogen abstraction in the CH oxidation process of an intermediate P450 Compound I at reasonable reduction potentials [43]. Modeling studies for biological systems have shown that cytochromes P450 (type 2B4 and 2E1) lose their monooxygenase activity when the thiolate is substituted with oxygen bound ligands Hys, Tyr and Ser[44].

Thiolates have been widely used in novel materials design – molecular magnets[45], heavy metal sponges[46] and polymers[47]. The sulfur atom has been employed as a bridge for certain heterometallic clusters exhibiting strong antiferromagnetic coupling with M-M bonds[48] (**Figure 3.5 A**). A tripodal tris(mercaptomethyl)ethane ligates to $VCl_3(THF)_3$ treated with 2-aminopyridine to form a tetranuclear $[V^{III}_4O(tmme)_4]^{2+}$ species with the oxygen atom bound to all four V atoms in a rare square planar arrangement[45], which contrasts the previously described hexametalate formed under the same reaction conditions if tris(hydroxymethyl) ethane is used[49]. The tetravanadate exhibits unusually strong antiferromagnetic coupling and reversible redox properties at mild potentials - attractive characteristics for magnetic information storage and quantum information processing devices (**Figure 3.5 B**).

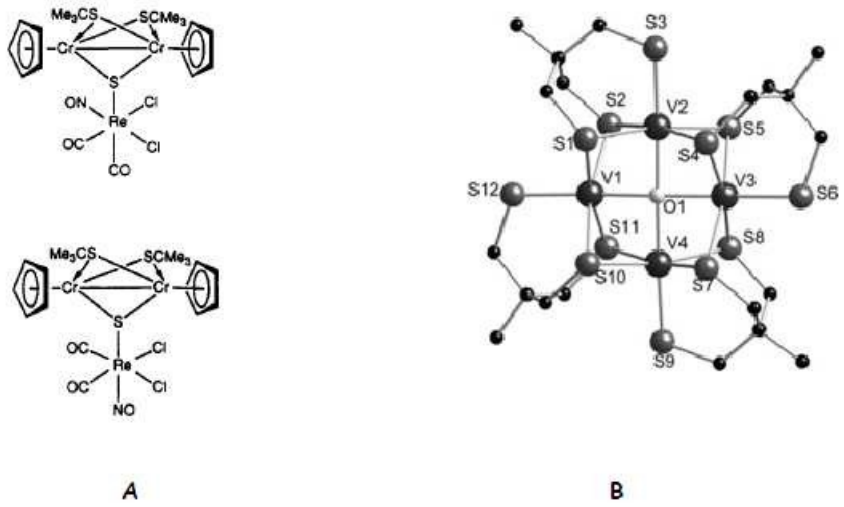

Figure 3.5 Molecular structures of multinuclear antiferromagnetic complexes featuring brinding thiolates (adapted from the original publications[48,49]).

Due to the chalcophilic nature of some of the heavy metals, such as lead, mercury and cadmium, thiolate-containing polymers make great ion absorbing sponges. Duolite G-73 is a very effective commercialized polythiol known to efficiently remove copper and mercury[46,50].

Many metal-based polymeric materials containing the thiolate moiety and cadmium[47], germanium[51] or other metals[52-54] have been synthesized for conductivity and photophysical studies. The most studied metal thiolates are Au-based due to gold's high affinity to sulfur. Thiolate ligands are often used to protect Au nanoparticles from clumping[55,56], as well as syntheses of self-organized structures based on aurophilic interactions[57,58] and metal-containing pharmaceuticals[59].

3.1.3 Introduction to self-organized monolayers.

Bare surfaces of metals and metal oxides tend to absorb organic materials to lower the free energy of the metal/metal oxide-environment interface. The concept of monolayers was first introduced in 1917 when Langmuir had realized that organic molecules on water surface form a

film that was one molecule thick[60]. Some of these adsorbates spontaneously form regular arrays that are referred to as self-assembled monolayers (SAMs)[61]. The organic moieties are connected to the surface through a junction group having a relatively high affinity to the surface. Several types of such linkers have been described – isonitriles[62], thiols[63], and siloxanes[64] among the most popular. SAMs are synthesized to be exlored in a variety of applications – from chromatography[61] to microelectronics[65]. The vast majority of monolayers assembled on gold are linked through the thiolate functionality, due to the strong gold-sulfur bond (1.7eV for methyl thiolate) and ease of preparation[66]. Thiolate monolayers are prepared by a variety of methods, including the adsorption of thiols and disulfides from gas phase or solution, and electrochemical deposition[67].

Alkyl thiolate films are arguably the most studied type of monolayers. Some of the examples of various aliphatic thiolate SAMs are shown in **Figure 3.6**. Carboxylates (**Figure 3.6A**) constitute attractive terminal SAM functionalities. Indeed, because of the gold's low affinity to oxygen, the carboxylate groups do not compete with the thiolate junctions for binding to the gold surface.

These systems' application in lithography was demonstrated by Abbot and coworkers who developed contact printing on 11-mercaprodecanoic acid layered on the Au(111) surface with Cu^{II} and Ni^{II} ions delivered by a poly(dimethylsiloxane) stamp[68]. A series of crown ether-terminated (18-crown-6, 15-crown-5 and 12-crown-4) aliphatic thiolate SAMs was synthesized and the ability of such films to sequester metal ions from solutions was investigated (**Figure 3.6B**). Electrochemical studies showed a predictable decay of responses that potentially allows employing such systems as cation sensors[69]. The guest-host interactions between the crown ethers and certain cationic guests are strong enough to provide an organizing force for monolayer formation and can be implied for planned patterns formation[70].

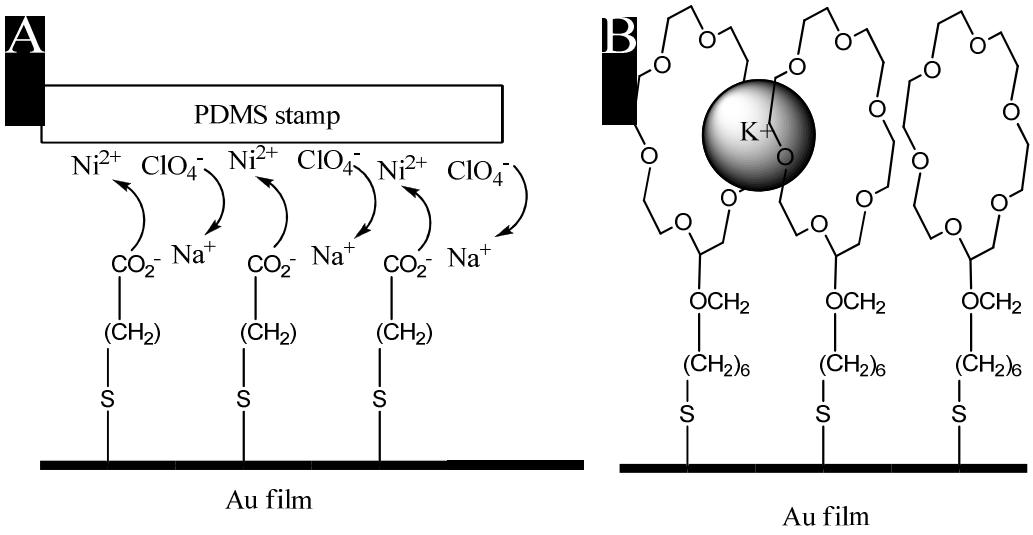

Figure 3.6 SAM applied for soft lithography (A) and cation sensor (B)[68,69,71].

Conjugated aromatic systems are attractive blocks for molecular conductor and charge transfer control applications, in part, because π-stacking interactions lead to tunable continuous patterns that define conducting behavior of the monolayer[71]. Strong π-π interactions allow functionalizing the ligand with various functional groups to adjust the properties of a system for a certain application without the loss of the pattern. An interesting example of such controlled monolayer formation is fullerene C_{60} bound to (4-mercaptophenyl)anthrylacetylene-based SAM on Au(111) surface that was synthesized to be used in electrode covering film application[72].

3.2 Work Described in Chapter Three

In this Chapter the synthesis and coordination chemistry of 2- and 6-azulenyl thiols is described. All of the thiols were synthesized in reasonable yields by SN_{Ar} reaction of 2- or 6-azulenyl halides with excess hydrosulfide nucleophile. Two of the azulenyl thiols were structurally characterized and all were shown to form air stable monolayers on Au(111) surfaces. The 2-azulenyl thiol ligand core was modified with IR-active cyano groups to permit observation of a strong surface IR signal of the azulene molecules tethered to the metal surface. Competition binding studies involving 2-isocyanoazulene and 2-azulenyl thiol suggest strongly preferential binding of the thiolate junction group to the Au surface. Air-stable dinuclear gold complexes $[Au_2(dcpm)(SAz)_2]$ (dcpm = (*bis*)dicyclohexylphosphinomethane; SAz= 2 – and 6- azulenyl thiolate units) of both 2- and 6-azulenyl thiol derivatives were synthesized and structurally characterized. Their UV/Visible absorption spectra and aurophilic interactions have been compared to those of previously known thioaryl analogues. The azulene-based complexes exhibit stronger Au-Au bonds than in previously described thiophenols and the absorption in the visible region of the UV/VIS spectrum that is assigned to LMCT is shifted towards lower energy. DFT studies of the electronic structures of both free ligands and dinuclear gold complexes were performed in line with systematic studies of ligands and their coordination chemistry. The comparison of dinuclear gold complexes with the isocyanide homologues has also revealed that the orientation of the planes of azulene ligands is not parallel.

3.3 Experimental Section

3.3.1 General procedures and starting materials. Synthetic operations that require inert atmosphere conditions were performed under an atmosphere of 99.5% argon purified by passage through columns of activated BASF catalyst and molecular sieves. Standard Schlenk

techniques were employed with a double manifold vacuum line. Solvents, including deuterated solvents, were freed of impurities by standard procedures and stored under argon.

Infrared spectra were recorded on a PerkinElmer Spectrum 100 FTIR spectrometer with samples sealed in 0.1 mm NaCl cells or between NaCl disks. NMR samples were analyzed on Bruker Avance 400 or 500 spectrometers. ^{1}H and ^{13}C NMR chemical shifts are given with reference to residual solvent resonances relative to $SiMe_4$. ^{31}P NMR chemical shifts are referenced to external 85% aqueous H_3PO_4. Melting points are uncorrected and were determined for samples in sealed capillary tubes. Elemental analyses were carried out by Chemisar Laboratories Inc. (Ontario, Canada) and Columbia Analytical Services (Tucson, Arizona). 1,3-Diethoxycarbonyl-2-chloroazulene[73], 1,3-diethoxycarbonyl-6-bromoazulene[74], 1,3-dicyano-2-aminoazulene[75], and $Au_2(dcpm)Cl_2$[76] (dcpm = bis(dicyclohexylphosphino)methane) were prepared according to published procedures. All other reagents were obtained from commercial sources and freed of oxygen and moisture if used in air- and/or water-sensitive syntheses. Davisil (200-425 mesh, type 60A) silica gel was used for chromatographic purifications.

3.3.2 Synthesis of 1,3-diethoxycarbonyl-2-mercaptoazulene (1).

1,3-Diethoxycarbonyl-2-chloroazulene (0.320 g, 1.04 mmol) and 3.00 g of 68% aqueous sodium hydrosulfide (36.4 mmol) were added to 30 mL of 70% aqueous ethanol. The resulting suspension was refluxed for 2 hours. After cooling to room temp, the mixture was stirred for an additional 10 hrs. Then the flask content was diluted with 100 mL of water and extracted with pentane (2×100 mL). Acidification of the aqueous layer with sulfuric acid afforded an orange precipitate, which was extracted with CH_2Cl_2 (2×100 mL). The combined methylene chloride extracts were dried over sodium sulfate and filtered. The filtrate was concentrated under vacuum and the residue was passed through a short silica gel column using

neat $CHCl_3$. After solvent removal and drying at 10^{-2} torr, brick-red crystalline **1** (0.208 g, 0.683 mmol) was isolated in a 66% yield. X-ray quality crystals of **1** were grown by slow diffusion of pentane into a solution of **1** in CH_2Cl_2. Anal. calcd. for $C_{16}H_{16}O_4S$: C, 63.14; H, 5.30. Found: C, 63.32; H, 4.93. IR ($CHCl_3$): ν_{CO} 1683 s, 1660 m sh cm^{-1}. ^1H NMR (400 MHz, $CDCl_3$, 25 °C): δ 1.50 (t, $^3J_{HH}$ = 8 Hz, 6H, C*H*$_3$), 4.49 (q, $^3J_{HH}$ = 8 Hz, 4H, C*H*$_2$), 7.58 (t, $^3J_{HH}$ = 10 Hz and 12 Hz, 2H, *H*^{5,7}), 7.69 (t, $^3J_{HH}$ = 12 Hz 1H, *H*^{6}), 7.71 (s, 1H, S*H*) 9.34 (dd, $^3J_{HH}$ = 10 Hz and 12Hz, 2H, *H*^{4,8}) ppm. ^{13}C NMR (100.6 MHz, $CDCl_3$, 25 °C): δ 14.5 (*C*H_3), 60.7 (*C*H_2), 113.7, 131.7, 135.5, 138.0, 143.9, 155.7 (azulenic *C*), 166.0 (*C*O_2Et) ppm.

3.3.3 Synthesis of 2-mercaptoazulene (2).

2-thio-1,3-diethoxycarbonylazulene (0. 150 g, 0.493 mmol) was heated in 25 ml of 86% H_3PO_4 at 130 ° C for 2 hours. Then the reaction mixture was cooled, diluted with 200 mL of water and extracted twice with 30 mL of benzene. The combined organic extracts were dried over sodium sulfate and then passed through a column with silica gel (using benzene as eluent). From the blue band 0.060 g (0.374 mmol, 76%) of purple crystals were collected that were found to be 2-thioazulene. Anal. calcd. for $C_{10}H_8S$: C, 74.96; H, 5.03. Found: C, 74.40; H, 4.43. IR ($CHCl_3$): ν_{SH} 2579 w cm^{-1}. ^1H NMR (400 MHz, $CDCl_3$, 25 °C): δ 3.88 (s, 1H, S*H*), 7.12 (s, 2H, *H*^{1,3}), 7.14 (dd, $^3J_{HH}$ = 12 Hz and 10 Hz, 2H, *H*^{5,7}), 7.44 (t, ^3J = 10 Hz, 1H, *H*^{6}), 8.04 (d, ^3J = 12 Hz, , 2H, *H*^{4,8}) ppm. ^{13}C NMR (100.6 MHz, $CDCl_3$, 25 °C): δ 116.6, 124.5, 133.0, 135.0, 135.4, 140.8 (azulenic *C*) ppm.

3.3.4 Synthesis of 1,3-diethoxycarbonyl-6-mercaptoazulene (3).

Magenta-colored 1,3-diethoxycarbonyl-6-bromoazulene (0.500 g, 1.424 mmol) and 16.0 g of 68% aqueous sodium hydrosulfide (285 mmol) were added to 240 mL of 70% aqueous

ethanol. The resulting suspension was refluxed for 20 minutes. After cooling to room temp., the reaction mixture was diluted with 250 mL of water. The resulting solution was acidified with aqueous sulfuric acid to afford a pink precipitate, which was extracted with methylene chloride (2×100 mL). The red methylene chloride extracts were combined, dried over sodium sulfate, and filtered. The solvent was removed under vacuum and the residue was recrystallized from benzene to provide blood red, crystalline **3** (0.302 g, 0.992 mmol) in a 71% yield. Anal. calcd. for $C_{16}H_{16}O_4S$: C, 63.14; H, 5.30. Found: C, 62.96; H, 5.03. IR ($CHCl_3$): ν_{CO} 1692 s, ν_{SH} 2587 w cm^{-1}. ^1H NMR (400 MHz, $CDCl_3$, 25 °C): δ 1.44 (t, $^3J_{HH}$ = 6 Hz, 6H, C*H*$_3$), 4.23 (s, 1H, S*H*), 4.41 (q, $^3J_{HH}$ = 6 Hz, 4H, C*H*$_2$), 7.60 (d, $^3J_{HH}$ = 12 Hz, 2H, $H^{5,7}$), 8.66 (s, 1H, H^2), 9.46 (d, $^3J_{HH}$ = 12 Hz, 2H, $H^{4,8}$) ppm. ^{13}C NMR (100.6 MHz, $CDCl_3$, 25 °C): δ 14.6 (*C*H$_3$), 60.1 (*C*H$_2$), 117.2, 128.9, 137.3, 141.4, 141.7, 152.3 (azulenic *C*), 165.0 (*C*O$_2$Et) ppm.

3.3.5 Synthesis of 1,3-dicyano-2-chloroazulene (4).

A solution/slurry of 1,3-dicyano-2-aminoazulene (0.200 g, 1.04 mmol) in 250 mL of toluene was saturated with dry hydrogen chloride. To this mixture, 0.15 mL of isoamylnitrite (1.1 mmol) was added and the resulting reaction mixture was stirred for 48 hours at room temp. The contents of the reaction flask were filtered and the filter-cake was washed with CH_2Cl_2 until the washings were colorless. The organic fractions were combined, washed with water, brine, and then dried over Na_2SO_4. The mixture was concentrated on a rotary evaporator and the oily residue was subject to column chromatography on silica with neat CH_2Cl_2. The first eluted band provided 0.081 g (0.381 mmol) of red microcrystalline **4** in a 37% yield after solvent removal. M.P. 316 – 318 °C (lit. "over 300 °C"[77]). IR (THF): ν_{CN} 2223 m cm^{-1}. ^1H NMR (500 MHz, DMF-d^7, 25 °C): δ 8.28 (t, $^3J_{HH}$ = 10 Hz, 2H, $H^{5,7}$), 8.53 (t, $^3J_{HH}$ = 10 Hz, 1H, H^6), 8.93 (d, $^3J_{HH}$ =10 Hz 2H, $H^{4,8}$) ppm. ^{13}C NMR (126 MHz, DMF-d^7, 25 °C): δ 97.5, 113.9, 134.7, 139.7, 143.4,

144.0, 145.0 ppm.

3.3.6 Synthesis of 1,3-dicyano-2-mercaptoazulene (5).

To a solution/slurry of 1,3-dicyano-2-chloro-azulene (0.100 g, 0.470 mmol) in 100 mL of ethanol, 6.0 g of 68% aqueous sodium hydrosulfide (73 mmol) in 20 mL of water was added and the reaction was refluxed for 45 min. The mixture was then diluted with 300 mL of H_2O and extracted Et_2O (2×100 mL). The aqueous fraction was acidified with concentrated sulfuric acid until a pink precipitate was formed. The resulting mixture was extracted with CH_2Cl_2 (3×100 mL) and the combined organic extracts were dried over Na_2SO_4. The solvent was then removed under vacuum to afford 0.076 g (0.257 mmol) of pink **5**·CH_2Cl_2 (55%). Anal. calcd. for $C_{13}H_8Cl_2N_2S$: C, 52.89; H, 2.73; N, 9.49. Found: C, 53.07; H, 2.68; N, 9.26. IR (nujol): ν_{CN} 2212 cm^{-1}, ν_{SH} 2559 cm^{-1}. ^1H NMR (500 MHz, C_5D_5N, 25 °C): δ 7.01 (t, $^3J_{HH}$ = 10 Hz, 1H, H^6), 7.13 (t, J = 10 Hz, 2H, $H^{5,7}$), 7.84 (d, J = 10 Hz, 2H, $H^{4,8}$) ppm. ^{13}C NMR (126.0 MHz, C_5D_5N , 25 °C): δ 104.14, 119.8, 125.3, 130.6, 131.5, 148.6 ppm.

3.3.7 Synthesis of [Au_2(dcpm)(1,3-diethoxycarbonyl-2-mercaptoazulene)$_2$]·CH_2Cl_2 (6).

Under argon atmosphere, triethylamine (0.50 mL, 3.6 mmol) was added to a solution of Au_2(dcpm)Cl_2 (0. 144 g, 0.165 mmol) and **1** (0.100 g, 0.329 mmol) in 20 mL. The reaction mixture was stirred at room temp. for a period of 72 hrs, during which formation of a white precipitate was observed. Then, the mixture was filtered through Celite. The Celite filtercake was washed with THF until the washings were colorless. All solvent was removed from the filtrate under vacuum to give a red oil. The oil was dissolved in 5 mL of CH_2Cl_2 and the resulting solution was carefully layered with 15 mL of pentane. After pentane diffusion, deep

red crystals formed. These were filtered off, washed with pentane, and dried at 10^{-2} torr to yield **6**·CH_2Cl_2 (0.160 g, 0.107 mmol) in a 65% yield.

Anal. calcd. for $C_{58}H_{78}Au_2Cl_2O_8P_2S_2$: C, 46.62; H, 5.26. Found: C, 46.50; H, 5.38. IR ($CHCl_3$): ν_{CO} = 1684 cm^{-1}. ^1H NMR (500 MHz, $CDCl_3$, 25 °C): δ 1.10 – 2. 20 (m, 44H, C_6H_{11}), 1.47 (t, $^3J_{HH}$ = 7 Hz, 12 H, CH_2CH_3), 4.46 (q, $^3J_{HH}$ = 7 Hz, 8H, CH_2CH_3), 5.30 (s, 2H, CH_2Cl_2 of crystallization), 7.38 (t, $^3J_{HH}$ = 10 Hz, 4H, $H^{5,7}$), 7.46 (t, $^3J_{HH}$ = 10 Hz, 2H, H^6), 8.74 (d, $^3J_{HH}$ = 10 Hz, 4H, $H^{4,8}$) ppm. ^{31}P NMR (162 MHz, $CDCl_3$, 25 °C) 43.6 ppm. ^{13}C NMR (126 MHz, $CDCl_3$, 25 C): δ 14.7 (CH_2CH_3), δ 25.6, 26.4, 26.6, 28.9, 29.9, 35.5 (t, $^1J_{PC}$ = 15.1 Hz, PCH_2P), 53.5 (CH_2Cl_2 of crystallization) 60.29 (CH_2CH_3), 122.0, 128.9, 132.3, 135.3, 141.7, 161.0 (azulenic *C*), 167.0 (CO_2Et) ppm.

3.3.8 Synthesis of [Au_2(dcpm)(1,3-diethoxycarbonyl-6-mercaptoazulene)$_2$] (7).

Under argon atmosphere, a slurry of potassium *tert*-butoxide (13 mg, 0.116 mmol) in 15 mL THF was added to a solution of $Au_2(dcpm)Cl_2$ (0.050 g, 0.057 mmol) and **3** (0.035 g, 0.115 mmol) in 20 mL of THF at room temp. with stirring. Gradual formation of a white precipitate was observed. After 24 hrs of stirring, the reaction mixture was filtered through Celite. The filtercake was washed with additional THF until the washings were colorless and the solvent was removed from the filtrate on a rotary evaporator. The oily residue was redissolved in CH_2Cl_2/Et_2O (2.5 mL/2.5 mL) and the resulting orange solution was allowed to crystallize at -18 °C for 15 hrs. The orange crystals formed were filtered off and dried at 10^{-2} torr to yield 0.056 g (0.040 mmol) of **7** in a 70% yield. Anal. calcd. for $C_{57}H_{76}Au_2O_8P_2S_2$: C, 48.58; H, 5.44. Found: C, 48.59; H, 5.04. IR ($CHCl_3$): ν_{CO} = 1675 cm^{-1}. ^1H NMR (500 MHz, $CDCl_3$, 25 °C): δ0.95–2.38 (m, 58H), δ 4.35 (q, 7.1 Hz, 8H), δ 8.05 (d, 10.6Hz, 4H), δ 8.41 (s, 2H), 9.05 (d, *J* = 10.7 Hz ,4H). ^{31}P NMR (162 MHz, $CDCl_3$, 25 °C) δ 50.99 ppm. ^{13}C NMR (126.0 MHz, $CDCl_3$,

25 °C): δ 14.6, δ 25.6, δ 26.5, δ 29.3, δ 30.2, δ 35.5, δ 59.6, δ 115.6, δ 134.7, δ 135.0, δ 139.0, δ 140.8, δ 165.4 ppm.

3.3.9 Synthesis of 2,2'-dimercapto-1,1',3,3'-tetraethoxycarbonyl -6,6'-biazulene.

Gaseous HCl was bubbled through a suspension of 2,2'-diamino-1,1',3,3'-tetraethoxycarbonyl -6,6'-biazulene (0.1 g, 0.174 mmol) in 25 mL of dry benzene for 4 hours, then 0.1 mL (0.58 mmol) of isoamylonitrite was added. The reaction was stirred overnight and then washed with water. The organic layer was stripped of the solvent on a rotary evaporator. The resulting dark oil was suspended in 75% ethanol and 2.0g of sodium hydrosulfide (68% hydrate, 24.3 mmol) were added. The resulting mixture was refluxed for 2 hours. The mixture was then diluted with 300 mL of H_2O and extracted with EtOAc (2×25 mL). The aqueous fraction was acidified with concentrated sulfuric acid until a precipitate formed. The resulting mixture was extracted with CH_2Cl_2 (3×30 mL) and the combined organic extracts were dried over Na_2SO_4. The solvent was then removed under vacuum to afford 0.014 g (0.023 mmol) of brown 2,2'-dimercapto-1,1',3,3'-tetraethoxycarbonyl -6,6'-biazulene (13%). MS (ES-, m/z) calc. for $C_{32}H_{29}O_8S_2$: 605.14; found: 605.12. ^{1}H NMR (400 MHz, $CDCl_3$, 25 °C): δ 1.54 (t, $^3J_{HH}$ = 7.1 Hz, 3H, *CH_3*), δ 4.56 (q, $^3J_{HH}$ = 7.1 Hz, 2H, *CH_2*), 7.79 (s, 1H, SH), 7.92 (d, J = 11.3 Hz, 2H, *$H^{5,7}$*), 9.54 (d, J = 11.3 Hz, 2H, *$H^{4,8}$*) ppm. ^{13}C NMR (101.0 MHz, $CDCl_3$, 25 °C): δ 14.77, 61.07, 114.68, 132.58, 134.74, 143.07, 152.83, 166.02 ppm.

3.3.10 X-ray structure determination for 1, 3, 6 and 7.

X-ray quality crystals of **1, 6** and **7** were grown by layering pentane over nearly saturated solutions of these compounds in CH_2Cl_2 at room temp. and then cooling the samples to +4 °C for several days. Single crystals of **3** suitable for X-ray analysis formed upon cooling a hot (*ca* 70

°C) saturated solution of **3** in benzene to room temp. All manipulations with the crystals prior to transfer to the goniometer were performed in air. Intensity data for all samples were collected using a Bruker SMART APEX CCD Single Crystal Diffraction System[78] employing graphite-monochromated Mo Kα radiation (λ = 0.71073 Å). Lattice constants were determined with the Bruker SAINT software package[78]. The data were corrected empirically for variable absorption effects using equivalent reflections. All structures were solved by direct methods and refined by full-matrix least-squares methods on F^2 with the SHELXTL Version 6.10 software package.[79]

The final structural models incorporated anisotropic thermal parameters for all nonhydrogen atoms and isotropic thermal parameters for all hydrogen atoms. The asymmetric unit of **3** contains two crystallographically-independent $C_{16}H_{16}O_4S$ molecules. For **6**, the 13 highest residual peaks (2.03 – 1.02 e $Å^{-3}$) in the final difference map were within 0.91 Å of a gold atom. Crystal data, data collection, solution, and refinement information for **1**, **3**,·and **6**·are summarized in **Table 3.1**. Full details of the crystallographic work are available in the Supporting Information.

Table 3.1. Crystal data, data collection and refinement information for **1**, **3**, **6** and **7**.

	1	**3**	**6**	**7**
Empirical formula	$C_{16}H_{16}O_4S$	$C_{16}H_{16}O_4S$	$C_{57}H_{76}Au_2O_8P_2S_2$	$C_{58}H_{77}Au_2Cl_3O_8P_2S_2$
Formula weight	304.35	304.35	1409.17	1528.53
Temperature (K)	100(2)	100(2)	100(2)	100(2)

Crystal system	triclinic	triclinic	monoclinic	Monoclinic
Space group	P1bar	P1bar	Cc	$P2_1/n$
a (Å)	6.782(1)	10.845(1)	16.438(2)	20.466(1)
b (Å)	9.952(1)	12.173(2)	24.216(2)	13.336(1)
c (Å)	11.066(2)	12.236(2)	14.768(1)	22.832(2)
α (deg)	100.453(3)	109.364(2)	90	90
β (deg)	94.859(3)	106.530(3)	109.588(1)	95.939(2)
γ (deg)	103.049(3)	98.626(2)	90	90
V ($Å^3$)	709.3(2)	1406.8(3)	5538.2(9)	6198.3(7)
Z'	2	4	4	4
D_{calc} (Mg m^{-3})	1.425	1.437	1.690	1.679
Absorption coefficient (mm^{-1})	0.241	0.243	5.478	5.029
F(000)	320	640	2808	3116
Crystal size (mm)	0.40×0.15×0.11	0.17×0.17×0.10	0.28×0.16×0.08	0.24×0.08×0.03
Crystal color	Orange	Red-orange	Red	Orange
θ Range for data collection (º)	2.5–5-30.52	2.76–26.00	2.23–29.16	2.49-21.5

Reflections collected	8429	12191	25563	33430
Reflections unique	4130	5491	13284	7101
R_{int} [a]	0.050	0.039	0.045	0.105
Absorption correction	Multi-can	Multi-scan	Multi-scan	Multi-scan
Max. and min. transmission	1.000 and 0.632	1.000 and 0.912	1.000 and 0.681	1.000 and 0.744
Refinement method	Full-matrix lest-squares on F^2			
Data/restraints/parameters	4139/0/251	5491/0/391	13284/2/644	7101/96/668
Goodness-of-fit on F^2	1.059	0.960	1.000	1.141
Final R indices $[I > 2\sigma(I)]$ [b,c]	R_1 = 0.056	R_1 = 0.052	0.032	0.086
	wR_2 = 0.136	wR_2 = 0.124	0.065	wR_2 = 0.183
R indices (all data) [b,c]	R_1 = 0.067	R_1 = 0.081	0.036	R_1 = 0.110
	wR_2 = 0.143	wR_2 = 0.135	0.066	wR_2 = 0.191
Absolute structure parameter	*n/a*	*n/a*	-0.012(4)	n/a
Largest diff. peak and hole ($e \cdot Å^{-3}$)	0.68 and -0.48	0.66 and -0.31	2.03 and -0.87	2.71 and -2.33

[a] $R_{int} = \sum|F_o^2 - \langle F_o^2 \rangle| / \sum|F_o^2|$. [b] $R1 = \sum||F_o| - |F_c|| / \sum|F_o|$. [c] $wR2 = [\sum(w(F_o^2 - F_c^2)^2) / \sum(w(F_o^2)^2)]^{1/2}$.

3.3.11 Surface studies.

Monolayer deposition and characterization were performed by at the University of Kansas by Brad M. Neal.

3.3.11a Self-assembled monolayer films of 1, 2, 3, and 5 on the Au(111) surface.

Gold-coated mica substrates were purchased from Agilent and Platypus Technology. The substrates were soaked in dichloromethane, acetone, and methanol for 2 hrs in each solvent, then rinsed thoroughly with hot methanol and dried under a stream of nitrogen immediately before use. Monolayer films of **1**, **2**, and **3** were formed by immersing the freshly cleaned metal substrate (gold on mica) into a *ca.* 2 mM solution of the corresponding mercaptoazulene in CH_2Cl_2., monolayer films of **5** were obtained by immersing the gold substrate into a *ca.* 2 mM solution of **5** in THF for 24 hrs. The gold samples were then rinsed with methanol and CH_2Cl_2, sonicated in methanol for 2 min., rinsed with methanol again, and dried in a flow of inert gas. No precautions to exclude air or ambient laboratory lighting were taken.

3.3.11b. Optical ellipsometry.

The film thicknesses were determined using an Auto EL III ellipsometer (Rudolph Research). All measurements were made with a HeNe laser at a wavelength of 632 nm and an incident angle of 70° to the surface normal. The optical constants for the gold films were determined for each sample individually from the measurements on the freshly cleaned bare gold sample. These optical constants were used in the determination of the thickness of the adsorbed organic layers. A refractive index of 1.45 was assumed[80] for all organic thin films described herein. A minimum of five different spots on each sample were used to take ellipsometric measurements. The reported thickness constitutes an average of the measurements over each of

those spots along with the standard deviation of the measurement given in parentheses.

3.3.11c Surface IR measurements.

The grazing incidence reflection absorption Fourier Transform Infrared Spectroscopy data for the monolayers of **5** on gold were obtained on a nitrogen-purged Thermo Nicolet 670 FTIR spectrometer with a VeeMax grazing angle accessory set at an angle of 70°. Before each experiment, a background spectrum was collected using a freshly cleaned bare gold substrate was used to collect before each experiment. Ten thousand scans from 600 to 4000 cm^{-1} at 4 cm^{-1} resolution were collected for each background/sample pair.

3.3.12 Computational work

All computational work was performed by A. D. Spaeth at the University of Kansas. The crystal structure coordinates of **1**, **3**, **6** and **7** served as a starting point for DFT energy minimizations. Energies of frontier orbitals of **1**, **3**, **6**, and **7** and their graphical representations were calculated with DFT theory using Orca 2.7.0 program (ZORA approximation was employed to account for relativistic effects associated with Au)[81]. Computations for **1** and **3** were performed using Becke's three parameter hybrid exchange functional with the LYP correlation functional. Computations for **6** and **7** were performed using Becke's three parameter hybrid exchange functional with the P86 correlation functional. ZORA approximation was used to account for large relativistic effects present for Au atoms. The TZVP valence split set was applied in all cases. UV/VIS transition energies were predicted with time-dependent DFT within the Tamm-Dancoff approximation. B3LYP functional and TZVP basis set have been used for these calculations.

3.4 Results and discussion.

3.4 Results and discussion.

3.4.1 Synthesis and characterization of 2- and 6-azulenyl thiols.

2-chloro-1,3-diethoxycarbonyl azulene and 6-bromo-1,3-diethoxycarbonyl were prepared by previously described procedures[73,74]. 2-chloro-1,3-dicyanoazulene (**4**) was synthesized from 2-amino-1,3-dicyanoazulene by diazotation in toluene saturated with hydrochloric acid. The mediocre yield of **2** is due to poor solubility of both parent compound and the product. Azulenyl thiols **1**,**3** and **5** were synthesized from corresponding azulenyl halides by direct nucleophilic substitution with >100 fold excess of sodium hydrosulfide(**Scheme 3.1**).

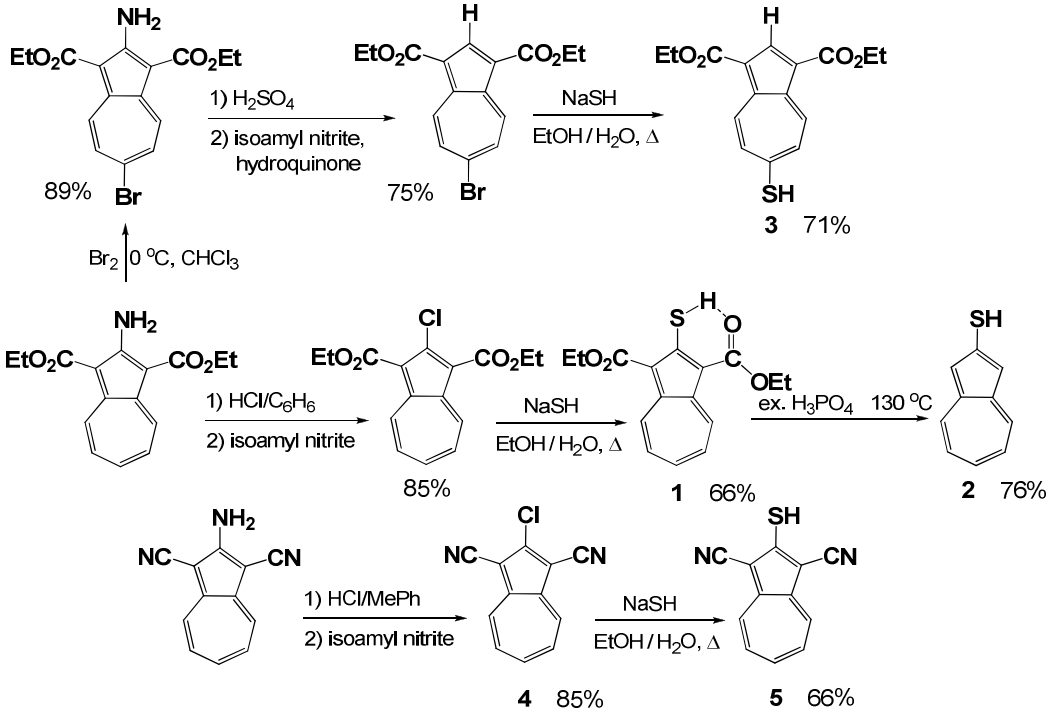

Scheme 3.1 Synthesis of azulenyl thiols

Thiols **1**, **2** and **3** were found robust enough to be stored in air. However, thiol **5** was found to slowly decompose at room temperature in air and, therefore, was stored at -18 °C. All of

the synthesized azulenyl thiols were soluble in basic aqueous solutions and precipitated upon acidification with mineral acids. They are reasonably soluble in organic solvents, except for 2-mercapto-1,3-dicyanoazulene that was found only slightly soluble in THF and DMF, but very soluble in amines or basic aqueous solutions.

Compounds **1** and **3** exhibit differences in thiolic acidities that can be observed by IR and ^{1}H NMR. The thiolic proton in **1** has a chemical shift of 7.71 ppm and a very broad IR signal centered around 2600 cm^{-1}, while the thiolic proton in **3** has a chemical shift of 4.23 ppm and a weak IR absorption peak at 2587 cm^{-1}, which is characteristic for aromatic thiols. This difference is due to hydrogen bonding of the thiolic proton and the carbonyl groups in *1* and *3* positions of the azulene; this hypothesis is also supported with XRD data that indicates that orientation of carbonyl groups in these molecules is opposite with carbonyls oriented towards *4* and *8* hydrogens of the azulenic ring in **3** (**Figure 3.7**) .

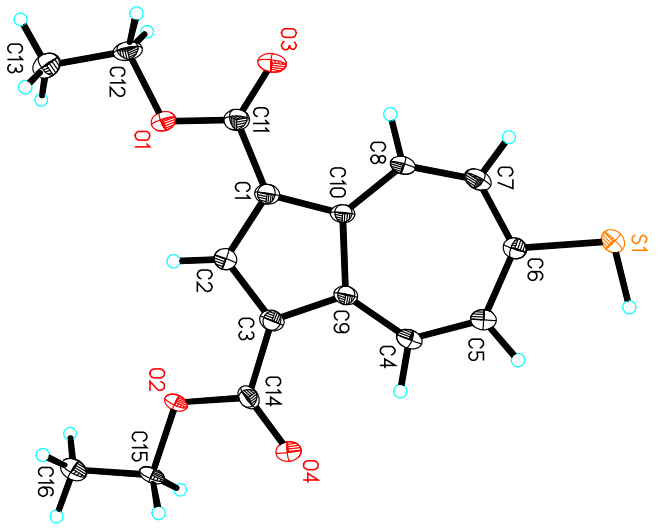

Figure 3.7 Molecular structure of **3**, 50% thermal ellipsoids

Carbonyl groups in **1** are oriented towards the thiol group (**Figure 3.8**). The different orientations of the carbonylethoxy groups was previously observed in case of diethyl 2-formamidoazulene dicarboxylate and its isocyanide derivative; it is thought to indicate hydrogen bonding between carboethoxy groups in positions *1* and *3* and acidic protons of a formamido group at *2* position of the azulene[40]. **1** was found to have a C-S-H bond angle of 109.5° and H-S bond distance of 1.2 Å with a H-O distance of 2.24 Å.

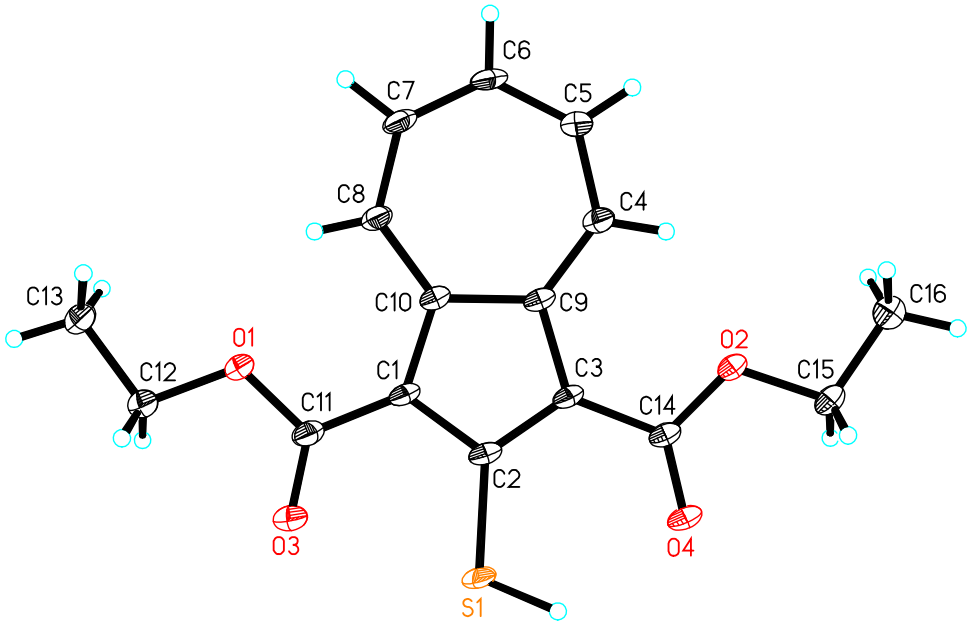

Figure 3.8 Molecular structure of **1**, 50% thermal ellipsoids

2-Azulenyl thiol (**2**) was synthesized by decarboxylation of **1** in 85% orthophosphoric acid with good yield. In the absence of carbonyls in ortho- positions, the chemical shift of the SH group has migrated to the expected 3.88 ppm (compared to 7.71 ppm in **1**) and the S-H stretching has become visible at 2579 cm^{-1} due to absence of hydrogen bonding.

Due to difficulties in characterization of monolayers on metal surfaces an IR active functional group should be introduced to the core ligand (this will be discussed in detail in **Section 3.4.4b** on this Chapter). To ease the characterization of monolayers, **5** was synthesized from 1,3-dicyano-2-chloroazulene (**4**). The resulting thiols are crystalline and have very little or no smell that makes it more pleasant to work with them.

3.4.2 Synthesis and characterization of $[Au_2(dcpm)(SAz)_2]$ 6 and 7

Thioazulenes **1** and **3** have reacted with $[Au_2(dcpm)]Cl_2$ in presence of base to form dinuclear gold complexes **6** and **7** in good yields (**Scheme 3.2**). These complexes are highly soluble in polar solvents and insoluble in hydrocarbons.

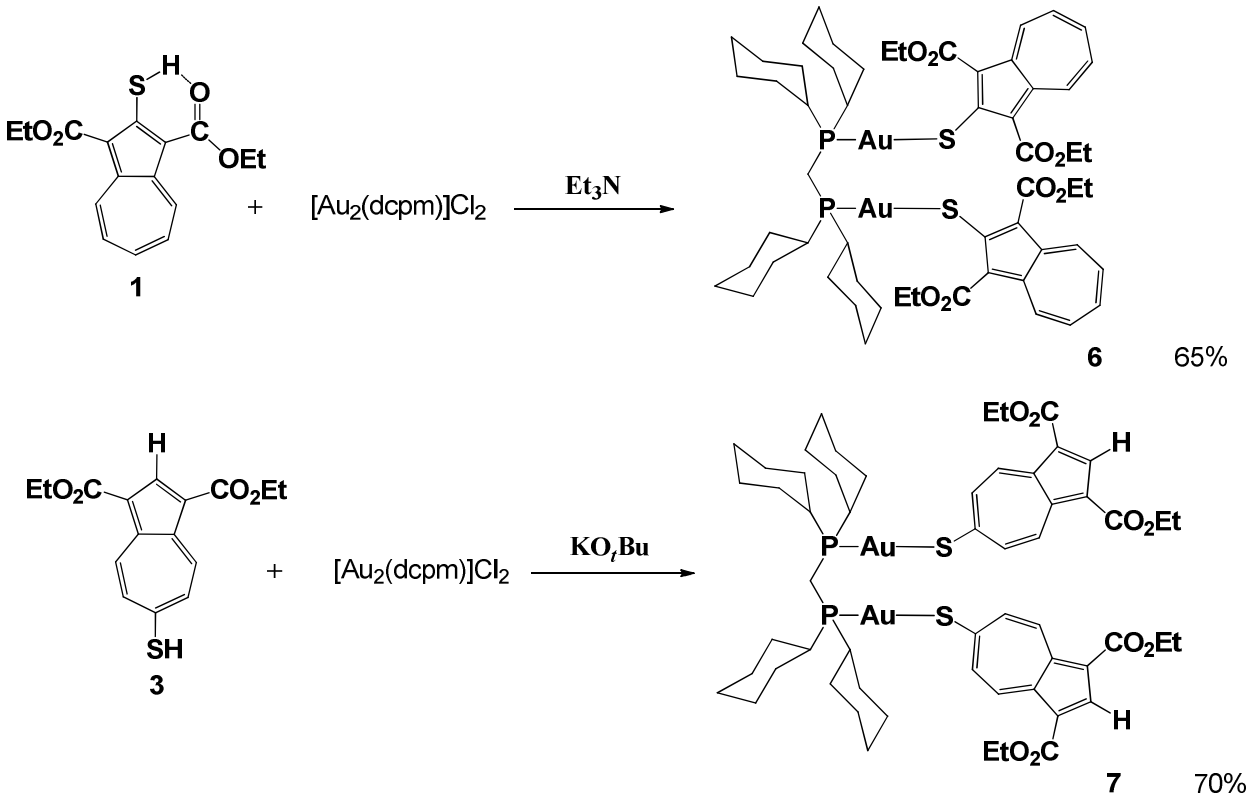

Scheme 3.2 Synthesis of **6** and **7**.

Diffusion of hexanes in chloroformic solutions of **6** and **7** produced XRD quality crystals. Unlike previously described analogous 2-isocyanoazulene $[Au_2(dcpm)]$ complexes where the

azulenes are stacked upon each other, the planes of azulene ligands are not parallel in either case (**Figure 3.9**).

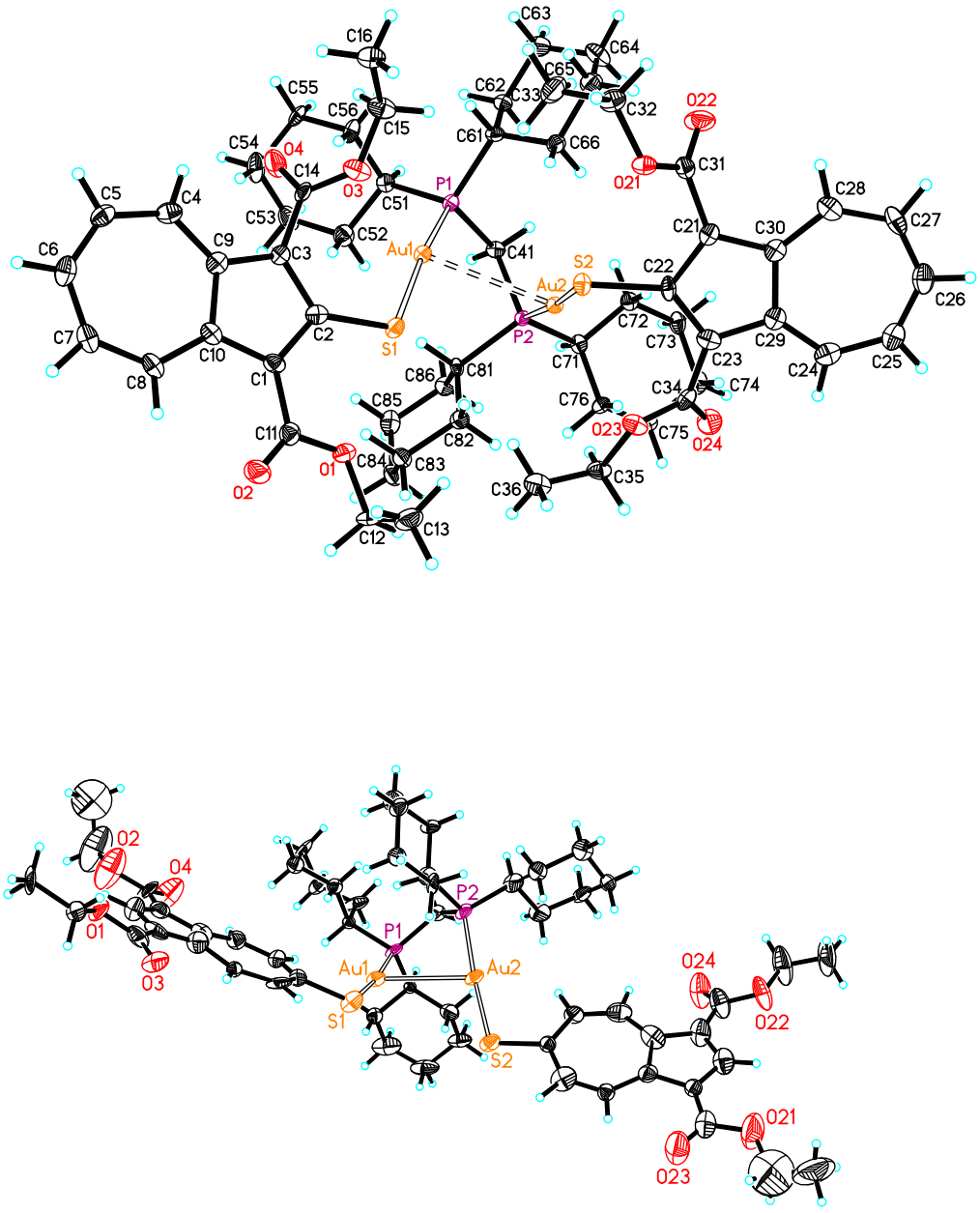

Figure 3.9 Molecular structures of **6** (top) and **7** (bottom), 50% ellipsoids

Interestingly enough, the orientation of the ester substituents in complex **6** changed from

the parent ligand: the carbonyl oxygen in this compound is rotated towards the 7-membered ring. The Au-S-C angles are 106.2°, 106.7° for **7** and 111.9°, 103.7° for **6**.

The aurophilic interactions remain strong with Au-Au bond distances of 3.036 Å and 3.084 Å for **6** and **7** respectively. Such interactions in aromatic thiolate complexes are thought to be the cause of the luminescent properties of polynuclear gold(I) complexes that some assign to ligand to metal-metal bond charge transfer[82]. Compared to the previously described complexes [Au2(dcpm)(SAr)], where SAr = 4'-mercaptobenzo-15-crown-5-benzene[83] (S-B15C5) or 4-nitrothiophenol[84] (4-$SC_6H_4NO_2$), and [Au2(dppm)(2-$SC_6H_4NH_2$)][85], where dppm = diphenylphosphinomethane, with the Au-Au distances of 3.284, 5.387 and 3.134 Å, respectively, compounds **6** and **7** clearly feature relatively strong Au-Au interactions.

3.4.3 UV/VIS studies of 1, 3, 6 and 7.

Previous studies of free aromatic thiols and their multinuclear Au(I) complexes have shown the potential for application of the polymetallic Au compounds in electronic devices due to their luminescent properties[86]. The UV/VIS spectroscopic studies of **1** and **3,** and the comparison of those to corresponding dinuclear gold complexes were performed in order to evaluate the electron transition energies. The UV/VIS spectra of **1** ($3.5*10^{-5}$M) and **6** (10^{-5}M) in CH_2Cl_2 are shown in **Figure 3.10**.

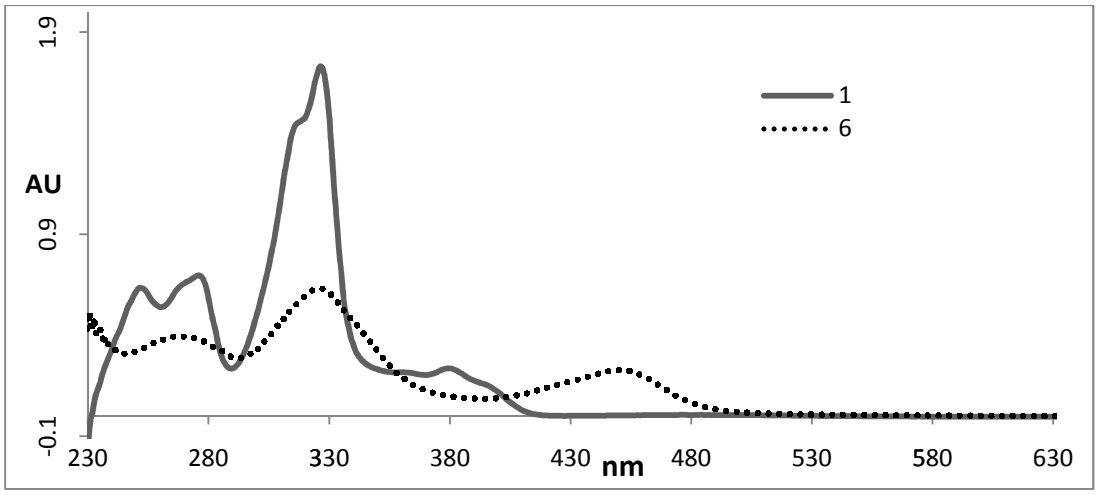

Figure 3.10 UV/VIS spectra of **1** and **6** in CH_2Cl_2.

The spectrum of the dinuclear gold complex **6** features the π(S)-π*(Az) transition at 450 nm. Related dinuclear gold(I) complexes with nitrothiophenols that possess no aurophilic interactions exhibit the same feature[84]. **Figure 3.11** shows the spectra of **3** ($3.45*10^{-5}$M) and **7** ($1.43*10^{-5}$M), where this transition is significantly stronger.

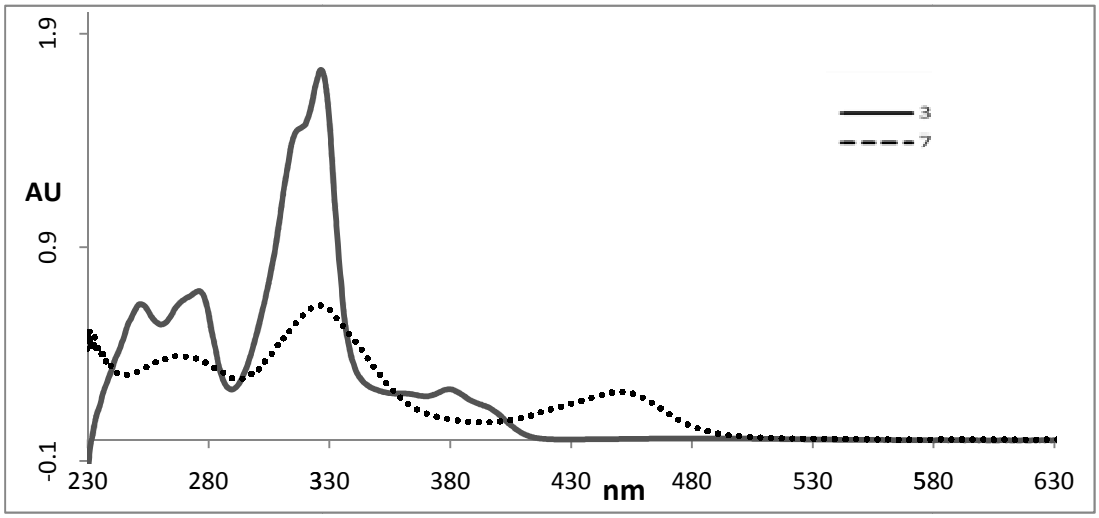

Figure 3.11 UV/VIS spectra of **3** and **7** in CH_2Cl_2.

The peak frequencies and ε values are summarized in **Table 3.2.** It is interesting to mention that the HOMO-LUMO transitions energies in both **6** and **7** are shifted towards the

visible region of the spectrum similar to some of the other aromatic [Au_2dcpm] thiolates[84,85], thus overlapping with the “blue valley” of the azulene.

Table 3.2 Maximum absorbance (nm) and molar extinction coefficients ($M^{-1}cm^{-1}$) of **6** (0.101 mmol/L) and **7** (0.143 mmol/L).

Compound	λ (ε)	λ (ε)	λ (ε)	λ (ε)
6	450.4 (22531)	325.7 (62537)	-	269.8 (38825)
7	426.0 (53856)	294.9 (27823)	266.9 (54393)	233.9 (56300)

As mentioned above, the LMMCT in dinuclear Au complexes is thought by some to be partially responsible for the photophosphorescent properties[82,87]. Previously synthesized complexes [Au_2(dcpm)(S-B15C5)] and [Au_2(dppm)(2-$SC_6H_4NH_2$) HOMO-LUMO transitions are higher in energy – 324nm and 308nm[84,85] respectively. If this absorption band in the visible region of the spectrum is indeed due to π(S)-π*(Az) transition, then the data aligns with the previously published work of Liu e*t. al*[84] who have assigned these transitions to be intraligand sulphur to π* strasitions in similar Au(I) thiophenolates. The DFT studies of **1**, **3**, **6** and **7** that were performed in order to assign the transitions and the energies of frontier orbitals of free and complexed ligand were calculated, support this hypothesis. (**Table 3.3**).

Table 3.3 Frontier orbital energies of **1**, **3**, **6** and **7**

Orbital	**3**	**1**	**6**	**7**
LUMO+1, eV	-2.1507	-2.1956	-2.4643	-2.4345
LUMO, eV	-2.4828	-2.5263	-2.6617	-2.7350
HOMO, eV	-6.1771	-6.1432	-4.5687	-4.8523
HOMO-1, eV	-6.2396	-6.4700	-4.5924	-4.8948

The HOMO-LUMO gap in gold complexes **6** and **7** is significantly lower than in the free ligands that is in good agreement with the intense absorption in the “blue valley” region. HOMO and LUMO orbitals of **1** and **6**, **3** and **7** are provided on Figure **3.12** and Figure **3.13** respectively. As seen on these diagrams, HOMOs of both complexex have thiolate character, thus destabilization of the HOMO seen in Au complexes **6** and **7** with respect to free ligands is likely due to interaction of sulfur’s lone pair and filled *d* orbitals of metal centers.

In both cases the junction between the aromatic π-systems and the metal centers participates in HOMO and LUMO, making these systems attractive for further investigation in the area of molecular wires and electron transport.

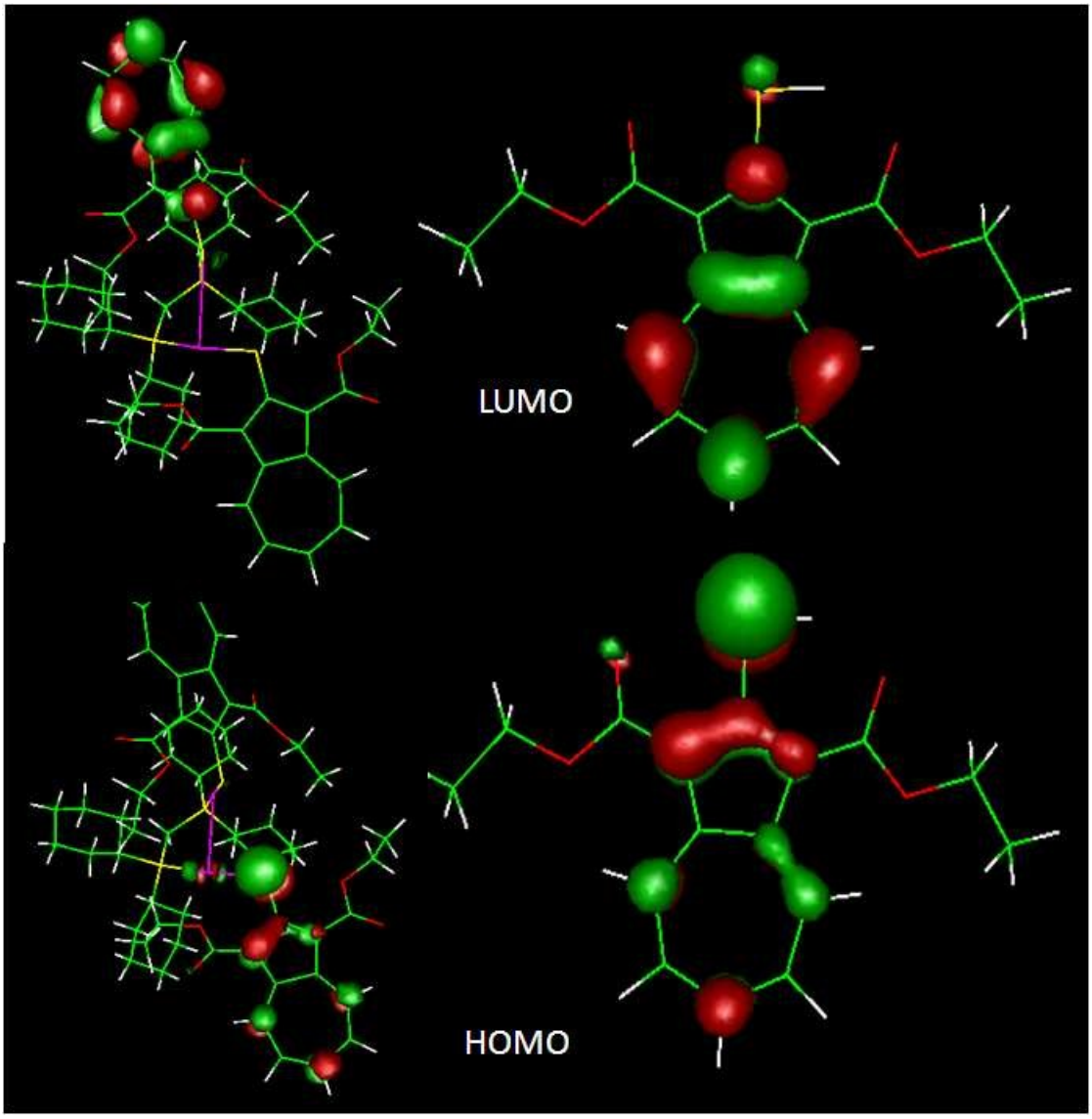

Figure 3.12 HOMO and LUMO diagram of **6** (left) and **1** (right)

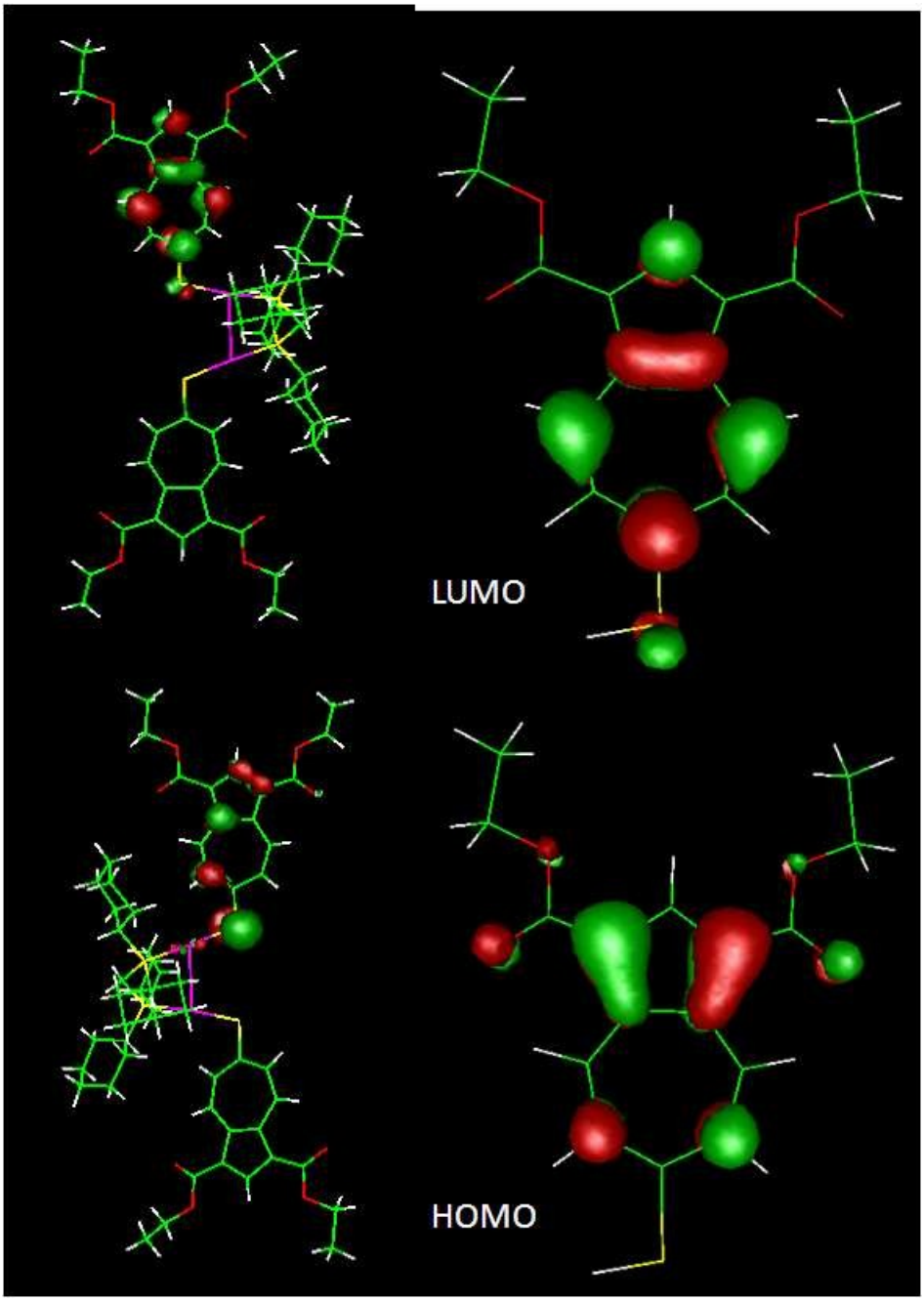

Figure 3.13 HOMO and LUMO diagram of **7** (left) and **3** (right)

3.4.4 Self assembled monolayers of 1, 2, 3 and 5 on Au(111)

3.4.4.a Synthesis of SAMs

The thiols **1**, **2**, **3** and **5** described above were readily absorbed by Au surfaces. All of the

monolayers were formed by soaking the gold films on mica in solutions of azulenes for 24 hours. Formed monolayers remained stable in air and have shown consistent thicknesses that are summarized in **Table 3.4**. While the ellipsometric studies were supportive of the monolayer formation, a ligand with an IR active functional group was needed to provide more certain data, thus **5** was synthesized and a free CN group was observed in the surface IR spectrum at 2216 cm^{-1}.

Table 3.4 Observed and calculated thicknesses of azulenyl thiol monolayers (Å).

	1	**2**	**3**	**5**
D_{obs} (Å)	10.9 ± 0.6	12.3 ± 2.0	11.7 ± 1.9	12.8 ± 1.9
D_{calc} (Å)	10.6	10.6	10.6	13.

3.4.4.b Monolayer displacement experiments.

Isocyanide based monolayers are one of the systems that are actively studied due to lower conduction barrier, although some of them are sensitive to air and undergo rapid Au promoted oxidation to form isocyanates[88]. Prior to this work, Barybin *et. al.* have shown that the 2- and 6-isocyanoazulenes are capable of forming monolayers on Au(111) surface that, unlike most isonitrile based SAMs[88], are stable in the air for *ca* 15 days. The formation of these SAMs was confirmed by surface IR where a significant shift of the signal from the bound isonitrile was detected; however a thiolate SH bending band is weak and cannot be used to evaluate the formation of the monolayer. In order to collect more information on the surface structure, a 1,3-dicyano-2-mercaptoazulene (**5**) was synthesized and then deposited on the surface. The IR

spectrum showed a clear signal from the nitrile group that is slightly shifted against the CN stretching frequency in THF. Azulenes **2** and **5** were subject for substitution studies with 1,3-dimethyl-2-isocyanoazulene and 1,3-dicyano-2-isocyanoazulene respectively. The monolayers of the isocyanoazulenes were soaked in THF solution of the mercaptoazulenes (**2** and **5** respectively) and vice versa (**Figure 3.14**) for 24 hours.

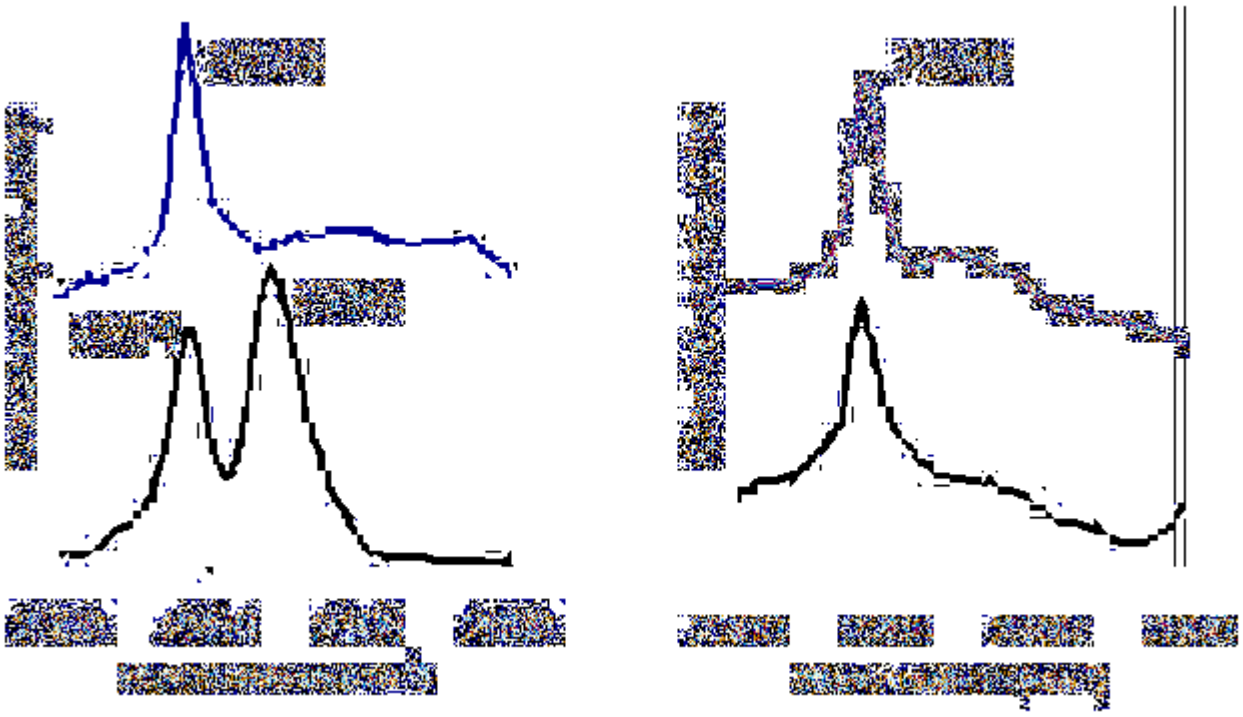

Figure 3.14 Surface IRs of SAM displacement experiments. Left: 1,3-dicyano-2-isocyanoazulene before soaking in solution of **2** (bottom) and after (top). Right: **2** before soaking in 1,3-dicyano-2-isocyanoazulene solution (bottom) and after (top).

It was found that 2-mercaptoazulenes displace isonitriles from the Au(111) surface almost irreversibly. As seen on **Figure 3.14**, while the surface IR of 1,3-dicyano-2-isocyanoazulene clearly indicates the presence of cyano and isocyano groups, after being soaked in solution of **2**,

the only signal observed is CN stretching at 2218 cm^{-1}. The reverse experiment has shown very little difference in the IR spectrum of SAM of **2** after soaking in 2 mM solution of 1,3-dicyano-2-isocyanoazulene. This observation is in line with the theoretical data that estimates the difference in bond energies Au-CN and Au-S to be ca. 20 kcal/mol[62].

3.5 Conclusions and future work.

In this chapter the synthesis and characterization of 2- and 6-azulenyl thiols were presented. The mercaptoazulenes **1** and **3** exhibit different orientations of the ethoxycarbonyl groups with respect to the azulenic core due to hydrogen bonding interaction of the carbonyl oxiden atoms with the S-H substituent in 2-mercapto-1,3-diethoxycarbonylazulene **1**.

The coordination chemistry of **1** and **3** was established by forming air stable dinuclear gold(I) complexes of these mercaptoazulenes that were structurally resolved and compared to the previously described 2-isocyanoazulene-containing dunuclear gold complex. The major difference is in the fact that the faces of the azulenyl thiolate moieties in **6** and **7** do not overlap and, thus, do not exhibit π-stacking interactions, unlike the azulenic scaffolds in their 2-isocyanoazulene containing analogue. This is in good agreement with the theoretical data suggesting that the *syn* orientation has the highest energy for all possible stacked π-complexes of azulene[89].

Up until now there have been no thiolate SAMs based on azulenyl scaffold described in the literature. All of the synthesized thiols were absorbed on the Au(111) surface from solution to form air stable monolayers. Their thicknesses were consistent with formation of one molecule thick films featuring approximately upright coordination of the mercaptoazulene moieties. The films showed no signs of significant decomposition after being stored for several days, which

suggests their inertness with respect to air, ambient lighting, and moisture.

2-Mercaptoazulenes **2** and **5** were subject to SAM displacement experiments with 1,3-methyl-2-isocyano- and 1,3-dicyano-2-isocyanoazulenes. Both mercaptoazulenes were found to displace the isocyanide ligands from the surface. However, isonitriles were unable to displace thiolate SAMs, which is in agreement with theoretical estimations of S-Au and NC-Au bond energies[62]. Modification of the azulene scaffold with IR-active cyano groups permitted observing chemisorption of **5** on gold film through by means of surface IR techniques. These cyano "spectroscopic handles" were particularly useful for following the SAM displacement experiments involving isocyanoazulene and mercaptoazulene "competitors".

Given that the 2,6-azulenic framework appears to have lower resistance to conductivity than its isomeric naphthalene scaffold[19], it is important to consider performing comparative conductivity studies on mercaptoazulene and mercaptonaphthalene SAMs in the future. The synthetic work will focus on the syntheses of azulene-dithiolates and hybrid linkers, such as -isocyanide/mercapto- and carboxylate/mercapto-substituted azulenes. Furthermore, the difference in ligating behavior of the above junction groups will permit achieving good control over azulenic dipole orientation upon SAM monolayer formation.

The growing interest in gold compounds with macrocyclic or oligomeric structures leads to potential application of polydentate mercaptoazulenes in photoluminescent materials synthesis[90]. Thus, solid state luminescence studies will be interesting to conduct as a further development of this work, especially on the systems containing 2,2'-dimercapto-6,6'-biazulene that appears to be accessible from 2,2'-diamino-1,1',3,3'-tetraethoxycarbonyl-6,6'biazulene[91].

3.6 References

(1) Piesse, S. *C. R. Hebd. Seances Acad. Sci.* **1863**, *57*, 1016.

(2) Anderson, A. G., Jr.; Stecker, B. M. *J. Am. Chem. Soc.* **1959**, *81*, 4941.

(3) Liu, R. S. H. *J. Chem. Ed* **2002**, *79*, 183.

(4) Plattner, P. A.; Pfau, A. S. *Helv. Chim. Acta* **1937**, *20*.

(5) Ziegler, K.; Hafner, K. *Angew. Chem.* **1955**, *67*, 301.

(6) Nozoe, T.; Seto, S.; Matsumura, S. *Proc. Jpn. Acad.* **1952**, *28*, 483.

(7) Tomiyama, T.; Yokota, M.; Wakabayashi, S.; Kokasai, K.; Yanagisawa, T. *J. Med. Chem.* **1993**, *36*, 791.

(8) Tanaka, Y.; Mitani, A.; Tigarashi, T.; Someya, S.; Otsuka, K.; Imai, T.; Yamaki, F.; Tanaka, H.; Saitoh, M.; Nakazawa, T.; Noguchi, K.; Hashimoto, K.; Shigenobu, K. *Naunyn-Schmiedeberg's Arch. Pharm.* **2001**, *363*, 344.

(9) Ueno, T. In *Jpn. Kokai Tokkyo Koho* Japan, 1990; Vol. JP 02015020.

(10) Chaudhuri, R. K.; Puccetti, G.; Marchio, F.; Lascu, Z. In *Eur. Pat. Appl.* 2005.

(11) Wang, F.; Yee-Hing, L. *Macromolecules* **2003**, *36*, 536.

(12) Wang, X.; Kok-Peng, J.; Jia, P.; Lin, T.; Cho, C. M.; Xu, J.; Lu, X.; He, C. *Macromolecules* **2009**, *42*, 5534.

(13) Ito, S.; Iida, T.; Kawakami, J.; Okujima, T.; Morita, N. *Eur. J. Org. Chem.* **2009**, 5355.

(14) Oda, M.; Thanh, N. C.; Ikai, M.; Fujikawa, H.; Nakajima, K.; Kuroda, S. *Tetrahedron* **2007**, *63*, 10608.

(15) Takaji, K.; Mizuno, A.; Iwamoto, H.; Kawashima, S.; Nishida, S.; Hashikawa, T.; Nozoe, T. *Dyes Pigh* **1994**, *26*, 51.

(16) Pham, W.; Weissleder, R.; Tung, C.-H. *Tetrahedron Lett.* **2003**, *44*, 3975.

(17) Estdale, S. E.; Brettle, R.; Dunmur, D. A.; Marson, C. M. *J. Mater. Chem.* **1997**, *7*,

391.

(18) Simpson, S. H.; Richardson, R. M.; Hanna, S. *J. Chem. Phys.* **2007**, *127*, 14.

(19) Dutta, S.; Lakshmi, S.; Pati, S. K. *Bull. Mater. Sci.* **2008**, *31*, 353.

(20) Biro, L. P.; Mark, I. M.; Koos, A. A.; Nagy, J. B.; Lambin, P. *Phys. Rev. B: Condens Matter Mater. Phys* **2002**, *66*.

(21) Wang, F.; Lai, Y.-H.; Kocherginsky, N. M.; Kosteski, Y. Y. *Org. Lett.* **2002**, *5*, 995.

(22) Wang, F.; Lai, Y.-H.; Han, M.-Y. *Macromolecules* **2004**, *37*, 3222.

(23) Ruiz, J. P.; Dharia, J. R.; Reynolds, J. R.; Buckley, L. J. *Macromolecules* **1992**, *25*, 1214.

(24) Reidl, F. X.; Kothe, O.; Rockl, K.; Bauer, W.; Daub, J. *Macromol. Chem. Phys* **2000**, *210*, 2091.

(25) Ito, S.; Morita, N. *Eur. J. Org. Chem.* **2009**, 4567.

(26) Shevyakov, S. V.; Li, H.; Muthyala, R.; Asato, A. E.; Croney, J. C.; Jameson, D. M.; Liu, R. S. H. *J. Phys. Chem. A* **2003**, *107*, 3295.

(27) Kurotobi, K.; Kim, K. S.; Noh, S. B.; Kim, D.; Osuka, A. *Angew. Chem. Int. Ed.* **2006**, *45*, 3944.

(28) Patalinghug, W. C.; Chang, M.; Solis, J. *J. Chem. Ed* **2007**, *84*, 1945.

(29) Muranaka, A.; Yonehara, M.; Uchiyama, M. *J. Am. Chem. Soc.* **2010**, *132*, 7844.

(30) King, R. B.; Ackermann, M. N. *Inorg. Chem.* **1973**, *13*, 637.

(31) Tofke, V. S.; Behrens, U. *Angew. Chem.* **1986**, *99*, 134.

(32) Churchill, M. R. *Progress in Inorganic Chemistry* **1970**, *11*, 53.

(33) Graham, S. R.; Ferrence, G. M.; Lash, T. D. *Chem. Commun.* **2002**, 894.

(34) Barybin, M. V.; Chisholm, M. H.; Dalal, N. S.; Holovics, T. C.; Patmore, N. J.; Robinson, R. E.; Zipse, D. J. *J. Am. Chem. Soc.* **2005**, *127*, 15182.

(35) Zhang, J.; Petoud, S. *Chem. Eur. J.* **2008**, *14*, 1264.

(36) Robinson, R. E.; Holovics, T. C.; Deplazes, S. F.; Powell, D. R.; Lushington, G. H.; Thompson, W. H.; Barybin, M. V. *Organometallics* **2005**, *24*, 2386.

(37) Lohr, H.-G.; Vogtle, F. *Acc. Chem. Res.* **1985**, *18*, 65.

(38) Lohr, H.-G.; Vogtle, F.; Schuh, W.; Puff, H. *Chem. Ber.* **2006**, *117*, 2839.

(39) Zielinski, T.; Kedziorek, M.; Jurczak, J. *Chem. Eur. J.* **2008**, *14*, 838.

(40) Holovics, T. C.; Robinson, R. E.; Weintrob, E. C.; Toriyama, M.; Lushington, G. H.; Barybin, M. V. *J. Am. Chem. Soc.* **2006**, *128*, 2300.

(41) Goldschmidt, V. M. *Geoehemische Verteilungsgesetze der Elemente*; X ed.; Norsk Videnskapsakademien: Oslo, 1938.

(42) Fartland, B. F.; Ke, J.; Anderson, M. D.; Maentzen, W. I.; Cui, L. W.; Allred, C. C.; Johnston, J. L.; Nikolau, B. J.; Wurtele, E. S. *Plant Physiol.* **2002**, *130*, 740.

(43) Green, M. T. *Curr. Opin. Chem. Biol.* **2009**, *13*, 84.

(44) Vatsis, K. P.; Peng, H.-M.; Coon, M. J. *J. Inorg. Biochem.* **2002**, *91*, 542.

(45) Batchelor, L. J.; Fitzgerald, E.; Wolowska, J.; McDouall, J. J. W.; McInnes, E. J. L. *Chem. Eur. J.* [Online Early Access]. DOI: DOI: 10.1002/chem.201000823. Published Online: 2010.

(46) Brower, J. B.; Ryan, R. L.; Pazirandeh, M. *Environ. Sci. Technol.* **1997**, *31*, 2910.

(47) Niu, H.; Gao, M. *Angew. Chem. Int. Ed.* **2006**, *45*, 6462.

(48) Eremenko, I. L.; Berke, H.; Kolobkov, B. I.; Novotortsev, V. M. *Organometallics* **1994**, *13*, 244.

(49) Batchelor, L. J.; Shaw, R.; Makrey, S. J.; Helliwell, M.; McInnes, E. J. L. *Chem. Eur. J.* **2010**, *16*, 5554.

(50) Orlando, U. S.; Baes, A. U.; Nishijima, W.; Okada, M. *Green Chem.* **2002**, *4*, 555.

(51) Shoda, S.-I.; Iwata, S.; Kim, H. J.; Hiraishi, M.; Kobayashi, S. *Macromol. Chem. Phys* **1996**, *197*, 2437.

(52) Jiang, D.; Dai, S. *J. Phys. Chem. C* **2009**, *113*, 7838.

(53) Wang, R.-H.; Hong, M.-C.; Su, W.-P.; Liang, Y.-C.; Cao, R.; Zhao, Y.-J.; Weng, J.-B. *Polyhedron* **2001**, *20*, 3165.

(54) Liu, X.; Yang, H.; Zheng, N.; Zheng, L. *Eur. J. Inorg. Chem.* **2010**, 2084.

(55) Jadzinsky, P. D.; Calero, G.; Ackerson, C. J.; Bushnell, D. A.; Kornberg, R. D. *Science* **2007**, *318*, 430.

(56) Benfield, R. E.; Grandjean, D. *J. Phys. Chem. B* **2001**, *105*, 1961.

(57) Mallick, K.; Witcomb, M.; Scurell, M. *Eur. Phys. J. E* **2006**, *20*, 347.

(58) Park, S.; Lim, J.-H.; Chung, S.-W.; Mirkin, C. A. *Science* **2004**, *303*, 348.

(59) Fricker, S. P. *Gold Bull.* **1996**, *29*, 53.

(60) Langmuir, I. *J. Am. Chem. Soc.* **1917**, *39*, 1848.

(61) Love, J. C.; Estroff, L. A.; Kriebel, J. K.; Nuzzo, R. G.; Whitesides, G. M. *Chem. Rev.* **2005**, *105*, 1103.

(62) Zhou, J.-H.; Shi, L.-W.; Zhang, T.; Chen, M.-B. *Chin. J. Chem.* **2007**, *25*, 1223.

(63) Nuzzo, R. G.; Zegarski, B. R.; Dubois, L. H. *J. Am. Chem. Soc.* **1987**, *109*, 733.

(64) Brandow, S. L.; Chen, M.-S.; Dulcey, C. S.; Dressick, W. J. *Langmuir* **2008**, *24*, 3888.

(65) Bent, S. F. *Surf. Sci.* **2002**, *500*, 879.

(66) Tielens, F.; Santos, E. *J. Phys. Chem. C* **2010**, *114*, 9444.

(67) Ulman, A. *Chem. Rev.* **1996**, *96*, 1533.

(68) Yang, K.-L.; Cadwell, K.; Abbott, N. L. *Adv. Mater.* **2003**, *15*, 1819.

(69) Flink, S.; van Veggel, F. C. J. M.; Reinhoudt, D. N. *J. Phys. Chem. B* **1999**, *103*, 6515.

(70) Bandyopadhyay, K.; Shu, L.; Liu, H.; Echegoyen, L. *Langmuir* **2000**, *16*, 2706.

(71) Zharnikov, M.; Grunze, M. J. *J. Phys. Condens. Matter* **2001**, *13*, 11333.

(72) Kang, S. H.; Ma, H.; Kang, M.-S.; Kim, K.-S.; Jen, A. K.-Y.; Zareie, M. H.; Sarikaya, A. *Angew. Chem. Int. Ed.* **2004**, *43*, 1512.

(73) McDonald, R. N.; Richmond, J. M. *J. Org. Chem,* **1975**, *40*, 1689.

(74) McDonald, R. N.; Richmond, J. M.; Curtis, J. R.; Petty, H. E.; Hoskind, T. L. *J. Org. Chem,* **1976**, *41*, 1811.

(75) Nozoe, T.; Seto, S.; Matsumura, S.; Yasuhiro, M. *Bull. Chem. Soc. Jpn.* **1962**, *35*, 1179.

(76) Irwin, M. J.; Rendina, L. M.; Vittal, J. J.; Puddephatt, R. J. *Chem. Commun.* **1996**, 1281.

(77) Morita, T.; Fujita, T.; Takase, K. *Bull. Chem. Soc. Jpn.* **1980**, *53*, 1647.

(78) Data Collection: SMART Software Reference Manual (1998). Bruker-AXS, 5465 E. Cheryl Parkway, Madison, WI 53711-5373 USA.

(79) Sheldrick, G. M.; Brucker-AXS: Madison, WI, 2000.

(80) Clear, C. S.; Nealey, P. F. *Langmuir* **2001**, *17*, 720.

(81) Neese, F.; Becker, U.; Ganyushin, D.; Hansen, A.; Liakos, D. G.; Kollmar, C.; Kossmann, S.; Petrenko, T.; Reimann, C.; Riplinger, C.; Sivalingam, K.; Valeev, E.,

(82) Wezisla, B.; Wennmohs, F.; 2.7.0 ed.; University of Bonn: Bonn, Germany, 2009.

(83) Yam, V. W.-W.; Chan, C.-L.; Li, C.-K.; Wong, K. M. C. *Coord. Chem. Rev.* **2001**, *216-217*, 173.

(84) Li, C.-K.; Lu, X.-X.; Wong, K.-M. C.; Chan, C.-L.; Zhu, N.; Yam, V. W.-W. *Inorg. Chem.* **2004**, *43*, 7421.

(85) Li, C.-H.; Kui, S. C.-F.; Sham, I. H. T.; Chui, S. S.-Y.; Che, C.-M. *Eur. J. Inorg. Chem.* **2008**, 2421.

(86) Bardaji, M.; Calhorda, M. J.; Costa, P. J.; Jones, P. G.; Laguna, A.; Perez, M. R.; Villacampa, M. D. *Inorg. Chem.* **2006**, *45*, 1059.

(87) Gimento, M. C.; Laguna, A. *Gold Bull.* **2003**, *36*, 83.

(88) Yam, V. W.-W.; Li, C.-K.; Chan, C.-L. *Angew. Chem. Int. Ed.* **1998**, *37*, 2857.

(89) Stapleton, J. J.; Daniel, T. A.; Uppili, S.; Cabarcos, O. M.; Naciri, J.; Shashidhar, R.; Allara, D. L. *Langmuir* **2005**, *21*, 11061.

(90) Piacensa, M.; Grimme, S. *J. Am. Chem. Soc.* **2005**, *127*, 14841.

(91) Brandys, M.-C.; Jennings, M. C.; Puddephatt, R. J. *J. Chem. Soc., Dalton Trans* **2000**, 4601.

(92) Kurotobi, K.; Tabata, H.; Miyauchi, M.; Murafuji, T.; Toshihiro, M.; Sugihara, Y. *Synthesis* **2002**, 1013.

Appendix A. Final GC trace of the reaction mixture 1.3.6.c1

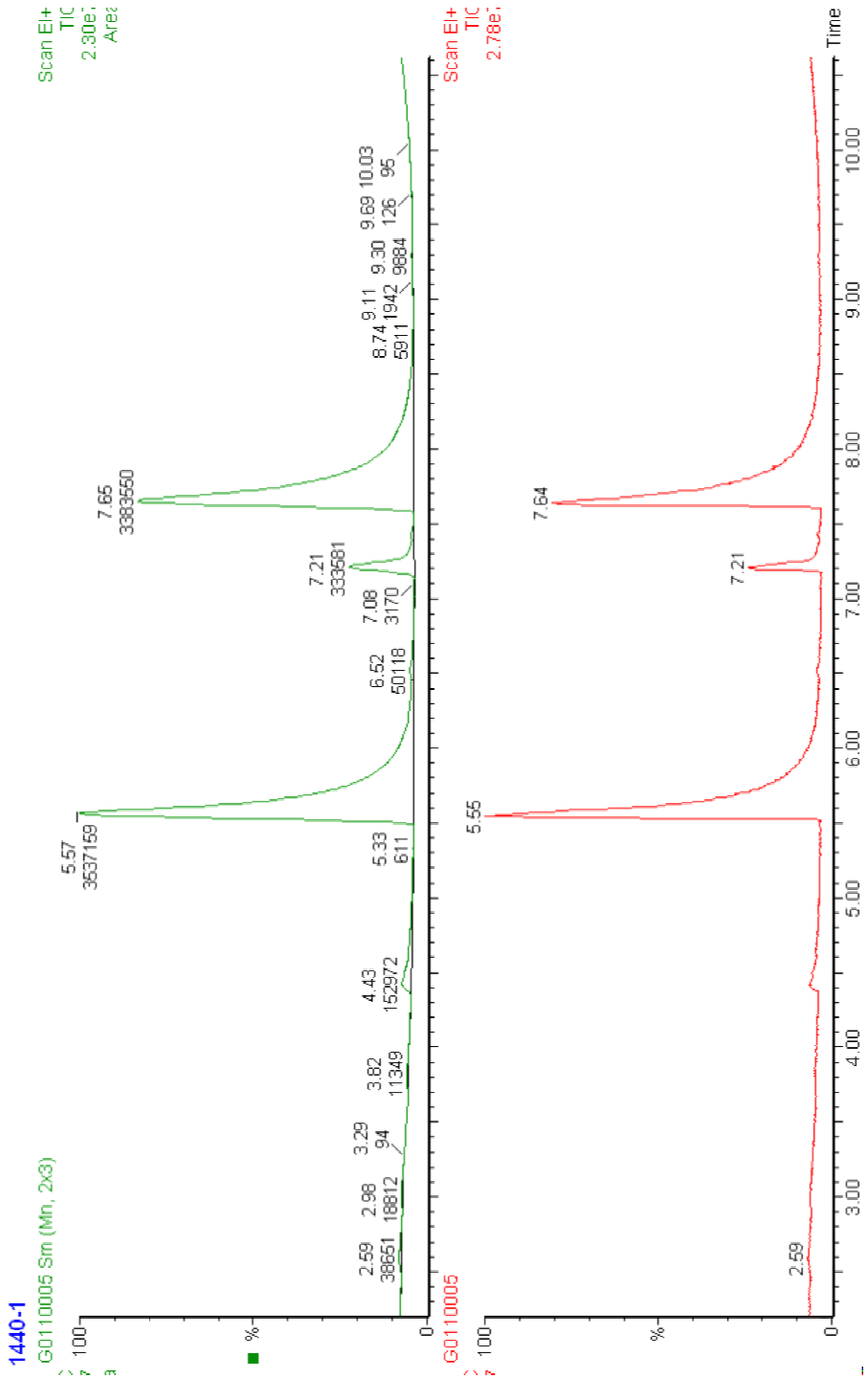

Appendix B. Final GC trace of the reaction mixture 1.3.6.c2

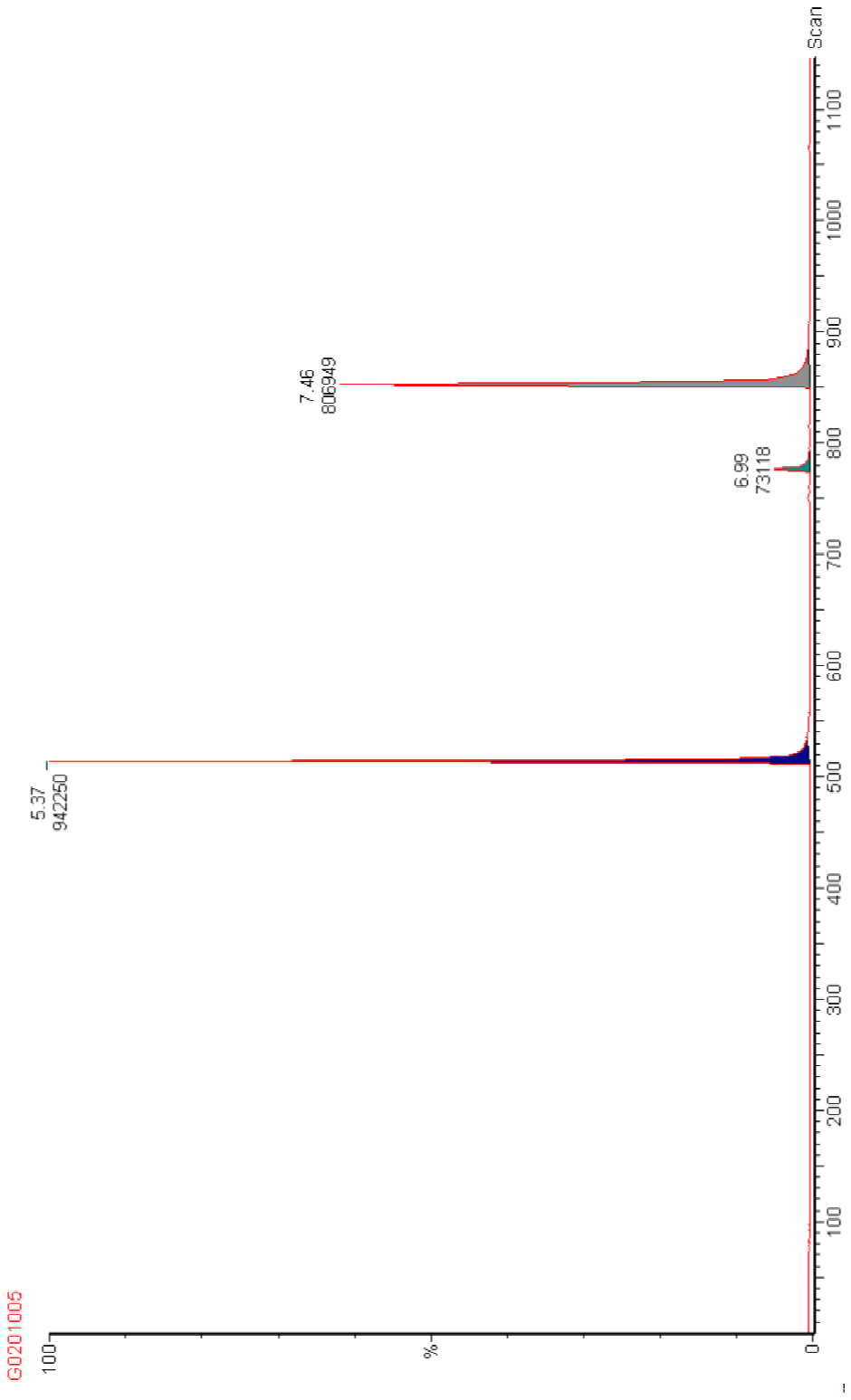

Appendix C. Final GC trace of the reaction mixture 1.3.6.c3

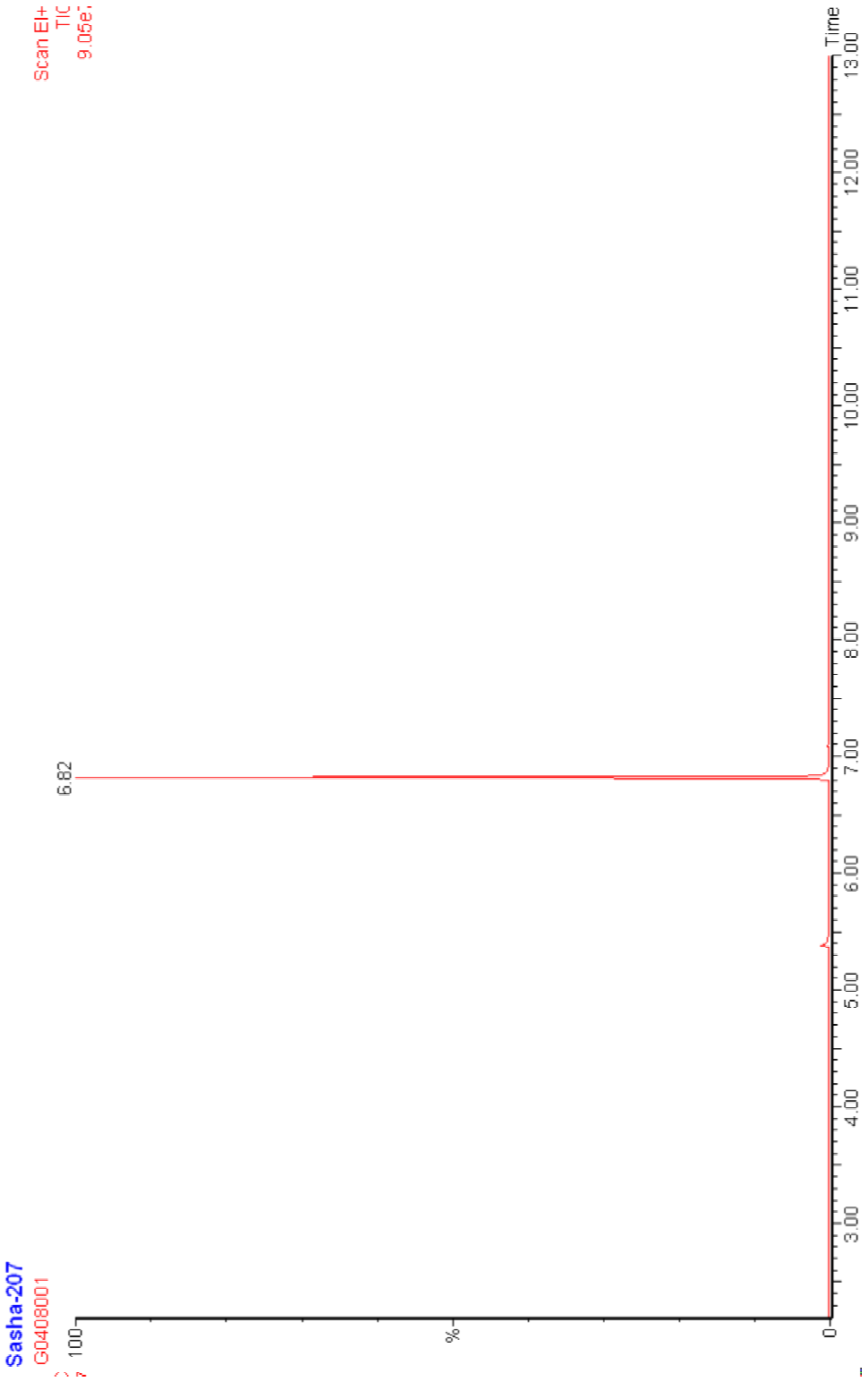

Appendix D. Final GC trace of the reaction mixture 1.3.6.c4

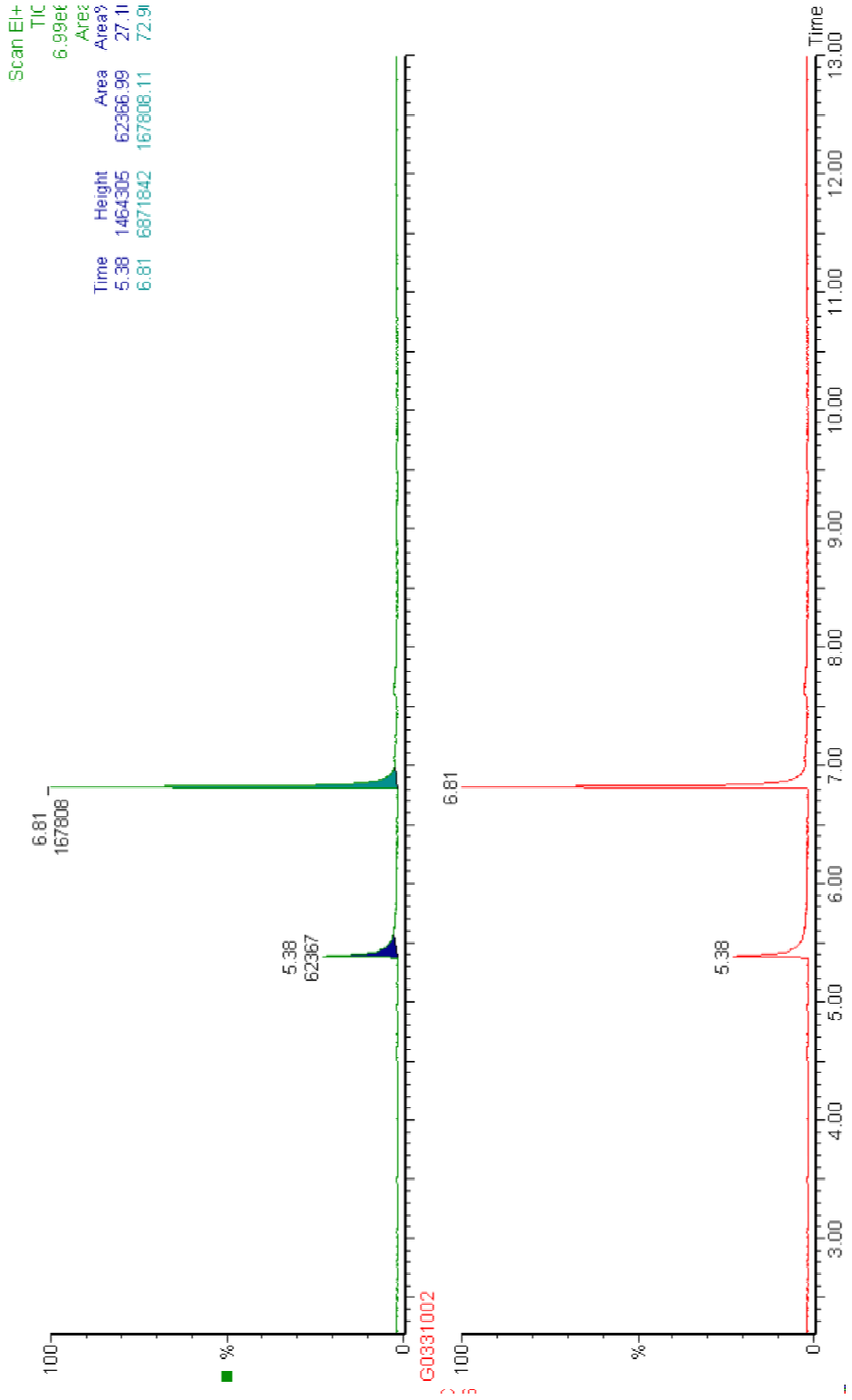

Appendix E. Final GC trace of the reaction mixture 1.3.6.c5

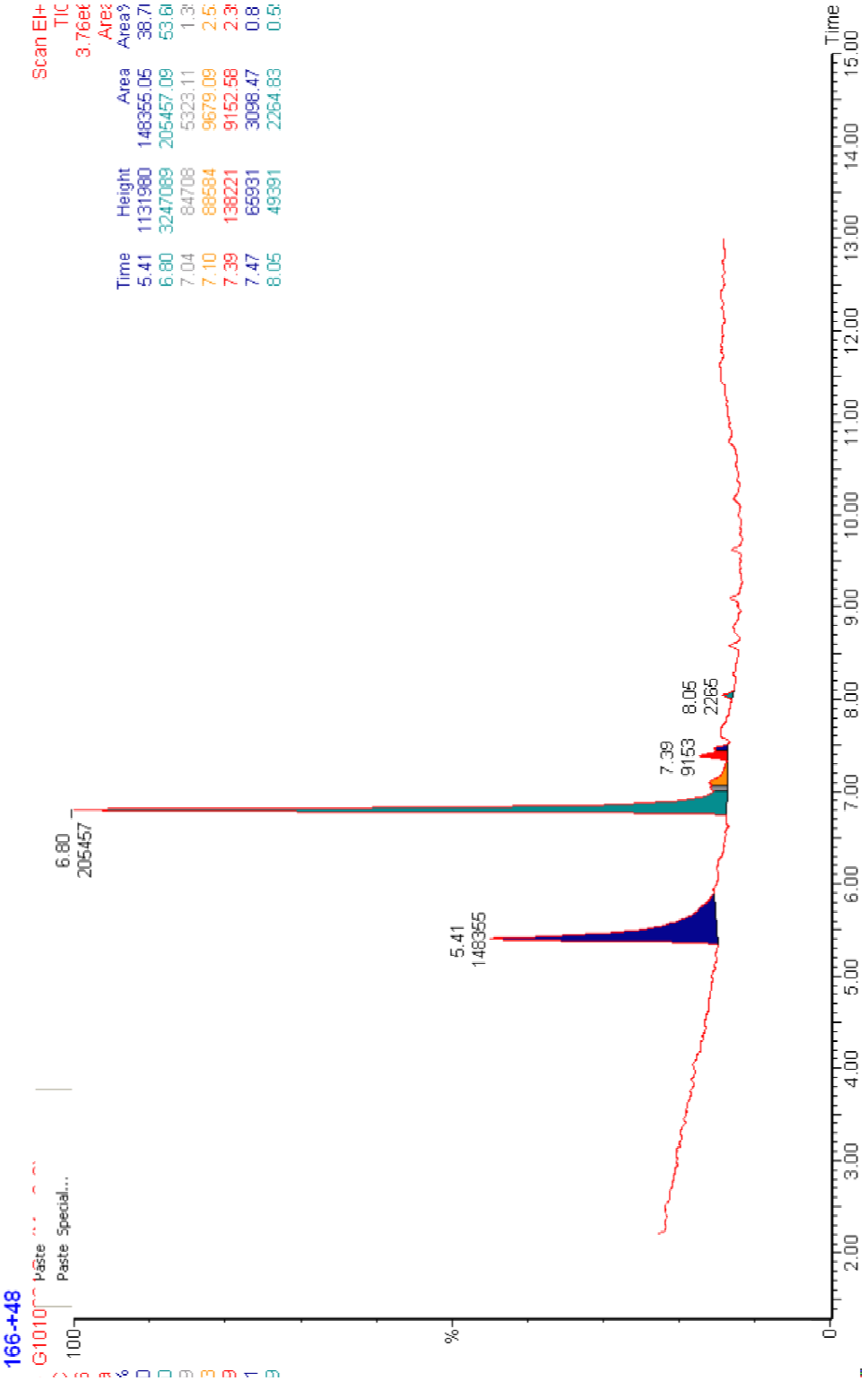

Appendix F. Final GC trace of the reaction mixture 1.3.6.c6

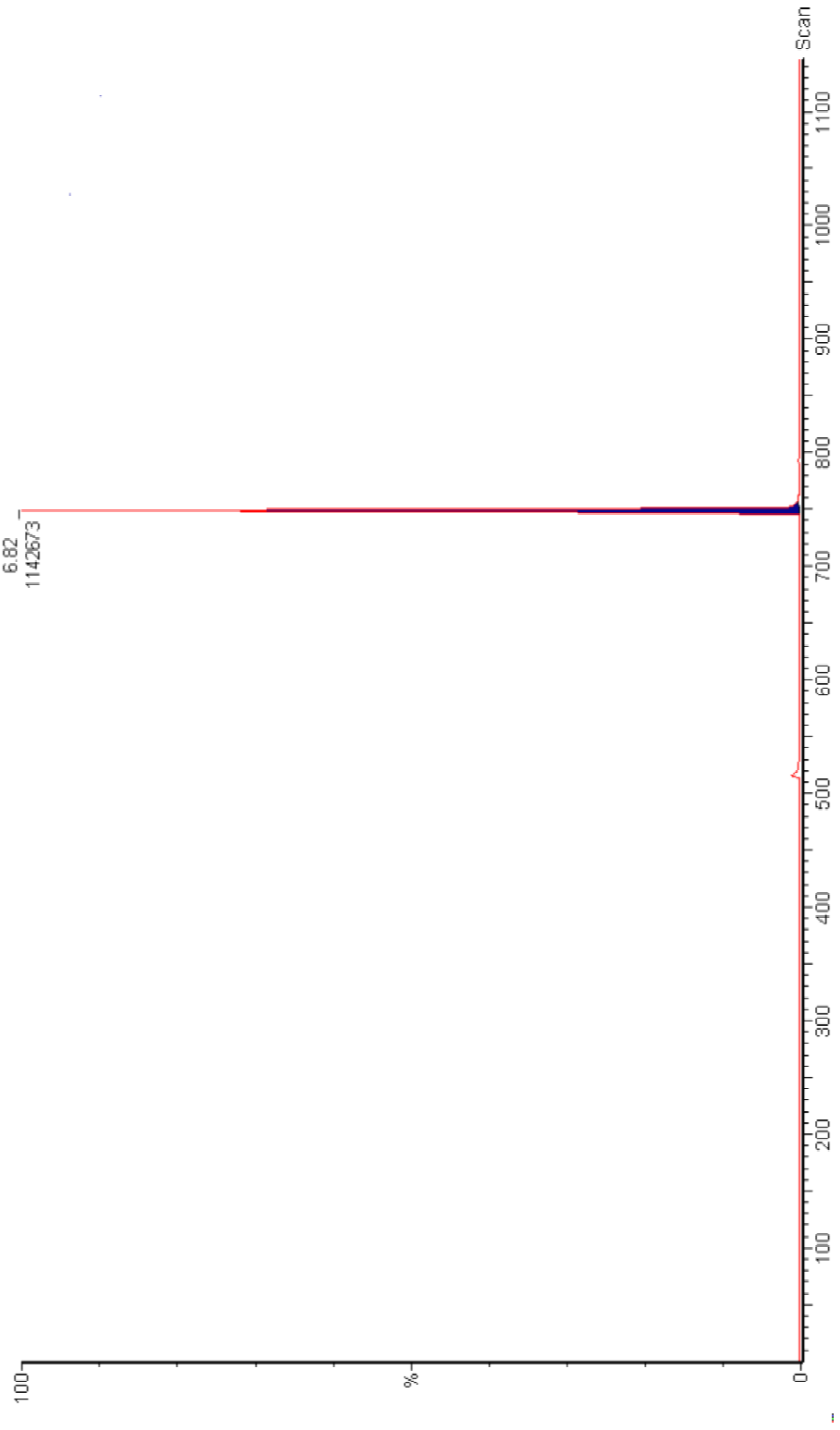

Appendix G. Final GC trace of the reaction mixture 1.3.8

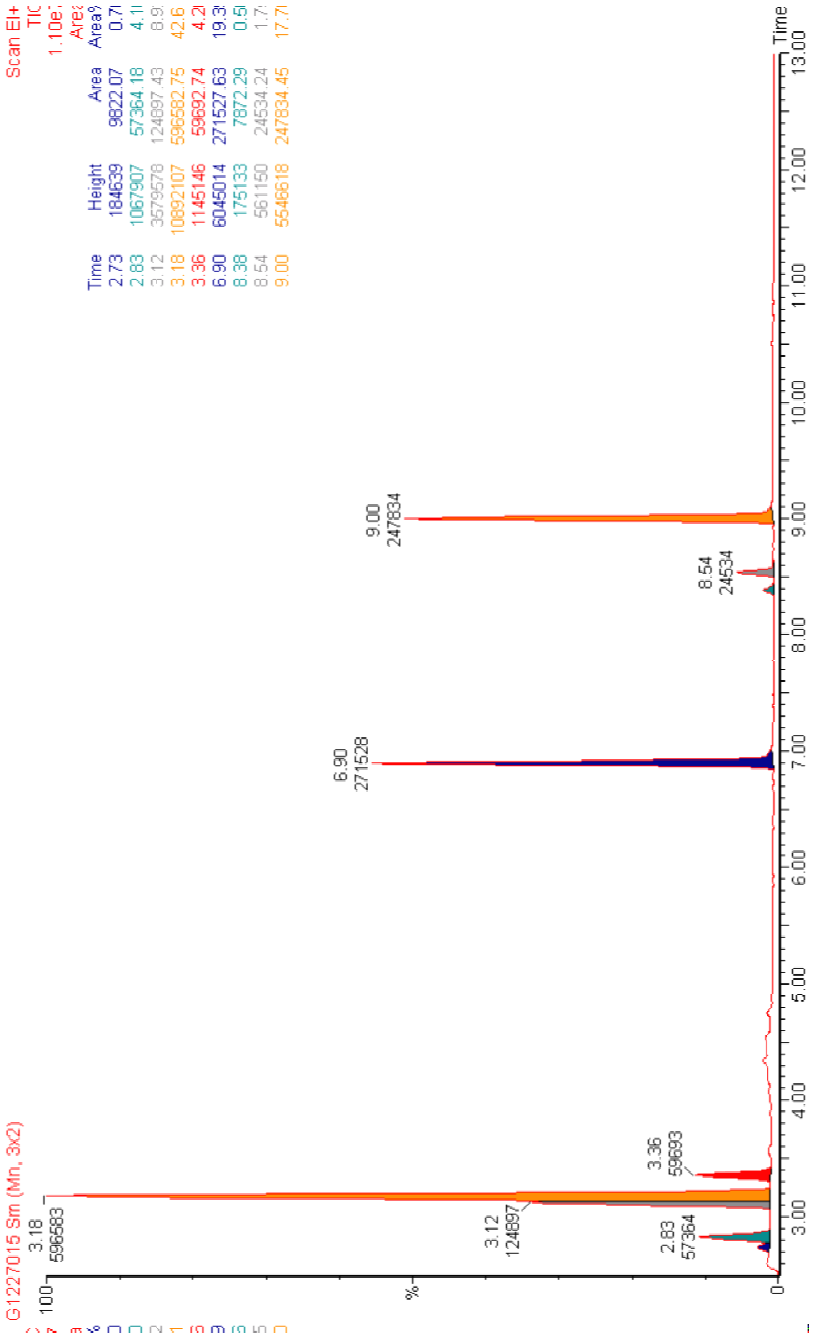

Appendix H. Crystallographic data for **1**.

Table H.1 Atomic coordinates (x 10^4) and equivalent isotropic displacement parameters ($Å^2$ x 10^3) for **1**. U(eq) is defined as one third of the trace of the orthogonalized U_{ij} tensor.

	x	y	z	U(eq)
S(1)	3433(1)	2955(1)	2779(1)	22(1)
O(1)	1979(2)	-1590(1)	829(1)	21(1)
O(2)	3299(2)	2368(1)	6833(1)	21(1)
O(3)	2719(2)	705(1)	760(1)	29(1)
O(4)	3481(2)	3877(1)	5552(1)	25(1)
C(1)	2498(2)	75(2)	2713(2)	17(1)
C(2)	2913(2)	1464(2)	3424(2)	17(1)
C(3)	2901(2)	1419(2)	4697(2)	17(1)
C(4)	2339(3)	-538(2)	5891(2)	19(1)
C(5)	2035(3)	-1914(2)	6069(2)	20(1)
C(6)	1783(3)	-3163(2)	5213(2)	21(1)
C(7)	1693(3)	-3351(2)	3934(2)	21(1)
C(8)	1873(3)	-2344(2)	3198(2)	19(1)
C(9)	2501(2)	-22(2)	4800(2)	16(1)
C(10)	2251(2)	-878(2)	3536(2)	16(1)
C(11)	2421(3)	-210(2)	1364(2)	19(1)
C(12)	1874(3)	-1907(2)	-514(2)	23(1)
C(13)	1273(3)	-3492(2)	-906(2)	26(1)
C(14)	3252(3)	2672(2)	5699(2)	18(1)
C(15)	3657(3)	3558(2)	7867(2)	24(1)
C(16)	3390(3)	2952(2)	9008(2)	26(1)

Table H.2. Bond lengths [Å] for **1**.

S(1)-C(2)	1.739(2)	C(6)-C(7)	1.387(3)
S(1)-H(1S)	1.20	C(6)-H(6)	0.92(2)
O(1)-C(11)	1.348(2)	C(7)-C(8)	1.393(2)
O(1)-C(12)	1.454(2)	C(7)-H(7)	0.98(2)
O(2)-C(14)	1.343(2)	C(8)-C(10)	1.397(2)
O(2)-C(15)	1.450(2)	C(8)-H(8)	0.90(2)
O(3)-C(11)	1.215(2)	C(9)-C(10)	1.473(2)
O(4)-C(14)	1.216(2)	C(12)-C(13)	1.508(3)
C(1)-C(2)	1.415(2)	C(12)-H(12A)	0.97(2)
C(1)-C(10)	1.423(2)	C(12)-H(12B)	0.94(2)
C(1)-C(11)	1.463(2)	C(13)-H(13A)	0.97(3)
C(2)-C(3)	1.418(2)	C(13)-H(13B)	0.95(2)
C(3)-C(9)	1.426(2)	C(13)-H(13C)	1.02(3)
C(3)-C(14)	1.470(2)	C(15)-C(16)	1.503(3)
C(4)-C(5)	1.391(2)	C(15)-H(15A)	0.94(2)
C(4)-C(9)	1.398(2)	C(15)-H(15B)	1.02(2)
C(4)-H(4)	0.96(2)	C(16)-H(16A)	0.95(2)
C(5)-C(6)	1.386(2)	C(16)-H(16B)	0.98(3)
C(5)-H(5)	0.94(2)	C(16)-H(16C)	0.93(3)

Table H.3. Bond angles [°] for **1**.

C(2)-S(1)-H(1S)	109.5	C(9)-C(3)-C(14)	127.9(2)
C(11)-O(1)-C(12)	115.5(1)	C(5)-C(4)-C(9)	129.9(2)
C(14)-O(2)-C(15)	116.1(1)	C(5)-C(4)-H(4)	113(1)
C(2)-C(1)-C(10)	108.3(1)	C(9)-C(4)-H(4)	117(1)
C(2)-C(1)-C(11)	121.9(1)	C(6)-C(5)-C(4)	129.8(2)
C(10)-C(1)-C(11)	129.8(2)	C(6)-C(5)-H(5)	120(1)
C(1)-C(2)-C(3)	109.5(1)	C(4)-C(5)-H(5)	110(1)
C(1)-C(2)-S(1)	123.1(1)	C(5)-C(6)-C(7)	128.0(2)
C(3)-C(2)-S(1)	127.4(1)	C(5)-C(6)-H(6)	116(1)
C(2)-C(3)-C(9)	107.9(1)	C(7)-C(6)-H(6)	116(1)
C(2)-C(3)-C(14)	124.2(1)	C(6)-C(7)-C(8)	129.0(2)

C(6)-C(7)-H(7)	117(1)	C(12)-C(13)-H(13B)	109(2)
C(8)-C(7)-H(7)	114(1)	H(13A)-C(13)-H(13B)	108(2)
C(7)-C(8)-C(10)	130.0(2)	C(12)-C(13)-H(13C)	108(1)
C(7)-C(8)-H(8)	116(1)	H(13A)-C(13)-H(13C)	111(2)
C(10)-C(8)-H(8)	114(1)	H(13B)-C(13)-H(13C)	111(2)
C(4)-C(9)-C(3)	126.7(2)	O(4)-C(14)-O(2)	121.7(2)
C(4)-C(9)-C(10)	126.0(2)	O(4)-C(14)-C(3)	125.1(2)
C(3)-C(9)-C(10)	107.3(1)	O(2)-C(14)-C(3)	113.2(1)
C(8)-C(10)-C(1)	125.9(2)	O(2)-C(15)-C(16)	106.3(1)
C(8)-C(10)-C(9)	127.1(2)	O(2)-C(15)-H(15A)	105(1)
C(1)-C(10)-C(9)	107.0(1)	C(16)-C(15)-H(15A)	112(1)
O(3)-C(11)-O(1)	122.0(2)	O(2)-C(15)-H(15B)	109(1)
O(3)-C(11)-C(1)	123.8(2)	C(16)-C(15)-H(15B)	110(1)
O(1)-C(11)-C(1)	114.3(1)	H(15A)-C(15)-H(15B)	114(2)
O(1)-C(12)-C(13)	106.2(2)	C(15)-C(16)-H(16A)	114(1)
O(1)-C(12)-H(12A)	107(1)	C(15)-C(16)-H(16B)	111(1)
C(13)-C(12)-H(12A)	109(1)	H(16A)-C(16)-H(16B)	109(2)
O(1)-C(12)-H(12B)	110(1)	C(15)-C(16)-H(16C)	111(2)
C(13)-C(12)-H(12B)	110(1)	H(16A)-C(16)-H(16C)	105(2)
H(12A)-C(12)-H(12B)	114(2)	H(16B)-C(16)-H(16C)	106(2)
C(12)-C(13)-H(13A)	110(2)		

Table H.4. Anisotropic displacement parameters ($Å^2 x\ 10^3$) for **1**. The anisotropic displacement factor exponent takes the form: $-2\pi^2[\ h^2 a^{*2} U_{11} + ... + 2\ h\ k\ a^*\ b^*\ U_{12}\ ]$

	U_{11}	U_{22}	U_{33}	U_{23}	U_{13}	U_{12}
S(1)	32(1)	9(1)	24(1)	7(1)	1(1)	5(1)
O(1)	33(1)	12(1)	19(1)	3(1)	3(1)	6(1)
O(2)	34(1)	11(1)	20(1)	2(1)	4(1)	8(1)
O(3)	50(1)	14(1)	24(1)	7(1)	5(1)	6(1)
O(4)	39(1)	10(1)	28(1)	5(1)	5(1)	7(1)
C(1)	20(1)	9(1)	22(1)	4(1)	2(1)	4(1)
C(2)	18(1)	10(1)	24(1)	6(1)	2(1)	4(1)

C(3)	20(1)	9(1)	22(1)	4(1)	2(1)	4(1)
C(4)	21(1)	13(1)	22(1)	5(1)	3(1)	5(1)
C(5)	25(1)	14(1)	21(1)	7(1)	3(1)	4(1)
C(6)	25(1)	11(1)	29(1)	9(1)	2(1)	4(1)
C(7)	26(1)	9(1)	27(1)	4(1)	1(1)	3(1)
C(8)	23(1)	11(1)	22(1)	3(1)	1(1)	3(1)
C(9)	16(1)	10(1)	23(1)	5(1)	2(1)	4(1)
C(10)	17(1)	11(1)	21(1)	4(1)	2(1)	4(1)
C(11)	23(1)	12(1)	23(1)	5(1)	2(1)	5(1)
C(12)	34(1)	16(1)	19(1)	4(1)	3(1)	7(1)
C(13)	38(1)	16(1)	23(1)	2(1)	2(1)	9(1)
C(14)	21(1)	11(1)	23(1)	4(1)	3(1)	6(1)
C(15)	36(1)	12(1)	23(1)	0(1)	4(1)	7(1)
C(16)	31(1)	22(1)	23(1)	4(1)	4(1)	6(1)

Table H.5. Hydrogen coordinates (x 10^4) and isotropic displacement parameters (Å^2 x 10^3) for **1**.

	x	y	z	U(eq)
H(1S)	3943	3990	3592	78(10)
H(4)	2620(30)	140(20)	6660(20)	27(6)
H(5)	2070(30)	-1920(20)	6920(20)	23(5)
H(6)	1640(30)	-3960(20)	5530(20)	29(6)
H(7)	1350(30)	-4320(20)	3470(20)	27(6)
H(8)	1730(30)	-2680(20)	2379(19)	20(5)
H(12A)	3230(30)	-1560(20)	-712(18)	23(5)
H(12B)	880(30)	-1530(20)	-869(19)	22(5)
H(13A)	1210(40)	-3760(30)	-1800(20)	41(7)
H(13B)	-40(40)	-3830(30)	-690(20)	38(7)
H(13C)	2330(40)	-3880(30)	-470(20)	42(7)
H(15A)	5010(30)	4060(20)	7869(18)	20(5)
H(15B)	2600(30)	4120(20)	7740(20)	26(5)
H(16A)	2060(30)	2370(20)	8994(18)	24(5)
H(16B)	3720(40)	3690(30)	9760(20)	39(7)

H(16C)	4270(40)	2370(30)	9100(20)	44(7)

Table H.6. Torsion angles [°] for **1**.

C(10)-C(1)-C(2)-C(3)	-1.1(2)	C(11)-C(1)-C(2)-S(1)	-1.7(2)
C(11)-C(1)-C(2)-C(3)	-179.7(1)	C(1)-C(2)-C(3)-C(9)	0.9(2)
C(10)-C(1)-C(2)-S(1)	177.0(1)	S(1)-C(2)-C(3)-C(9)	-177.0(1)
C(1)-C(2)-C(3)-C(14)	-179.3(2)	C(4)-C(9)-C(10)-C(8)	-2.1(3)
S(1)-C(2)-C(3)-C(14)	2.9(3)	C(3)-C(9)-C(10)-C(8)	178.9(2)
C(9)-C(4)-C(5)-C(6)	-0.8(3)	C(4)-C(9)-C(10)-C(1)	178.7(2)
C(4)-C(5)-C(6)-C(7)	-2.8(3)	C(3)-C(9)-C(10)-C(1)	-0.3(2)
C(5)-C(6)-C(7)-C(8)	1.5(3)	C(12)-O(1)-C(11)-O(3)	-0.3(2)
C(6)-C(7)-C(8)-C(10)	2.1(3)	C(12)-O(1)-C(11)-C(1)	179.5(1)
C(5)-C(4)-C(9)-C(3)	-177.1(2)	C(2)-C(1)-C(11)-O(3)	0.7(3)
C(5)-C(4)-C(9)-C(10)	4.0(3)	C(10)-C(1)-C(11)-O(3)	-177.7(2)
C(2)-C(3)-C(9)-C(4)	-179.4(2)	C(2)-C(1)-C(11)-O(1)	-179.1(1)
C(14)-C(3)-C(9)-C(4)	0.8(3)	C(10)-C(1)-C(11)-O(1)	2.5(3)
C(2)-C(3)-C(9)-C(10)	-0.3(2)	C(11)-O(1)-C(12)-C(13)	-177.5(2)
C(14)-C(3)-C(9)-C(10)	179.8(2)	C(15)-O(2)-C(14)-O(4)	-0.6(2)
C(7)-C(8)-C(10)-C(1)	177.1(2)	C(15)-O(2)-C(14)-C(3)	179.5(1)
C(7)-C(8)-C(10)-C(9)	-1.9(3)	C(2)-C(3)-C(14)-O(4)	4.2(3)
C(2)-C(1)-C(10)-C(8)	-178.4(2)	C(9)-C(3)-C(14)-O(4)	-175.9(2)
C(11)-C(1)-C(10)-C(8)	0.2(3)	C(2)-C(3)-C(14)-O(2)	-175.9(2)
C(2)-C(1)-C(10)-C(9)	0.8(2)	C(9)-C(3)-C(14)-O(2)	4.0(2)
C(11)-C(1)-C(10)-C(9)	179.4(2)		
C(14)-O(2)-C(15)-C(16)	173.3(2)		

Appendix I. Crystallographic data for **3**.

Table I.1. Atomic coordinates (x 10^4) and equivalent isotropic displacement parameters ($Å^2$ x 10^3) for **3**. U(eq) is defined as one third of the trace of the orthogonalized U_{ij} tensor.

	x	y	z	U(eq)
S(1)	2224(1)	3473(1)	8672(1)	25(1)
O(1)	5726(2)	1221(2)	3273(2)	23(1)
O(2)	2300(2)	-2497(1)	2726(2)	22(1)
O(3)	5948(2)	2946(2)	4835(2)	26(1)
O(4)	1126(2)	-2138(2)	3988(2)	25(1)
C(1)	4329(2)	1145(2)	4390(2)	19(1)
C(2)	3725(2)	-91(2)	3676(2)	19(1)
C(3)	2756(2)	-507(2)	4097(2)	19(1)
C(4)	1873(2)	445(2)	5765(2)	20(1)
C(5)	1776(2)	1338(2)	6752(2)	22(1)
C(6)	2547(2)	2549(2)	7389(2)	20(1)
C(7)	3566(2)	3146(2)	7123(2)	22(1)
C(8)	4072(2)	2699(2)	6206(2)	20(1)
C(9)	2716(2)	472(2)	5100(2)	17(1)
C(10)	3740(2)	1536(2)	5294(2)	18(1)
C(11)	5398(2)	1876(2)	4213(2)	20(1)
C(12)	6786(2)	1855(2)	3022(2)	25(1)
C(13)	6930(3)	963(2)	1902(2)	29(1)
C(14)	1968(2)	-1761(2)	3625(2)	19(1)
C(15)	1679(3)	-3776(2)	2330(2)	24(1)
C(16)	2213(3)	-4459(2)	1388(2)	28(1)
S(2)	1265(1)	4742(1)	6231(1)	26(1)
O(21)	4471(2)	2350(2)	629(2)	22(1)
O(22)	1065(2)	-1315(1)	204(2)	21(1)
O(23)	4710(2)	4106(2)	2156(2)	29(1)
O(24)	-18(2)	-926(2)	1543(2)	24(1)
C(21)	3164(2)	2306(2)	1833(2)	20(1)
C(22)	2538(2)	1069(2)	1134(2)	20(1)
C(23)	1614(2)	677(2)	1610(2)	17(1)

C(24)	831(2)	1653(2)	3344(2)	20(1)
C(25)	773(2)	2572(2)	4352(2)	21(1)
C(26)	1527(2)	3789(2)	4931(2)	21(1)
C(27)	2513(3)	4356(2)	4618(2)	24(1)
C(28)	2991(2)	3898(2)	3685(2)	21(1)
C(29)	1627(2)	1670(2)	2629(2)	18(1)
C(30)	2626(2)	2720(2)	2777(2)	18(1)
C(31)	4173(2)	3029(2)	1585(2)	22(1)
C(32)	5430(3)	2979(2)	276(3)	27(1)
C(33)	5630(3)	2048(2)	-785(2)	27(1)
C(34)	803(2)	-568(2)	1144(2)	18(1)
C(35)	285(2)	-2563(2)	-311(2)	21(1)
C(36)	680(3)	-3257(2)	-1359(2)	25(1)

Table I.2. Bond lengths [Å] for **3**.

S(1)-C(6)	1.765(3)	C(8)-C(10)	1.397(3)
S(1)-H(1S)	1.23(3)	C(9)-C(10)	1.477(3)
O(1)-C(11)	1.340(3)	C(12)-C(13)	1.506(3)
O(1)-C(12)	1.451(3)	C(15)-C(16)	1.498(3)
O(2)-C(14)	1.346(3)	S(2)-C(26)	1.758(2)
O(2)-C(15)	1.453(3)	S(2)-H(2S)	1.26(3)
O(3)-C(11)	1.217(3)	O(21)-C(31)	1.346(3)
O(4)-C(14)	1.217(3)	O(21)-C(32)	1.446(3)
C(1)-C(2)	1.401(3)	O(22)-C(34)	1.342(3)
C(1)-C(10)	1.415(3)	O(22)-C(35)	1.447(3)
C(1)-C(11)	1.464(3)	O(23)-C(31)	1.216(3)
C(2)-C(3)	1.396(3)	O(24)-C(34)	1.221(3)
C(3)-C(9)	1.416(3)	C(21)-C(22)	1.403(3)
C(3)-C(14)	1.462(3)	C(21)-C(30)	1.420(3)
C(4)-C(5)	1.375(3)	C(21)-C(31)	1.463(3)
C(4)-C(9)	1.390(3)	C(22)-C(23)	1.394(3)
C(5)-C(6)	1.405(3)	C(23)-C(29)	1.415(3)
C(6)-C(7)	1.406(3)	C(23)-C(34)	1.462(3)
C(7)-C(8)	1.376(3)	C(24)-C(25)	1.388(3)

C(24)-C(29)	1.396(3)	C(28)-C(30)	1.403(3)
C(25)-C(26)	1.406(3)	C(29)-C(30)	1.469(3)
C(26)-C(27)	1.397(3)	C(32)-C(33)	1.508(3)
C(27)-C(28)	1.374(3)	C(35)-C(36)	1.498(3)

Table I.3. Bond angles [°] for **3**.

C(6)-S(1)-H(1S)	100(1)	O(4)-C(14)-C(3)	126.2(2)
C(11)-O(1)-C(12)	116.4(2)	O(2)-C(14)-C(3)	111.7(2)
C(14)-O(2)-C(15)	114.4(2)	O(2)-C(15)-C(16)	107.2(2)
C(2)-C(1)-C(10)	108.3(2)	C(26)-S(2)-H(2S)	98(1)
C(2)-C(1)-C(11)	124.5(2)	C(31)-O(21)-C(32)	116.4(2)
C(10)-C(1)-C(11)	127.1(2)	C(34)-O(22)-C(35)	115.0(2)
C(3)-C(2)-C(1)	109.7(2)	C(22)-C(21)-C(30)	108.5(2)
C(2)-C(3)-C(9)	108.8(2)	C(22)-C(21)-C(31)	124.6(2)
C(2)-C(3)-C(14)	125.5(2)	C(30)-C(21)-C(31)	126.9(2)
C(9)-C(3)-C(14)	125.7(2)	C(23)-C(22)-C(21)	109.4(2)
C(5)-C(4)-C(9)	130.8(2)	C(22)-C(23)-C(29)	108.8(2)
C(4)-C(5)-C(6)	128.7(2)	C(22)-C(23)-C(34)	125.0(2)
C(5)-C(6)-C(7)	127.8(2)	C(29)-C(23)-C(34)	126.2(2)
C(5)-C(6)-S(1)	118.2(2)	C(25)-C(24)-C(29)	130.5(2)
C(7)-C(6)-S(1)	114.1(2)	C(24)-C(25)-C(26)	128.5(2)
C(8)-C(7)-C(6)	129.2(2)	C(27)-C(26)-C(25)	127.8(2)
C(7)-C(8)-C(10)	130.3(2)	C(27)-C(26)-S(2)	114.0(2)
C(4)-C(9)-C(3)	126.9(2)	C(25)-C(26)-S(2)	118.2(2)
C(4)-C(9)-C(10)	126.7(2)	C(28)-C(27)-C(26)	130.1(2)
C(3)-C(9)-C(10)	106.4(2)	C(27)-C(28)-C(30)	129.6(2)
C(8)-C(10)-C(1)	126.7(2)	C(24)-C(29)-C(23)	126.4(2)
C(8)-C(10)-C(9)	126.4(2)	C(24)-C(29)-C(30)	126.8(2)
C(1)-C(10)-C(9)	106.9(2)	C(23)-C(29)-C(30)	106.8(2)
O(3)-C(11)-O(1)	122.9(2)	C(28)-C(30)-C(21)	126.7(2)
O(3)-C(11)-C(1)	125.4(2)	C(28)-C(30)-C(29)	126.8(2)
O(1)-C(11)-C(1)	111.7(2)	C(21)-C(30)-C(29)	106.6(2)
O(1)-C(12)-C(13)	106.9(2)	O(23)-C(31)-O(21)	122.3(2)
O(4)-C(14)-O(2)	122.1(2)	O(23)-C(31)-C(21)	126.1(2)

O(21)-C(31)-C(21)	111.6(2)
O(21)-C(32)-C(33)	107.3(2)
O(24)-C(34)-O(22)	122.0(2)
O(24)-C(34)-C(23)	125.9(2)
O(22)-C(34)-C(23)	112.0(2)
O(22)-C(35)-C(36)	107.9(2)

Table I.4. Anisotropic displacement parameters ($Å^2 \times 10^3$)for **3**. The anisotropic displacement factor exponent takes the form: $-2\pi^2[h^2 a^{*2} U_{11} + ... + 2 h k a^* b^* U_{12}]$

	U_{11}	U_{22}	U_{33}	U_{23}	U_{13}	U_{12}
S(1)	29(1)	16(1)	25(1)	2(1)	13(1)	1(1)
O(1)	23(1)	19(1)	28(1)	7(1)	15(1)	0(1)
O(2)	27(1)	9(1)	25(1)	1(1)	13(1)	-2(1)
O(3)	26(1)	16(1)	31(1)	5(1)	12(1)	-4(1)
O(4)	25(1)	18(1)	29(1)	6(1)	14(1)	-2(1)
C(1)	18(1)	15(1)	22(1)	6(1)	6(1)	1(1)
C(2)	20(1)	16(1)	19(1)	5(1)	7(1)	2(1)
C(3)	18(1)	14(1)	21(1)	5(1)	6(1)	2(1)
C(4)	21(1)	13(1)	22(1)	4(1)	6(1)	0(1)
C(5)	23(1)	17(1)	26(1)	7(1)	10(1)	0(1)
C(6)	20(1)	15(1)	23(1)	6(1)	9(1)	3(1)
C(7)	21(1)	14(1)	23(1)	3(1)	4(1)	0(1)
C(8)	20(1)	12(1)	22(1)	4(1)	6(1)	-2(1)
C(9)	15(1)	13(1)	20(1)	5(1)	6(1)	1(1)
C(10)	16(1)	13(1)	22(1)	6(1)	7(1)	1(1)
C(11)	18(1)	19(1)	21(1)	8(1)	6(1)	1(1)
C(12)	20(1)	22(1)	33(2)	12(1)	12(1)	-1(1)
C(13)	33(2)	27(2)	33(2)	13(1)	20(1)	6(1)
C(14)	20(1)	13(1)	18(1)	2(1)	7(1)	4(1)
C(15)	30(1)	8(1)	28(1)	1(1)	12(1)	-4(1)
C(16)	33(2)	15(1)	30(2)	2(1)	13(1)	0(1)

S(2)	32(1)	18(1)	24(1)	2(1)	14(1)	4(1)
O(21)	23(1)	16(1)	28(1)	5(1)	15(1)	0(1)
O(22)	22(1)	11(1)	24(1)	1(1)	11(1)	-3(1)
O(23)	31(1)	16(1)	36(1)	5(1)	16(1)	-3(1)
O(24)	27(1)	15(1)	26(1)	3(1)	14(1)	-5(1)
C(21)	18(1)	14(1)	22(1)	5(1)	5(1)	0(1)
C(22)	22(1)	16(1)	20(1)	5(1)	9(1)	4(1)
C(23)	14(1)	14(1)	19(1)	4(1)	4(1)	0(1)
C(24)	18(1)	14(1)	24(1)	6(1)	6(1)	-1(1)
C(25)	20(1)	17(1)	23(1)	6(1)	9(1)	2(1)
C(26)	26(1)	18(1)	18(1)	4(1)	9(1)	7(1)
C(27)	28(1)	11(1)	24(1)	3(1)	7(1)	-2(1)
C(28)	23(1)	13(1)	25(1)	4(1)	12(1)	-1(1)
C(29)	18(1)	14(1)	19(1)	5(1)	6(1)	2(1)
C(30)	17(1)	13(1)	21(1)	6(1)	6(1)	0(1)
C(31)	20(1)	18(1)	25(1)	8(1)	8(1)	3(1)
C(32)	23(1)	23(1)	33(2)	9(1)	15(1)	-1(1)
C(33)	26(1)	24(1)	31(2)	11(1)	14(1)	2(1)
C(34)	19(1)	16(1)	17(1)	4(1)	6(1)	2(1)
C(35)	20(1)	11(1)	25(1)	1(1)	9(1)	-3(1)
C(36)	27(1)	14(1)	29(1)	4(1)	10(1)	0(1)

Table I.5. Hydrogen coordinates (x 10^4) and isotropic displacement parameters (Å^2 x 10^3) for **3**.

	x	y	z	U(eq)
H(1S)	1430(30)	2720(20)	8770(20)	35(8)
H(2)	3941	-573	3006	23
H(4)	1260	-321	5491	24
H(5)	1097	1107	7043	27
H(7)	3961	3976	7653	26
H(8)	4758	3273	6191	24
H(12A)	7633	2153	3743	30

H(12B)	6557	2554	2855	30
H(13A)	7628	1362	1691	44
H(13B)	6081	663	1201	44
H(13C)	7176	284	2086	44
H(15A)	696	-3952	1961	29
H(15B)	1899	-4013	3047	29
H(16A)	1826	-5329	1109	42
H(16B)	3187	-4267	1761	42
H(16C)	1975	-4227	677	42
H(2S)	310(30)	4000(30)	6220(20)	34(8)
H(22)	2717	575	444	24
H(24)	231	889	3102	24
H(25)	142	2350	4696	25
H(27)	2916	5189	5132	28
H(28)	3670	4462	3648	25
H(32A)	6286	3387	985	32
H(32B)	5090	3597	14	32
H(33A)	6253	2449	-1067	40
H(33B)	4770	1632	-1470	40
H(33C)	5996	1458	-506	40
H(35A)	-679	-2616	-617	25
H(35B)	461	-2901	332	25
H(36A)	184	-4111	-1708	38
H(36B)	1640	-3181	-1050	38
H(36C)	474	-2933	-2003	38

Table I.6. Torsion angles [°] for **3**.

C(10)-C(1)-C(2)-C(3)	0.1(3)	C(5)-C(6)-C(7)-C(8)	-1.3(4)
C(11)-C(1)-C(2)-C(3)	179.4(2)	S(1)-C(6)-C(7)-C(8)	179.4(2)
C(1)-C(2)-C(3)-C(9)	0.4(3)	C(6)-C(7)-C(8)-C(10)	-0.9(5)
C(1)-C(2)-C(3)-C(14)	-176.5(2)	C(5)-C(4)-C(9)-C(3)	179.1(2)
C(9)-C(4)-C(5)-C(6)	-1.6(5)	C(5)-C(4)-C(9)-C(10)	-1.6(4)
C(4)-C(5)-C(6)-C(7)	3.2(4)	C(2)-C(3)-C(9)-C(4)	178.8(2)
C(4)-C(5)-C(6)-S(1)	-177.5(2)	C(14)-C(3)-C(9)-C(4)	-4.4(4)

C(2)-C(3)-C(9)-C(10)	-0.7(3)	C(25)-C(26)-C(27)-C(28)	0.6(5)
C(14)-C(3)-C(9)-C(10)	176.2(2)	S(2)-C(26)-C(27)-C(28)	179.0(2)
C(7)-C(8)-C(10)-C(1)	-179.0(2)	C(26)-C(27)-C(28)-C(30)	-0.3(5)
C(7)-C(8)-C(10)-C(9)	0.1(4)	C(25)-C(24)-C(29)-C(23)	179.9(2)
C(2)-C(1)-C(10)-C(8)	178.7(2)	C(25)-C(24)-C(29)-C(30)	-0.8(4)
C(11)-C(1)-C(10)-C(8)	-0.5(4)	C(22)-C(23)-C(29)-C(24)	179.0(2)
C(2)-C(1)-C(10)-C(9)	-0.5(3)	C(34)-C(23)-C(29)-C(24)	-2.7(4)
C(11)-C(1)-C(10)-C(9)	-179.8(2)	C(22)-C(23)-C(29)-C(30)	-0.4(3)
C(4)-C(9)-C(10)-C(8)	2.0(4)	C(34)-C(23)-C(29)-C(30)	177.9(2)
C(3)-C(9)-C(10)-C(8)	-178.5(2)	C(27)-C(28)-C(30)-C(21)	179.9(3)
C(4)-C(9)-C(10)-C(1)	-178.7(2)	C(27)-C(28)-C(30)-C(29)	-1.0(4)
C(3)-C(9)-C(10)-C(1)	0.8(3)	C(22)-C(21)-C(30)-C(28)	179.2(2)
C(12)-O(1)-C(11)-O(3)	0.0(3)	C(31)-C(21)-C(30)-C(28)	-2.3(4)
C(12)-O(1)-C(11)-C(1)	-179.5(2)	C(22)-C(21)-C(30)-C(29)	0.0(3)
C(2)-C(1)-C(11)-O(3)	-178.9(2)	C(31)-C(21)-C(30)-C(29)	178.5(2)
C(10)-C(1)-C(11)-O(3)	0.3(4)	C(24)-C(29)-C(30)-C(28)	1.6(4)
C(2)-C(1)-C(11)-O(1)	0.6(3)	C(23)-C(29)-C(30)-C(28)	-179.0(2)
C(10)-C(1)-C(11)-O(1)	179.7(2)	C(24)-C(29)-C(30)-C(21)	-179.2(2)
C(11)-O(1)-C(12)-C(13)	-177.3(2)	C(23)-C(29)-C(30)-C(21)	0.2(3)
C(15)-O(2)-C(14)-O(4)	-6.2(3)	C(32)-O(21)-C(31)-O(23)	-2.5(3)
C(15)-O(2)-C(14)-C(3)	172.3(2)	C(32)-O(21)-C(31)-C(21)	178.1(2)
C(2)-C(3)-C(14)-O(4)	179.5(2)	C(22)-C(21)-C(31)-O(23)	178.2(2)
C(9)-C(3)-C(14)-O(4)	3.1(4)	C(30)-C(21)-C(31)-O(23)	-0.1(4)
C(2)-C(3)-C(14)-O(2)	1.0(3)	C(22)-C(21)-C(31)-O(21)	-2.4(3)
C(9)-C(3)-C(14)-O(2)	-175.4(2)	C(30)-C(21)-C(31)-O(21)	179.2(2)
C(14)-O(2)-C(15)-C(16)	-176.9(2)	C(31)-O(21)-C(32)-C(33)	178.9(2)
C(30)-C(21)-C(22)-C(23)	-0.2(3)	C(35)-O(22)-C(34)-O(24)	1.2(3)
C(31)-C(21)-C(22)-C(23)	-178.8(2)	C(35)-O(22)-C(34)-C(23)	-179.4(2)
C(21)-C(22)-C(23)-C(29)	0.4(3)	C(22)-C(23)-C(34)-O(24)	-179.4(2)
C(21)-C(22)-C(23)-C(34)	-178.0(2)	C(29)-C(23)-C(34)-O(24)	2.5(4)
C(29)-C(24)-C(25)-C(26)	-0.3(5)	C(22)-C(23)-C(34)-O(22)	1.2(3)
C(24)-C(25)-C(26)-C(27)	0.2(4)	C(29)-C(23)-C(34)-O(22)	-176.8(2)
C(24)-C(25)-C(26)-S(2)	-178.2(2)	C(34)-O(22)-C(35)-C(36)	178.7(2)

Appendix J. Crystallographic data for **6**.

Table J.1. Atomic coordinates (x 10^4) and equivalent isotropic displacement parameters ($Å^2$ x 10^3) for **6**. U(eq) is defined as one third of the trace of the orthogonalized U_{ij} tensor.

	x	y	z	U(eq)
Au(1)	5005(1)	1155(1)	2511(1)	14(1)
Au(2)	4996(1)	2409(1)	2492(1)	13(1)
S(1)	6440(1)	1167(1)	2635(1)	17(1)
S(2)	6039(1)	2504(1)	3992(1)	16(1)
P(1)	3544(1)	1221(1)	2094(1)	13(1)
P(2)	3963(1)	2229(1)	1054(1)	12(1)
O(1)	7860(3)	1154(2)	1897(3)	22(1)
O(2)	8965(3)	563(2)	2357(3)	28(1)
O(3)	5926(2)	388(2)	4304(3)	25(1)
O(4)	5296(3)	-314(2)	3338(3)	34(1)
O(21)	6143(2)	2574(2)	6158(3)	20(1)
O(22)	4831(3)	2923(2)	5948(3)	35(1)
O(23)	6640(2)	3370(2)	2749(3)	21(1)
O(24)	5655(3)	4041(2)	2228(3)	30(1)
C(1)	7670(3)	348(2)	2676(4)	17(1)
C(2)	6898(3)	516(2)	2857(4)	16(1)
C(3)	6611(3)	50(2)	3262(4)	14(1)
C(4)	7121(4)	-900(2)	3779(4)	21(1)
C(5)	7658(4)	-1353(2)	3916(4)	22(1)
C(6)	8368(4)	-1435(2)	3638(4)	23(1)
C(7)	8736(4)	-1073(2)	3162(4)	21(1)
C(8)	8526(3)	-531(2)	2885(4)	18(1)
C(9)	7166(4)	-393(3)	3345(5)	18(1)
C(10)	7854(3)	-210(2)	2968(4)	17(1)
C(11)	8236(4)	684(2)	2301(4)	20(1)
C(12)	8411(4)	1542(3)	1634(4)	20(1)
C(13)	8986(4)	1835(3)	2526(5)	31(2)
C(14)	5863(3)	21(2)	3608(4)	17(1)
C(15)	5271(4)	383(3)	4753(4)	25(1)

C(16)	5654(4)	173(3)	5765(4)	29(1)
C(21)	5697(3)	3331(2)	5125(4)	16(1)
C(22)	5922(3)	3193(2)	4310(4)	16(1)
C(23)	5969(3)	3688(2)	3817(4)	17(1)
C(24)	5714(4)	4690(2)	4038(4)	24(1)
C(25)	5511(4)	5151(2)	4491(4)	25(1)
C(26)	5302(4)	5174(3)	5321(4)	27(1)
C(27)	5201(4)	4750(2)	5914(4)	25(1)
C(28)	5329(3)	4189(2)	5837(4)	21(1)
C(29)	5764(3)	4139(2)	4317(4)	18(1)
C(30)	5581(3)	3905(2)	5156(4)	17(1)
C(31)	5497(4)	2927(2)	5774(4)	19(1)
C(32)	5987(4)	2135(2)	6744(4)	24(1)
C(33)	5473(5)	1669(3)	6139(5)	33(2)
C(34)	6067(4)	3729(2)	2865(4)	18(1)
C(35)	6602(4)	3260(2)	1772(4)	20(1)
C(36)	7191(4)	2785(3)	1811(4)	24(1)
C(41)	3119(3)	1773(2)	1201(4)	15(1)
C(51)	3018(3)	583(2)	1517(4)	17(1)
C(52)	3393(4)	397(2)	734(4)	23(1)
C(53)	3030(4)	-161(2)	309(4)	28(1)
C(54)	3151(4)	-601(3)	1080(5)	31(2)
C(55)	2740(5)	-415(3)	1805(5)	21(2)
C(56)	3143(4)	127(2)	2270(4)	20(1)
C(61)	3104(3)	1366(2)	3065(4)	16(1)
C(62)	2116(3)	1334(2)	2732(4)	16(1)
C(63)	1783(5)	1444(3)	3558(5)	26(2)
C(64)	2107(4)	1984(3)	4058(4)	30(2)
C(65)	3088(4)	2003(3)	4411(4)	26(1)
C(66)	3435(4)	1910(2)	3574(4)	18(1)
C(71)	3392(3)	2839(2)	407(4)	15(1)
C(72)	2946(4)	3141(2)	1022(4)	19(1)
C(73)	2526(4)	3680(2)	560(4)	21(1)
C(74)	3157(4)	4055(2)	286(4)	21(1)
C(75)	3559(3)	3748(2)	-350(4)	18(1)
C(76)	4020(4)	3230(2)	141(4)	15(1)

C(81)	4403(3)	1829(2)	258(3)	13(1)
C(82)	5319(3)	2015(2)	351(4)	18(1)
C(83)	5686(4)	1653(2)	-268(4)	21(1)
C(84)	5087(4)	1644(2)	-1309(4)	24(1)
C(85)	4189(4)	1448(3)	-1382(4)	24(1)
C(86)	3799(4)	1806(2)	-784(4)	19(1)

Table J.2. Bond lengths [Å] for **6**.

Au(1)-P(1)	2.277(2)	C(1)-C(2)	1.441(7)
Au(1)-S(1)	2.304(2)	C(1)-C(11)	1.476(7)
Au(1)-Au(2)	3.0360(4)	C(2)-C(3)	1.430(7)
Au(2)-P(2)	2.273(1)	C(3)-C(9)	1.387(8)
Au(2)-S(2)	2.313(1)	C(3)-C(14)	1.483(7)
S(1)-C(2)	1.728(6)	C(4)-C(5)	1.382(8)
S(2)-C(22)	1.762(5)	C(4)-C(9)	1.397(8)
P(1)-C(51)	1.834(6)	C(5)-C(6)	1.375(8)
P(1)-C(41)	1.842(5)	C(6)-C(7)	1.384(8)
P(1)-C(61)	1.844(5)	C(7)-C(8)	1.383(8)
P(2)-C(71)	1.837(5)	C(8)-C(10)	1.389(7)
P(2)-C(41)	1.841(5)	C(9)-C(10)	1.485(8)
P(2)-C(81)	1.847(5)	C(12)-C(13)	1.517(8)
O(1)-C(11)	1.338(7)	C(15)-C(16)	1.503(8)
O(1)-C(12)	1.444(7)	C(21)-C(30)	1.406(7)
O(2)-C(11)	1.209(7)	C(21)-C(22)	1.412(8)
O(3)-C(14)	1.337(6)	C(21)-C(31)	1.481(8)
O(3)-C(15)	1.442(6)	C(22)-C(23)	1.417(7)
O(4)-C(14)	1.198(6)	C(23)-C(29)	1.422(8)
O(21)-C(31)	1.334(7)	C(23)-C(34)	1.471(7)
O(21)-C(32)	1.448(6)	C(24)-C(29)	1.390(8)
O(22)-C(31)	1.205(7)	C(24)-C(25)	1.399(8)
O(23)-C(34)	1.335(7)	C(25)-C(26)	1.381(8)
O(23)-C(35)	1.448(6)	C(26)-C(27)	1.396(8)
O(24)-C(34)	1.219(6)	C(27)-C(28)	1.385(8)
C(1)-C(10)	1.421(8)	C(28)-C(30)	1.391(8)

C(29)-C(30)	1.481(8)	C(65)-C(66)	1.542(8)
C(32)-C(33)	1.509(8)	C(71)-C(72)	1.531(7)
C(35)-C(36)	1.492(8)	C(71)-C(76)	1.545(8)
C(51)-C(56)	1.532(8)	C(72)-C(73)	1.527(7)
C(51)-C(52)	1.548(8)	C(73)-C(74)	1.531(8)
C(52)-C(53)	1.525(8)	C(74)-C(75)	1.513(7)
C(53)-C(54)	1.521(9)	C(75)-C(76)	1.518(7)
C(54)-C(55)	1.514(9)	C(81)-C(86)	1.527(7)
C(55)-C(56)	1.526(8)	C(81)-C(82)	1.533(7)
C(61)-C(66)	1.524(7)	C(82)-C(83)	1.529(7)
C(61)-C(62)	1.533(7)	C(83)-C(84)	1.523(8)
C(62)-C(63)	1.519(9)	C(84)-C(85)	1.520(8)
C(63)-C(64)	1.508(10)	C(85)-C(86)	1.522(8)
C(64)-C(65)	1.519(8)		

Table J.3. Bond angles [°] for **6**.

P(1)-Au(1)-S(1)	168.47(5)	C(41)-P(2)-Au(2)	111.2(2)
P(1)-Au(1)-Au(2)	85.76(4)	C(81)-P(2)-Au(2)	111.5(2)
S(1)-Au(1)-Au(2)	89.46(4)	C(11)-O(1)-C(12)	115.9(5)
P(2)-Au(2)-S(2)	174.51(6)	C(14)-O(3)-C(15)	118.1(4)
P(2)-Au(2)-Au(1)	79.44(4)	C(31)-O(21)-C(32)	116.7(4)
S(2)-Au(2)-Au(1)	95.20(4)	C(34)-O(23)-C(35)	116.8(4)
C(2)-S(1)-Au(1)	111.9(2)	C(10)-C(1)-C(2)	108.9(5)
C(22)-S(2)-Au(2)	103.7(2)	C(10)-C(1)-C(11)	122.8(5)
C(51)-P(1)-C(41)	105.8(3)	C(2)-C(1)-C(11)	128.3(5)
C(51)-P(1)-C(61)	106.0(2)	C(3)-C(2)-C(1)	106.7(5)
C(41)-P(1)-C(61)	105.4(2)	C(3)-C(2)-S(1)	128.0(4)
C(51)-P(1)-Au(1)	110.9(2)	C(1)-C(2)-S(1)	125.2(4)
C(41)-P(1)-Au(1)	110.9(2)	C(9)-C(3)-C(2)	110.4(5)
C(61)-P(1)-Au(1)	117.1(2)	C(9)-C(3)-C(14)	122.0(5)
C(71)-P(2)-C(41)	105.7(2)	C(2)-C(3)-C(14)	127.5(5)
C(71)-P(2)-C(81)	109.3(2)	C(5)-C(4)-C(9)	129.4(6)
C(41)-P(2)-C(81)	103.4(2)	C(6)-C(5)-C(4)	129.5(6)
C(71)-P(2)-Au(2)	115.0(2)	C(5)-C(6)-C(7)	128.3(6)

C(8)-C(7)-C(6)	130.1(6)	C(27)-C(28)-C(30)	129.3(6)
C(7)-C(8)-C(10)	129.1(6)	C(24)-C(29)-C(23)	125.7(5)
C(3)-C(9)-C(4)	125.8(6)	C(24)-C(29)-C(30)	127.4(5)
C(3)-C(9)-C(10)	107.3(5)	C(23)-C(29)-C(30)	106.9(5)
C(4)-C(9)-C(10)	126.7(6)	C(28)-C(30)-C(21)	126.1(5)
C(8)-C(10)-C(1)	126.8(5)	C(28)-C(30)-C(29)	127.5(5)
C(8)-C(10)-C(9)	126.5(5)	C(21)-C(30)-C(29)	106.5(5)
C(1)-C(10)-C(9)	106.7(5)	O(22)-C(31)-O(21)	123.6(5)
O(2)-C(11)-O(1)	122.4(5)	O(22)-C(31)-C(21)	124.0(5)
O(2)-C(11)-C(1)	125.2(5)	O(21)-C(31)-C(21)	112.4(5)
O(1)-C(11)-C(1)	112.4(5)	O(21)-C(32)-C(33)	111.7(5)
O(1)-C(12)-C(13)	109.6(5)	O(24)-C(34)-O(23)	122.5(5)
O(4)-C(14)-O(3)	123.9(5)	O(24)-C(34)-C(23)	124.7(5)
O(4)-C(14)-C(3)	124.0(5)	O(23)-C(34)-C(23)	112.8(5)
O(3)-C(14)-C(3)	112.0(4)	O(23)-C(35)-C(36)	107.0(4)
O(3)-C(15)-C(16)	109.4(5)	P(2)-C(41)-P(1)	113.6(3)
C(30)-C(21)-C(22)	109.8(5)	C(56)-C(51)-C(52)	110.0(5)
C(30)-C(21)-C(31)	124.7(5)	C(56)-C(51)-P(1)	110.0(4)
C(22)-C(21)-C(31)	125.0(5)	C(52)-C(51)-P(1)	110.4(4)
C(21)-C(22)-C(23)	108.2(5)	C(53)-C(52)-C(51)	111.5(5)
C(21)-C(22)-S(2)	122.3(4)	C(54)-C(53)-C(52)	112.1(5)
C(23)-C(22)-S(2)	129.4(5)	C(55)-C(54)-C(53)	110.1(5)
C(22)-C(23)-C(29)	108.6(5)	C(54)-C(55)-C(56)	110.2(5)
C(22)-C(23)-C(34)	126.2(5)	C(82)-C(81)-P(2)	111.9(3)
C(29)-C(23)-C(34)	124.5(5)	C(83)-C(82)-C(81)	110.5(4)
C(29)-C(24)-C(25)	128.6(6)	C(84)-C(83)-C(82)	111.1(5)
C(26)-C(25)-C(24)	128.8(6)	C(85)-C(84)-C(83)	111.0(5)
C(25)-C(26)-C(27)	130.1(6)	C(84)-C(85)-C(86)	111.6(5)
C(28)-C(27)-C(26)	128.1(5)	C(85)-C(86)-C(81)	110.4(4
C(55)-C(56)-C(51)	111.2(5)	C(63)-C(62)-C(61)	111.1(5)
C(66)-C(61)-C(62)	111.6(4)	C(64)-C(63)-C(62)	112.5(6)
C(66)-C(61)-P(1)	112.4(4)	C(63)-C(64)-C(65)	110.7(5)
C(62)-C(61)-P(1)	112.9(4)	C(64)-C(65)-C(66)	110.9(5)
C(61)-C(66)-C(65)	110.8(5)		
C(72)-C(71)-C(76)	110.7(4)		
C(72)-C(71)-P(2)	109.7(4)		

C(76)-C(71)-P(2)	110.9(3)
C(73)-C(72)-C(71)	112.2(4)
C(72)-C(73)-C(74)	112.3(5)
C(75)-C(74)-C(73)	110.5(4)
C(74)-C(75)-C(76)	111.2(5)
C(75)-C(76)-C(71)	111.0(4)
C(86)-C(81)-C(82)	112.8(4)
C(86)-C(81)-P(2)	113.6(4)

Table J.4. Anisotropic displacement parameters ($Å^2 \times 10^3$) for **6**. The anisotropic displacement factor exponent takes the form: $-2\pi^2[h^2 a^{*2} U_{11} + ... + 2 h k a^* b^* U_{12}]$

	U_{11}	U_{22}	U_{33}	U_{23}	U_{13}	U_{12}
Au(1)	12(1)	14(1)	14(1)	1(1)	2(1)	0(1)
Au(2)	14(1)	14(1)	10(1)	0(1)	3(1)	-1(1)
S(1)	13(1)	13(1)	24(1)	2(1)	5(1)	0(1)
S(2)	18(1)	15(1)	12(1)	-1(1)	1(1)	2(1)
P(1)	13(1)	13(1)	13(1)	2(1)	2(1)	1(1)
P(2)	14(1)	12(1)	10(1)	1(1)	3(1)	0(1)
O(1)	25(2)	19(2)	25(2)	5(2)	13(2)	0(2)
O(2)	21(2)	30(2)	35(2)	5(2)	14(2)	5(2)
O(3)	21(2)	35(2)	20(2)	-5(2)	9(2)	-6(2)
O(4)	27(2)	25(2)	57(3)	-15(2)	25(2)	-7(2)
O(21)	20(2)	23(2)	15(2)	4(2)	7(2)	0(2)
O(22)	32(3)	35(3)	48(3)	16(2)	28(2)	12(2)
O(23)	17(2)	31(2)	13(2)	-2(2)	3(2)	-1(2)
O(24)	41(3)	26(2)	22(2)	6(2)	10(2)	6(2)
C(1)	13(2)	21(3)	19(3)	-4(2)	7(2)	-3(2)
C(2)	14(3)	21(3)	12(3)	-2(2)	1(2)	-4(2)
C(3)	12(2)	15(3)	14(2)	1(2)	2(2)	-1(2)
C(4)	16(3)	25(3)	21(3)	2(2)	5(2)	-4(2)
C(5)	25(3)	18(3)	24(3)	1(2)	8(2)	-6(2)
C(6)	19(3)	17(3)	27(3)	-3(2)	-1(2)	0(2)
C(7)	15(3)	24(3)	21(3)	-8(2)	1(2)	3(2)

C(8)	12(3)	24(3)	17(3)	-9(2)	2(2)	0(2)
C(9)	15(3)	19(3)	15(3)	-2(2)	1(2)	-3(2)
C(10)	13(3)	21(3)	14(2)	-4(2)	2(2)	0(2)
C(11)	25(3)	18(3)	17(3)	-2(2)	7(2)	-1(2)
C(12)	21(3)	23(3)	19(3)	5(3)	12(3)	-3(3)
C(13)	38(4)	27(4)	36(4)	-6(3)	20(3)	-15(3)
C(14)	18(3)	10(3)	22(3)	6(2)	7(2)	3(2)
C(15)	21(3)	36(4)	19(3)	-4(3)	7(2)	-6(3)
C(16)	36(4)	32(4)	23(3)	4(3)	15(3)	0(3)
C(21)	11(3)	15(3)	19(3)	1(2)	1(2)	0(2)
C(22)	12(3)	13(3)	17(3)	-8(2)	-1(2)	0(2)
C(23)	8(2)	27(3)	14(3)	0(2)	0(2)	0(2)
C(24)	21(3)	28(3)	20(3)	3(3)	2(2)	-3(3)
C(25)	22(3)	20(3)	26(3)	1(2)	1(2)	1(2)
C(26)	22(3)	23(3)	31(3)	-4(3)	2(3)	5(3)
C(27)	24(3)	30(3)	17(3)	-7(2)	3(2)	8(3)
C(28)	14(3)	30(3)	16(3)	0(2)	1(2)	4(2)
C(29)	12(3)	21(3)	18(3)	-1(2)	-1(2)	-2(2)
C(30)	13(3)	19(3)	15(3)	1(2)	-1(2)	0(2)
C(31)	20(3)	18(3)	19(3)	-4(2)	7(2)	0(2)
C(32)	24(3)	25(3)	21(3)	5(2)	7(2)	0(3)
C(33)	44(4)	21(4)	33(4)	3(3)	13(3)	-5(3)
C(34)	17(3)	13(3)	20(3)	0(2)	2(2)	-4(2)
C(35)	22(3)	26(3)	12(3)	2(2)	6(2)	-3(2)
C(36)	19(3)	35(4)	17(3)	-5(3)	4(2)	-6(3)
C(41)	13(2)	18(3)	13(2)	1(2)	3(2)	0(2)
C(51)	14(3)	17(3)	18(3)	-1(2)	4(2)	0(2)
C(52)	23(3)	22(3)	24(3)	-4(2)	6(2)	-3(2)
C(53)	27(3)	29(3)	28(3)	-13(3)	8(3)	-3(3)
C(54)	27(3)	19(3)	41(4)	-14(3)	4(3)	-3(3)
C(55)	26(4)	9(3)	27(4)	0(2)	8(3)	-6(3)
C(56)	22(3)	11(3)	22(3)	-2(2)	0(2)	-3(2)
C(61)	17(3)	17(3)	13(2)	3(2)	6(2)	0(2)
C(62)	15(3)	18(3)	13(3)	1(2)	4(2)	1(2)
C(63)	20(3)	34(4)	23(3)	9(3)	6(3)	6(3)
C(64)	31(4)	40(4)	23(3)	-8(3)	14(3)	1(3)

C(65)	34(3)	24(3)	19(3)	-1(2)	9(3)	-5(3)
C(66)	23(3)	17(3)	15(3)	-1(2)	6(2)	-4(2)
C(71)	12(2)	16(3)	14(3)	2(2)	1(2)	5(2)
C(72)	22(3)	18(3)	20(3)	1(2)	9(2)	2(2)
C(73)	23(3)	16(3)	21(3)	0(2)	5(2)	7(2)
C(74)	25(3)	16(3)	14(3)	1(2)	-1(2)	4(2)
C(75)	18(3)	18(3)	16(3)	2(2)	5(2)	-2(2)
C(76)	15(3)	14(3)	15(3)	3(2)	4(2)	-1(2)
C(81)	17(3)	11(2)	8(2)	-2(2)	3(2)	3(2)
C(82)	16(3)	17(3)	19(3)	2(2)	6(2)	1(2)
C(83)	25(3)	20(3)	20(3)	1(2)	11(2)	3(2)
C(84)	36(4)	21(3)	20(3)	0(2)	15(3)	7(3)
C(85)	29(3)	22(3)	16(3)	-1(2)	1(2)	4(3)
C(86)	23(3)	21(3)	10(2)	0(2)	2(2)	0(2)

Table J.5. Hydrogen coordinates (x 10^4) and isotropic displacement parameters (Å^{2}x 10^3) for **6**.

	x	y	z	U(eq)
H(4)	6652	-937	4014	25
H(5)	7517	-1653	4251	27
H(6)	8641	-1785	3792	28
H(7)	9207	-1218	3001	26
H(8)	8893	-353	2596	22
H(12A)	8052	1816	1173	23
H(12B)	8770	1344	1319	23
H(13A)	9300	2133	2339	47
H(13B)	9399	1571	2937	47
H(13C)	8631	1990	2880	47
H(15A)	4786	142	4384	30
H(15B)	5043	761	4759	30
H(16A)	5221	194	6086	44
H(16B)	6155	399	6116	44

H(16C)	5835	-212	5753	44
H(24)	5834	4762	3463	29
H(25)	5519	5496	4186	30
H(26)	5214	5536	5521	33
H(27)	5021	4859	6435	30
H(28)	5231	3966	6319	25
H(32A)	5668	2285	7152	28
H(32B)	6546	1990	7174	28
H(33A)	5462	1355	6554	49
H(33B)	5742	1556	5668	49
H(33C)	4881	1794	5802	49
H(35A)	6790	3588	1496	24
H(35B)	6004	3166	1367	24
H(36A)	7166	2688	1158	36
H(36B)	7010	2466	2108	36
H(36C)	7783	2887	2194	36
H(41A)	2800	1603	573	18
H(41B)	2705	1999	1398	18
H(51)	2386	655	1207	20
H(52A)	3254	676	216	28
H(52B)	4030	371	1019	28
H(53A)	2407	-121	-57	34
H(53B)	3322	-282	-144	34
H(54A)	2883	-951	778	37
H(54B)	3775	-668	1409	37
H(55A)	2825	-702	2306	25
H(55B)	2111	-364	1481	25
H(56A)	3767	71	2612	24
H(56B)	2874	242	2748	24
H(61)	3325	1068	3555	19
H(62A)	1867	1609	2216	19
H(62B)	1927	962	2463	19
H(63A)	1144	1449	3309	31
H(63B)	1968	1139	4030	31
H(64A)	1899	2028	4610	36
H(64B)	1874	2294	3608	36

H(65A)	3320	1715	4905	31
H(65B)	3286	2367	4711	31
H(66A)	3249	2218	3110	22
H(66B)	4074	1906	3825	22
H(71)	2941	2714	-199	18
H(72A)	2498	2897	1119	23
H(72B)	3375	3222	1661	23
H(73A)	2303	3879	1014	25
H(73B)	2029	3595	-23	25
H(74A)	2846	4384	-57	25
H(74B)	3615	4181	876	25
H(75A)	3976	3993	-506	21
H(75B)	3104	3646	-959	21
H(76A)	4499	3333	730	18
H(76B)	4271	3036	-294	18
H(81)	4458	1441	499	15
H(82A)	5307	2405	145	21
H(82B)	5696	1990	1032	21
H(83A)	6258	1796	-239	25
H(83B)	5765	1271	-11	25
H(84A)	5050	2020	-1585	29
H(84B)	5328	1395	-1687	29
H(85A)	4221	1061	-1157	29
H(85B)	3809	1458	-2063	29
H(86A)	3235	1651	-809	23
H(86B)	3701	2184	-1055	23

Table J.6. Torsion angles [°] for **6**.

P(1)-Au(1)-Au(2)-P(2)	-48.97(5)	P(1)-Au(1)-S(1)-C(2)	-123.4(3)
S(1)-Au(1)-Au(2)-P(2)	120.52(6)	Au(2)-Au(1)-S(1)-C(2)	171.2(2)
P(1)-Au(1)-Au(2)-S(2)	129.80(6)	P(2)-Au(2)-S(2)-C(22)	-150.0(6)
S(1)-Au(1)-Au(2)-S(2)	-60.71(6)	Au(1)-Au(2)-S(2)-C(22)	-162.7(2)

S(1)-Au(1)-P(1)-C(51)	92.3(3)	C(2)-C(1)-C(10)-C(9)	-0.1(6)
Au(2)-Au(1)-P(1)-C(51)	158.0(2)	C(11)-C(1)-C(10)-C(9)	177.1(5)
S(1)-Au(1)-P(1)-C(41)	-25.0(3)	C(3)-C(9)-C(10)-C(8)	-177.5(5)
Au(2)-Au(1)-P(1)-C(41)	40.8(2)	C(4)-C(9)-C(10)-C(8)	7.4(10)
S(1)-Au(1)-P(1)-C(61)	-145.9(3)	C(3)-C(9)-C(10)-C(1)	0.3(6)
Au(2)-Au(1)-P(1)-C(61)	-80.1(2)	C(4)-C(9)-C(10)-C(1)	-174.8(6)
S(2)-Au(2)-P(2)-C(71)	161.6(6)	C(12)-O(1)-C(11)-O(2)	-7.3(8)
Au(1)-Au(2)-P(2)-C(71)	174.5(2)	C(12)-O(1)-C(11)-C(1)	171.6(5)
S(2)-Au(2)-P(2)-C(41)	41.5(7)	C(10)-C(1)-C(11)-O(2)	-13.6(9)
Au(1)-Au(2)-P(2)-C(41)	54.4(2)	C(2)-C(1)-C(11)-O(2)	162.9(6)
S(2)-Au(2)-P(2)-C(81)	-73.2(6)	C(10)-C(1)-C(11)-O(1)	167.6(5)
Au(1)-Au(2)-P(2)-C(81)	-60.3(2)	C(2)-C(1)-C(11)-O(1)	-15.9(8)
C(10)-C(1)-C(2)-C(3)	-0.2(6)	C(11)-O(1)-C(12)-C(13)	-76.6(6)
C(11)-C(1)-C(2)-C(3)	-177.1(5)	C(15)-O(3)-C(14)-O(4)	-0.3(8)
C(10)-C(1)-C(2)-S(1)	178.8(4)	C(15)-O(3)-C(14)-C(3)	-176.0(4)
C(11)-C(1)-C(2)-S(1)	1.8(8)	C(9)-C(3)-C(14)-O(4)	-57.8(8)
Au(1)-S(1)-C(2)-C(3)	-22.0(6)	C(2)-C(3)-C(14)-O(4)	125.7(6)
Au(1)-S(1)-C(2)-C(1)	159.3(4)	C(9)-C(3)-C(14)-O(3)	118.0(6)
C(1)-C(2)-C(3)-C(9)	0.4(6)	C(2)-C(3)-C(14)-O(3)	-58.6(7)
S(1)-C(2)-C(3)-C(9)	-178.5(5)	C(14)-O(3)-C(15)-C(16)	109.7(6)
C(1)-C(2)-C(3)-C(14)	177.3(5)	C(30)-C(21)-C(22)-C(23)	1.1(6)
S(1)-C(2)-C(3)-C(14)	-1.6(8)	C(31)-C(21)-C(22)-C(23)	173.5(5)
C(9)-C(4)-C(5)-C(6)	-2.1(11)	C(30)-C(21)-C(22)-S(2)	-175.2(4)
C(4)-C(5)-C(6)-C(7)	1.5(10)	C(31)-C(21)-C(22)-S(2)	-2.8(8)
C(5)-C(6)-C(7)-C(8)	3.7(10)	Au(2)-S(2)-C(22)-C(21)	118.4(4)
C(6)-C(7)-C(8)-C(10)	-3.6(10)	Au(2)-S(2)-C(22)-C(23)	-57.2(5)
C(2)-C(3)-C(9)-C(4)	174.7(6)	C(21)-C(22)-C(23)-C(29)	-0.6(6)
C(14)-C(3)-C(9)-C(4)	-2.4(9)	S(2)-C(22)-C(23)-C(29)	175.4(4)
C(2)-C(3)-C(9)-C(10)	-0.5(6)	C(21)-C(22)-C(23)-C(34)	-171.1(5)
C(14)-C(3)-C(9)-C(10)	-177.6(5)	S(2)-C(22)-C(23)-C(34)	4.9(8)
C(5)-C(4)-C(9)-C(3)	-178.0(6)	C(29)-C(24)-C(25)-C(26)	-0.7(10)
C(5)-C(4)-C(9)-C(10)	-3.7(10)	C(24)-C(25)-C(26)-C(27)	-2.9(11)
C(7)-C(8)-C(10)-C(1)	179.5(5)	C(25)-C(26)-C(27)-C(28)	3.5(10)
C(7)-C(8)-C(10)-C(9)	-3.1(9)	C(26)-C(27)-C(28)-C(30)	-0.6(10)
C(2)-C(1)-C(10)-C(8)	177.7(5)	C(25)-C(24)-C(29)-C(23)	179.6(5)
C(11)-C(1)-C(10)-C(8)	-5.1(8)	C(25)-C(24)-C(29)-C(30)	2.3(10)

C(22)-C(23)-C(29)-C(24)	-177.8(5)	Au(1)-P(1)-C(51)-C(56)	74.0(4)
C(34)-C(23)-C(29)-C(24)	-7.1(8)	C(41)-P(1)-C(51)-C(52)	72.8(4)
C(22)-C(23)-C(29)-C(30)	-0.1(6)	C(61)-P(1)-C(51)-C(52)	-175.6(4)
C(34)-C(23)-C(29)-C(30)	170.6(5)	Au(1)-P(1)-C(51)-C(52)	-47.5(4)
C(27)-C(28)-C(30)-C(21)	-179.9(6)	C(56)-C(51)-C(52)-C(53)	53.0(6)
C(27)-C(28)-C(30)-C(29)	-1.2(10)	P(1)-C(51)-C(52)-C(53)	174.5(4)
C(22)-C(21)-C(30)-C(28)	177.8(5)	C(51)-C(52)-C(53)-C(54)	-53.9(6)
C(31)-C(21)-C(30)-C(28)	5.3(9)	C(52)-C(53)-C(54)-C(55)	56.6(7)
C(22)-C(21)-C(30)-C(29)	-1.2(6)	C(53)-C(54)-C(55)-C(56)	-58.9(7)
C(31)-C(21)-C(30)-C(29)	-173.6(5)	C(54)-C(55)-C(56)-C(51)	59.7(7)
C(24)-C(29)-C(30)-C(28)	-0.5(9)	C(52)-C(51)-C(56)-C(55)	-56.1(6)
C(23)-C(29)-C(30)-C(28)	-178.1(5)	P(1)-C(51)-C(56)-C(55)	-177.9(4)
C(24)-C(29)-C(30)-C(21)	178.4(5)	C(51)-P(1)-C(61)-C(66)	-176.1(4)
C(23)-C(29)-C(30)-C(21)	0.8(6)	C(41)-P(1)-C(61)-C(66)	-64.2(4)
C(32)-O(21)-C(31)-O(22)	5.7(8)	Au(1)-P(1)-C(61)-C(66)	59.6(4)
C(32)-O(21)-C(31)-C(21)	-175.3(5)	C(51)-P(1)-C(61)-C(62)	-48.8(4)
C(30)-C(21)-C(31)-O(22)	47.7(9)	C(41)-P(1)-C(61)-C(62)	63.1(4)
C(22)-C(21)-C(31)-O(22)	-123.6(7)	Au(1)-P(1)-C(61)-C(62)	-173.1(3)
C(30)-C(21)-C(31)-O(21)	-131.2(5)	C(66)-C(61)-C(62)-C(63)	-53.5(6)
C(22)-C(21)-C(31)-O(21)	57.5(7)	P(1)-C(61)-C(62)-C(63)	178.8(4)
C(31)-O(21)-C(32)-C(33)	79.8(6)	C(61)-C(62)-C(63)-C(64)	54.4(7)
C(35)-O(23)-C(34)-O(24)	-15.5(8)	C(62)-C(63)-C(64)-C(65)	-56.2(7)
C(35)-O(23)-C(34)-C(23)	162.1(4)	C(63)-C(64)-C(65)-C(66)	56.6(7)
C(22)-C(23)-C(34)-O(24)	135.3(6)	C(62)-C(61)-C(66)-C(65)	54.7(6)
C(29)-C(23)-C(34)-O(24)	-33.8(8)	P(1)-C(61)-C(66)-C(65)	-177.3(4)
C(22)-C(23)-C(34)-O(23)	-42.2(7)	C(64)-C(65)-C(66)-C(61)	-56.3(7)
C(29)-C(23)-C(34)-O(23)	148.7(5)	C(41)-P(2)-C(71)-C(72)	63.4(4)
C(34)-O(23)-C(35)-C(36)	-170.7(5)	C(81)-P(2)-C(71)-C(72)	174.1(4)
C(71)-P(2)-C(41)-P(1)	-165.0(3)	Au(2)-P(2)-C(71)-C(72)	-59.6(4)
C(81)-P(2)-C(41)-P(1)	80.1(3)	C(41)-P(2)-C(71)-C(76)	-173.9(4)
Au(2)-P(2)-C(41)-P(1)	-39.6(3)	C(81)-P(2)-C(71)-C(76)	-63.2(4)
C(51)-P(1)-C(41)-P(2)	-132.6(3)	Au(2)-P(2)-C(71)-C(76)	63.0(4)
C(61)-P(1)-C(41)-P(2)	115.3(3)	C(76)-C(71)-C(72)-C(73)	52.3(6)
Au(1)-P(1)-C(41)-P(2)	-12.3(3)	P(2)-C(71)-C(72)-C(73)	175.0(4)
C(41)-P(1)-C(51)-C(56)	-165.7(4)	C(71)-C(72)-C(73)-C(74)	-52.6(6)
C(61)-P(1)-C(51)-C(56)	-54.1(4)	C(72)-C(73)-C(74)-C(75)	54.7(6)

C(73)-C(74)-C(75)-C(76)	-57.6(6)	Au(2)-P(2)-C(81)-C(82)	-38.1(4)
C(74)-C(75)-C(76)-C(71)	58.4(6)	C(86)-C(81)-C(82)-C(83)	-54.0(6)
C(72)-C(71)-C(76)-C(75)	-55.1(6)	P(2)-C(81)-C(82)-C(83)	176.4(4)
P(2)-C(71)-C(76)-C(75)	-177.2(4)	C(81)-C(82)-C(83)-C(84)	54.8(6)
C(71)-P(2)-C(81)-C(86)	-39.0(4)	C(82)-C(83)-C(84)-C(85)	-56.8(6)
C(41)-P(2)-C(81)-C(86)	73.3(4)	C(83)-C(84)-C(85)-C(86)	57.1(6)
Au(2)-P(2)-C(81)-C(86)	-167.2(3)	C(84)-C(85)-C(86)-C(81)	-55.1(6)
C(71)-P(2)-C(81)-C(82)	90.1(4)	C(82)-C(81)-C(86)-C(85)	54.0(6)
C(41)-P(2)-C(81)-C(82)	-157.6(4)	P(2)-C(81)-C(86)-C(85)	-177.4(4)

Appendix K. Crystallographic data for **7**.

Table K.1. Atomic coordinates (x 10^4) and equivalent isotropic displacement parameters ($Å^2$ x 10^3) for **7**. U(eq) is defined as one third of the trace of the orthogonalized U_{ij} tensor.

	x	y	z	U(eq)
Au(1)	2662(1)	5397(1)	3656(1)	29(1)
Au(2)	3196(1)	6410(1)	2589(1)	29(1)
S(1)	2946(3)	3783(4)	3416(2)	38(2)
S(2)	2822(3)	5459(4)	1779(2)	36(1)
P(1)	2469(3)	6970(4)	3997(2)	26(1)
P(2)	3675(3)	7341(4)	3342(2)	28(1)
O(1)	4346(7)	-698(10)	5815(6)	40(4)
O(2)	3411(13)	2124(17)	6993(9)	105(8)
O(3)	4097(7)	-597(10)	4850(7)	43(4)
O(4)	2911(11)	3322(16)	6477(8)	84(7)
O(21)	3620(13)	6397(17)	-1720(9)	106(9)
O(22)	4197(9)	9711(11)	-515(8)	63(5)
O(23)	3299(12)	5130(14)	-1157(8)	81(7)
O(24)	3614(10)	9767(12)	257(9)	69(6)
C(1)	3795(10)	693(14)	5465(11)	34(6)
C(2)	3681(11)	1046(15)	6012(10)	36(6)
C(3)	3382(10)	1981(17)	5999(10)	36(6)
C(4)	3017(10)	3194(16)	5173(9)	33(5)
C(5)	2950(10)	3558(15)	4614(9)	33(6)
C(6)	3123(10)	3127(15)	4090(9)	27(5)
C(7)	3386(10)	2191(15)	4029(10)	37(6)
C(8)	3571(9)	1449(14)	4463(8)	20(5)
C(9)	3580(11)	1476(18)	5112(10)	42(6)
C(10)	3302(10)	2277(15)	5387(10)	34(6)
C(11)	4081(12)	-245(16)	5333(12)	41(6)
C(12)	4688(11)	-1640(14)	5732(9)	32(5)
C(13)	4917(12)	-2027(16)	6332(10)	46(7)
C(14)	3210(12)	2570(20)	6502(10)	46(7)
C(15)	3250(20)	2670(30)	7535(15)	130(16)
C(16)	3900(20)	2900(40)	7900(20)	160(17)

C(21)	3510(10)	6756(15)	-734(9)	27(5)
C(22)	3716(11)	7749(18)	-777(12)	49(7)
C(23)	3698(13)	8220(17)	-250(11)	48(7)
C(24)	3481(11)	7665(18)	773(11)	46(7)
C(25)	3308(11)	7033(15)	1205(10)	35(6)
C(26)	3080(9)	6063(14)	1165(9)	24(5)
C(27)	3005(12)	5493(17)	649(10)	46(6)
C(28)	3133(9)	5681(15)	90(9)	26(5)
C(29)	3391(10)	6543(16)	-146(9)	32(5)
C(30)	3505(10)	7522(15)	181(12)	40(6)
C(31)	3458(15)	6020(20)	-1203(12)	71(9)
C(32)	3500(30)	5780(40)	-2260(30)	179(19)
C(33)	3840(20)	5950(40)	-2669(16)	170(20)
C(34)	3828(13)	9297(19)	-135(13)	55(7)
C(35)	4336(17)	10779(19)	-428(15)	86(11)
C(36)	4766(18)	11040(20)	-858(14)	100(12)
C(37)	3116(9)	7854(15)	3828(9)	27(5)
C(41)	2473(9)	6917(13)	4802(8)	17(4)
C(42)	2339(11)	7923(17)	5098(10)	44(7)
C(43)	2296(11)	7801(16)	5744(9)	40(6)
C(44)	2944(12)	7380(20)	6037(9)	50(7)
C(45)	3117(10)	6440(16)	5768(9)	32(5)
C(46)	3148(9)	6512(15)	5084(8)	25(5)
C(51)	1698(8)	7557(14)	3707(8)	17(4)
C(52)	1633(10)	7707(16)	3026(10)	38(6)
C(53)	990(10)	8189(17)	2817(10)	40(6)
C(54)	422(12)	7592(18)	3008(12)	56(8)
C(55)	450(13)	7411(19)	3651(12)	60(8)
C(56)	1118(9)	6946(15)	3888(9)	28(5)
C(61)	4265(10)	6558(15)	3832(9)	33(5)
C(62)	4598(11)	5756(14)	3502(9)	29(5)
C(63)	4993(10)	5091(15)	3944(9)	30(5)
C(64)	5477(10)	5682(14)	4349(9)	32(5)
C(65)	5143(12)	6491(17)	4686(10)	45(6)
C(66)	4770(10)	7188(14)	4240(9)	30(5)
C(71)	4099(10)	8450(15)	3102(10)	37(6)

C(72)	3587(11)	9073(17)	2708(11)	47(7)
C(73)	3892(12)	9953(16)	2444(10)	40(6)
C(74)	4467(12)	9663(17)	2111(10)	43(6)
C(75)	4987(11)	9110(17)	2529(10)	43(6)
C(76)	4689(10)	8093(16)	2766(9)	34(5)
Cl(1S)	6872(6)	9772(9)	1724(5)	123(4)
Cl(2S)	5978(6)	11101(8)	2219(5)	123(4)
Cl(3S)	7144(6)	10494(9)	2907(5)	131(4)
C(1S)	6786(18)	10770(40)	2186(17)	140(20)
N(1S)	5141(17)	4500(30)	-1057(16)	133(12)
C(2S)	4730(40)	3620(60)	-220(30)	250(30)
C(3S)	5010(30)	4950(50)	-320(20)	190(20)

Table K.2. Bond lengths [Å] for **7**.

Au(1)-P(1)	2.286(5)	O(21)-C(32)	1.48(6)
Au(1)-S(1)	2.310(5)	O(22)-C(34)	1.33(3)
Au(1)-Au(2)	3.084(1)	O(22)-C(35)	1.46(3)
Au(2)-P(2)	2.263(5)	O(23)-C(31)	1.23(3)
Au(2)-S(2)	2.306(5)	O(24)-C(34)	1.21(3)
S(1)-C(6)	1.77(2)	C(1)-C(9)	1.36(3)
S(2)-C(26)	1.74(2)	C(1)-C(2)	1.38(3)
P(1)-C(51)	1.82(2)	C(1)-C(11)	1.43(3)
P(1)-C(41)	1.84(2)	C(2)-C(3)	1.39(3)
P(1)-C(37)	1.84(2)	C(3)-C(10)	1.45(3)
P(2)-C(37)	1.81(2)	C(3)-C(14)	1.46(3)
P(2)-C(71)	1.83(2)	C(4)-C(5)	1.36(3)
P(2)-C(61)	1.87(2)	C(4)-C(10)	1.42(3)
O(1)-C(11)	1.32(3)	C(5)-C(6)	1.40(3)
O(1)-C(12)	1.46(2)	C(6)-C(7)	1.37(3)
O(2)-C(14)	1.29(3)	C(7)-C(8)	1.42(3)
O(2)-C(15)	1.50(4)	C(8)-C(9)	1.48(3)
O(3)-C(11)	1.20(3)	C(9)-C(10)	1.39(3)
O(4)-C(14)	1.18(3)	C(12)-C(13)	1.49(3)
O(21)-C(31)	1.36(3)	C(15)-C(16)	1.52(5)

C(21)-C(22)	1.40(3)	C(52)-C(53)	1.50(3)
C(21)-C(29)	1.42(3)	C(53)-C(54)	1.51(3)
C(21)-C(31)	1.45(4)	C(54)-C(55)	1.48(4)
C(22)-C(23)	1.36(3)	C(55)-C(56)	1.55(3)
C(23)-C(30)	1.44(3)	C(61)-C(62)	1.51(3)
C(23)-C(34)	1.48(3)	C(61)-C(66)	1.56(3)
C(24)-C(25)	1.37(3)	C(62)-C(63)	1.51(3)
C(24)-C(30)	1.37(3)	C(63)-C(64)	1.51(3)
C(25)-C(26)	1.38(3)	C(64)-C(65)	1.53(3)
C(26)-C(27)	1.40(3)	C(65)-C(66)	1.52(3)
C(27)-C(28)	1.35(3)	C(71)-C(72)	1.55(3)
C(28)-C(29)	1.40(3)	C(71)-C(76)	1.57(3)
C(29)-C(30)	1.51(3)	C(72)-C(73)	1.49(3)
C(32)-C(33)	1.25(6)	C(73)-C(74)	1.52(3)
C(35)-C(36)	1.43(4)	C(74)-C(75)	1.54(3)
C(41)-C(42)	1.54(3)	C(75)-C(76)	1.60(3)
C(41)-C(46)	1.56(3)	Cl(1S)-C(1S)	1.72(4)
C(42)-C(43)	1.49(3)	Cl(2S)-C(1S)	1.72(4)
C(43)-C(44)	1.53(3)	Cl(3S)-C(1S)	1.77(4)
C(44)-C(45)	1.46(3)	N(1S)-C(3S)	1.84(6)
C(45)-C(46)	1.57(3)	C(2S)-C(3S)	1.89(9)
C(51)-C(56)	1.53(3)	C(3S)-C(3S)#1	1.45(10)
C(51)-C(52)	1.56(3)		

Symmetry transformations used to generate equivalent atoms: #1: -x+1, -y+1, -z.

Table K.3. Bond angles [°] for **7**.

P(1)-Au(1)-S(1)	172.9(2)	C(51)-P(1)-C(41)	107.1(8)
P(1)-Au(1)-Au(2)	87.4(2)	C(51)-P(1)-C(37)	105.2(9)
S(1)-Au(1)-Au(2)	95.9(2)	C(41)-P(1)-C(37)	107.7(9)
P(2)-Au(2)-S(2)	173.5(2)	C(51)-P(1)-Au(1)	116.4(6)
P(2)-Au(2)-Au(1)	78.5(2)	C(41)-P(1)-Au(1)	108.8(6)
S(2)-Au(2)-Au(1)	106.1(2	C(37)-P(1)-Au(1)	111.3(7)
C(6)-S(1)-Au(1)	106.7(7)	C(37)-P(2)-C(71)	103(1)
C(26)-S(2)-Au(2)	106.7(7)	C(37)-P(2)-C(61)	105(1)

C(71)-P(2)-C(61)	110(1)	C(22)-C(21)-C(29)	110(2)
C(37)-P(2)-Au(2)	115(1)	C(22)-C(21)-C(31)	126(2)
C(71)-P(2)-Au(2)	113(1)	C(29)-C(21)-C(31)	124(2)
C(61)-P(2)-Au(2)	111(1)	C(23)-C(22)-C(21)	110(2)
C(11)-O(1)-C(12)	117(2)	C(22)-C(23)-C(30)	110(2)
C(14)-O(2)-C(15)	115(2)	C(22)-C(23)-C(34)	126(2)
C(31)-O(21)-C(32)	119(3)	C(30)-C(23)-C(34)	124(2)
C(34)-O(22)-C(35)	116(2)	C(25)-C(24)-C(30)	131(2)
C(9)-C(1)-C(2)	102(2)	C(24)-C(25)-C(26)	130(2)
C(9)-C(1)-C(11)	131(2)	C(25)-C(26)-C(27)	125(2)
C(2)-C(1)-C(11)	127(2)	C(25)-C(26)-S(2)	121(2)
C(1)-C(2)-C(3)	114(2)	C(27)-C(26)-S(2)	114(2)
C(2)-C(3)-C(10)	106(2)	C(28)-C(27)-C(26)	133(2)
C(2)-C(3)-C(14)	127(2)	C(27)-C(28)-C(29)	129(2)
C(10)-C(3)-C(14)	127(2)	C(28)-C(29)-C(21)	130(2)
C(5)-C(4)-C(10)	129(2)	C(28)-C(29)-C(30)	125(2)
C(4)-C(5)-C(6)	130(2)	C(21)-C(29)-C(30)	105(2)
C(7)-C(6)-C(5)	127(2)	C(24)-C(30)-C(23)	129(2)
C(7)-C(6)-S(1)	114(2)	C(24)-C(30)-C(29)	126(2)
C(5)-C(6)-S(1)	119(2)	C(23)-C(30)-C(29)	105(2)
C(6)-C(7)-C(8)	130(2)	O(23)-C(31)-O(21)	122(3)
C(7)-C(8)-C(9)	131(2)	O(23)-C(31)-C(21)	126(3)
C(1)-C(9)-C(10)	116(2)	O(21)-C(31)-C(21)	113(3)
C(1)-C(9)-C(8)	123(2)	C(33)-C(32)-O(21)	118(5)
C(10)-C(9)-C(8)	120(2)	O(24)-C(34)-O(22)	123(2)
C(9)-C(10)-C(4)	133(2)	O(24)-C(34)-C(23)	124(2)
C(9)-C(10)-C(3)	102(2)	O(22)-C(34)-C(23)	113(2)
C(4)-C(10)-C(3)	125(2)	C(36)-C(35)-O(22)	106(2)
O(3)-C(11)-O(1)	123(2)	P(2)-C(37)-P(1)	114(1)
O(3)-C(11)-C(1)	126(2)	C(42)-C(41)-C(46)	108(2)
O(1)-C(11)-C(1)	111(2)	C(42)-C(41)-P(1)	115(1)
O(1)-C(12)-C(13)	107(2)	C(46)-C(41)-P(1)	110(1)
O(4)-C(14)-O(2)	123(3)	C(43)-C(42)-C(41)	112(2)
O(4)-C(14)-C(3)	126(2)	C(42)-C(43)-C(44)	110(2)
O(2)-C(14)-C(3)	111(2)	C(45)-C(44)-C(43)	112(2)
O(2)-C(15)-C(16)	108(3)	C(44)-C(45)-C(46)	114(2)

C(41)-C(46)-C(45)	108(2)	C(65)-C(66)-C(61)	109(2)
C(56)-C(51)-C(52)	110(2)	C(72)-C(71)-C(76)	113(2)
C(56)-C(51)-P(1)	110(1)	C(72)-C(71)-P(2)	107(2)
C(52)-C(51)-P(1)	114(1)	C(76)-C(71)-P(2)	108(1)
C(53)-C(52)-C(51)	111(2)	C(73)-C(72)-C(71)	112(2)
C(52)-C(53)-C(54)	111(2)	C(72)-C(73)-C(74)	113(2)
C(55)-C(54)-C(53)	115(2)	C(73)-C(74)-C(75)	110(2)
C(54)-C(55)-C(56)	111(2)	C(74)-C(75)-C(76)	111(2)
C(51)-C(56)-C(55)	112(2)	C(71)-C(76)-C(75)	104(2)
C(62)-C(61)-C(66)	112(2)	Cl(1S)-C(1S)-Cl(2S)	113(2)
C(62)-C(61)-P(2)	113(1)	Cl(1S)-C(1S)-Cl(3S)	111(2)
C(66)-C(61)-P(2)	114(1)	Cl(2S)-C(1S)-Cl(3S)	109(2)
C(61)-C(62)-C(63)	109(2)	C(3S)#1-C(3S)-N(1S)	164(7)
C(64)-C(63)-C(62)	112(2)	C(3S)#1-C(3S)-C(2S)	85(6)
C(63)-C(64)-C(65)	112(2)	N(1S)-C(3S)-C(2S)	83(4)
C(66)-C(65)-C(64)	108(2)		

Symmetry transformations used to generate equivalent atoms: #1: -x+1, -y+1, -z.

Table K.4. Anisotropic displacement parameters ($Å^2 x\ 10^3$) for **7**. The anisotropic displacement factor exponent takes the form: $-2\pi^2[\ h^2\ a^{*2}U_{11} + ... + 2\ h\ k\ a^*\ b^*\ U_{12}\ ]$.

	U_{11}	U_{22}	U_{33}	U_{23}	U_{13}	U_{12}
Au(1)	38(1)	14(1)	30(1)	-3(1)	-10(1)	4(1)
Au(2)	39(1)	19(1)	25(1)	-1(1)	-13(1)	5(1)
S(1)	55(4)	23(3)	33(3)	-5(2)	-5(3)	14(3)
S(2)	53(4)	21(3)	30(3)	-2(2)	-11(3)	-1(3)
P(1)	36(3)	16(3)	21(3)	0(2)	-16(3)	6(3)
P(2)	37(3)	19(3)	25(3)	6(2)	-12(3)	4(3)
O(1)	52(10)	28(9)	35(9)	8(7)	-18(8)	10(8)
O(2)	170(20)	101(18)	47(14)	-3(12)	20(14)	61(17)
O(3)	48(10)	24(9)	52(11)	-6(8)	-21(9)	17(7)
O(4)	117(18)	91(16)	41(12)	-24(11)	0(11)	63(15)
O(21)	190(30)	85(16)	47(13)	-12(12)	42(15)	-49(17)
O(22)	78(13)	27(10)	91(14)	18(9)	47(12)	-1(9)

O(23)	140(20)	47(12)	55(13)	-6(10)	28(13)	-19(13)
O(24)	112(17)	25(10)	77(14)	8(9)	47(13)	14(10)
C(1)	23(13)	14(12)	64(17)	-9(11)	4(12)	-3(10)
C(2)	47(15)	25(13)	35(15)	-2(11)	8(12)	14(11)
C(3)	32(14)	46(15)	32(15)	-4(12)	6(11)	-15(12)
C(4)	33(5)	33(5)	33(5)	0(1)	3(1)	0(1)
C(5)	35(13)	17(11)	43(14)	12(10)	-14(11)	5(10)
C(6)	27(5)	26(5)	27(5)	0(1)	3(1)	0(1)
C(7)	38(14)	25(12)	42(14)	-15(10)	-23(11)	-1(11)
C(8)	20(5)	20(5)	20(5)	0(1)	2(1)	0(1)
C(9)	42(6)	43(6)	42(6)	0(1)	4(1)	0(1)
C(10)	17(12)	28(13)	58(17)	3(11)	2(11)	2(10)
C(11)	50(16)	20(14)	53(18)	-5(13)	8(14)	-13(12)
C(12)	39(14)	18(12)	37(14)	0(10)	-4(11)	4(10)
C(13)	73(18)	24(13)	41(15)	25(11)	1(13)	0(12)
C(14)	43(16)	59(18)	29(15)	10(14)	-23(12)	10(14)
C(15)	190(50)	150(40)	60(20)	0(20)	40(30)	60(30)
C(16)	160(17)	160(17)	160(17)	0(1)	17(2)	0(1)
C(22)	47(16)	47(16)	53(18)	10(14)	13(13)	8(13)
C(23)	70(19)	23(14)	54(18)	10(13)	13(14)	11(12)
C(24)	47(16)	41(15)	49(18)	-16(13)	0(13)	-2(12)
C(25)	53(16)	15(12)	35(14)	-4(10)	-5(12)	-8(11)
C(27)	56(17)	25(13)	54(17)	-2(12)	-3(13)	20(12)
C(28)	26(5)	26(5)	26(5)	0(1)	2(1)	0(1)
C(29)	23(12)	42(14)	30(13)	2(11)	0(10)	3(11)
C(30)	30(14)	19(13)	71(19)	2(12)	7(13)	14(10)
C(31)	90(20)	80(20)	44(19)	12(16)	12(16)	-26(19)
C(32)	179(19)	179(19)	179(19)	0(1)	19(2)	0(1)
C(33)	140(40)	300(70)	60(30)	-80(30)	10(30)	-80(40)
C(34)	61(18)	39(17)	70(20)	7(15)	36(16)	6(14)
C(35)	130(30)	36(17)	100(30)	18(16)	60(20)	-4(18)
C(36)	150(30)	70(20)	80(20)	43(19)	40(20)	-20(20)
C(37)	27(5)	27(5)	27(5)	0(1)	2(1)	0(1)
C(42)	37(14)	42(15)	47(16)	-5(12)	-25(12)	14(12)
C(43)	56(16)	30(13)	31(14)	2(10)	-13(12)	8(12)
C(44)	51(16)	90(20)	12(12)	12(12)	-4(11)	16(15)

C(45)	32(5)	32(5)	32(5)	0(1)	3(1)	0(1)
C(46)	25(5)	25(5)	25(5)	0(1)	3(1)	0(1)
C(52)	31(13)	28(13)	51(15)	10(11)	-11(12)	-2(11)
C(53)	32(14)	35(14)	49(16)	-8(11)	-18(12)	4(12)
C(54)	44(16)	33(15)	80(20)	-6(14)	-38(15)	11(13)
C(55)	55(18)	41(16)	80(20)	-17(14)	-23(16)	12(13)
C(56)	28(5)	28(5)	28(5)	0(1)	3(1)	0(1)
C(61)	33(5)	33(5)	33(5)	0(1)	3(1)	0(1)
C(62)	51(15)	11(11)	24(12)	10(9)	3(11)	3(10)
C(63)	30(5)	30(5)	30(5)	0(1)	3(1)	0(1)
C(64)	40(14)	23(12)	30(13)	4(10)	-7(11)	3(10)
C(65)	45(6)	45(6)	45(6)	0(1)	4(1)	0(1)
C(66)	27(12)	16(11)	41(14)	4(10)	-18(11)	4(10)
C(71)	41(14)	24(12)	44(14)	10(11)	-11(11)	8(11)
C(72)	33(14)	37(14)	65(18)	22(13)	-20(13)	5(12)
C(73)	62(17)	25(13)	29(14)	5(10)	-21(13)	-7(12)
C(74)	58(17)	32(14)	35(14)	13(11)	-10(13)	-26(13)
C(75)	43(6)	43(6)	43(6)	0(1)	4(1)	0(1)
C(76)	34(5)	34(5)	34(5)	0(1)	3(1)	0(1)
Cl(1S)	131(9)	145(10)	92(7)	-3(7)	11(6)	39(8)
Cl(2S)	130(9)	101(8)	146(10)	28(7)	51(8)	20(7)
Cl(3S)	164(11)	133(9)	93(7)	-6(7)	-1(7)	-51(8)
C(1S)	80(30)	210(50)	120(30)	-90(30)	-60(20)	60(30)

Table K.5. Hydrogen coordinates (x 10^4) and isotropic displacement parameters ($Å^2$ x 10^3) for **7**.

	x	y	z	U(eq)
H(2)	3797	683	6366	43
H(4)	2851	3612	5461	39
H(5)	2755	4204	4570	40
H(7)	3456	2010	3637	44
H(8)	3712	832	4311	24

H(12A)	5067	-1527	5504	38
H(12B)	4388	-2128	5517	38
H(13A)	5150	-2662	6298	69
H(13B)	4537	-2134	6553	69
H(13C)	5213	-1537	6540	69
H(15A)	2969	2250	7762	156
H(15B)	3014	3301	7424	156
H(16A)	3808	3269	8259	239
H(16B)	4175	3309	7673	239
H(16C)	4123	2272	8018	239
H(22)	3850	8051	-1122	58
H(24)	3607	8318	909	55
H(25)	3353	7307	1591	42
H(27)	2830	4843	701	55
H(28)	3033	5150	-182	31
H(32A)	3558	5069	-2144	215
H(32B)	3030	5867	-2413	215
H(33A)	3722	5475	-2991	249
H(33B)	4305	5871	-2527	249
H(33C)	3760	6636	-2813	249
H(35A)	3926	11176	-486	103
H(35B)	4550	10904	-25	103
H(36A)	4870	11759	-826	150
H(36B)	4551	10898	-1253	150
H(36C)	5172	10651	-790	150
H(37A)	2907	8462	3644	32
H(37B)	3371	8060	4201	32
H(41)	2126	6431	4895	21
H(42A)	2695	8401	5036	53
H(42B)	1921	8207	4912	53
H(43A)	1932	7338	5810	49
H(43B)	2205	8457	5921	49
H(44A)	3298	7877	6004	61
H(44B)	2905	7269	6461	61
H(45A)	2791	5924	5848	38
H(45B)	3551	6218	5956	38

H(46A)	3505	6971	4997	30
H(46B)	3235	5843	4922	30
H(51)	1680	8234	3892	21
H(52A)	1998	8134	2918	45
H(52B)	1665	7049	2830	45
H(53A)	947	8239	2382	48
H(53B)	979	8877	2979	48
H(54A)	9	7950	2879	68
H(54B)	407	6936	2804	68
H(55A)	91	6951	3733	72
H(55B)	388	8052	3857	72
H(56A)	1147	6910	4323	34
H(56B)	1145	6254	3735	34
H(61)	3992	6193	4102	40
H(62A)	4891	6068	3235	34
H(62B)	4264	5352	3262	34
H(63A)	4691	4728	4181	36
H(63B)	5234	4587	3731	36
H(64A)	5802	6001	4115	38
H(64B)	5718	5219	4634	38
H(65A)	4836	6180	4940	54
H(65B)	5477	6876	4939	54
H(66A)	5081	7526	4000	36
H(66B)	4537	7708	4447	36
H(71)	4269	8856	3454	45
H(72A)	3379	8640	2389	56
H(72B)	3240	9306	2947	56
H(73A)	4045	10431	2761	49
H(73B)	3557	10297	2172	49
H(74A)	4663	10272	1953	51
H(74B)	4313	9223	1776	51
H(75A)	5135	9549	2867	52
H(75B)	5373	8951	2318	52
H(76A)	4534	7644	2435	41
H(76B)	5020	7734	3035	41

H(1S)	7022	11356	2036	171

Table K.6. Torsion angles [°] for **7**.

P(1)-Au(1)-Au(2)-P(2)	44.8(2)	C(6)-C(7)-C(8)-C(9)	-5(4)
S(1)-Au(1)-Au(2)-P(2)	-128.9(2)	C(2)-C(1)-C(9)-C(10)	-4(3)
P(1)-Au(1)-Au(2)-S(2)	-140.0(2)	C(11)-C(1)-C(9)-C(10)	178(2)
S(1)-Au(1)-Au(2)-S(2)	46.3(2)	C(2)-C(1)-C(9)-C(8)	-177(2)
P(1)-Au(1)-S(1)-C(6)	32(2)	C(11)-C(1)-C(9)-C(8)	4(4)
Au(2)-Au(1)-S(1)-C(6)	149(1)	C(7)-C(8)-C(9)-C(1)	-178(2)
P(2)-Au(2)-S(2)-C(26)	-49(2)	C(7)-C(8)-C(9)-C(10)	9(3)
Au(1)-Au(2)-S(2)-C(26)	177(1)	C(1)-C(9)-C(10)-C(4)	-179(2)
S(1)-Au(1)-P(1)-C(51)	-158(2)	C(8)-C(9)-C(10)-C(4)	-5(4)
Au(2)-Au(1)-P(1)-C(51)	84(1)	C(1)-C(9)-C(10)-C(3)	3(3)
S(1)-Au(1)-P(1)-C(41)	-37(2)	C(8)-C(9)-C(10)-C(3)	177(2)
Au(2)-Au(1)-P(1)-C(41)	-155(1)	C(5)-C(4)-C(10)-C(9)	-1(4)
S(1)-Au(1)-P(1)-C(37)	81(2)	C(5)-C(4)-C(10)-C(3)	177(2)
Au(2)-Au(1)-P(1)-C(37)	-36(1)	C(2)-C(3)-C(10)-C(9)	-1(2)
S(2)-Au(2)-P(2)-C(37)	172(2)	C(14)-C(3)-C(10)-C(9)	176(2)
Au(1)-Au(2)-P(2)-C(37)	-53(1)	C(2)-C(3)-C(10)-C(4)	-180(2)
S(2)-Au(2)-P(2)-C(71)	53(2)	C(14)-C(3)-C(10)-C(4)	-2(3)
Au(1)-Au(2)-P(2)-C(71)	-172(1)	C(12)-O(1)-C(11)-O(3)	2(3)
S(2)-Au(2)-P(2)-C(61)	-70(2)	C(12)-O(1)-C(11)-C(1)	-177(2)
Au(1)-Au(2)-P(2)-C(61)	65(1)	C(9)-C(1)-C(11)-O(3)	-12(4)
C(9)-C(1)-C(2)-C(3)	3(3)	C(2)-C(1)-C(11)-O(3)	169(2)
C(11)-C(1)-C(2)-C(3)	-179(2)	C(9)-C(1)-C(11)-O(1)	167(2)
C(1)-C(2)-C(3)-C(10)	-1(3)	C(2)-C(1)-C(11)-O(1)	-12(3)
C(1)-C(2)-C(3)-C(14)	-179(2)	C(11)-O(1)-C(12)-C(13)	-178(2)
C(10)-C(4)-C(5)-C(6)	2(4)	C(15)-O(2)-C(14)-O(4)	-2(5)
C(4)-C(5)-C(6)-C(7)	3(4)	C(15)-O(2)-C(14)-C(3)	-180(3)
C(4)-C(5)-C(6)-S(1)	178(2)	C(2)-C(3)-C(14)-O(4)	-174(3)
Au(1)-S(1)-C(6)-C(7)	-172(1)	C(10)-C(3)-C(14)-O(4)	9(4)
Au(1)-S(1)-C(6)-C(5)	12(2)	C(2)-C(3)-C(14)-O(2)	4(4)
C(5)-C(6)-C(7)-C(8)	-3(4)	C(10)-C(3)-C(14)-O(2)	-173(2)
S(1)-C(6)-C(7)-C(8)	-178(2)	C(14)-O(2)-C(15)-C(16)	-121(4)

C(29)-C(21)-C(22)-C(23)	-4(3)	C(35)-O(22)-C(34)-C(23)	179(2)
C(31)-C(21)-C(22)-C(23)	180(2)	C(22)-C(23)-C(34)-O(24)	155(3)
C(21)-C(22)-C(23)-C(30)	3(3)	C(30)-C(23)-C(34)-O(24)	-22(4)
C(21)-C(22)-C(23)-C(34)	-175(2)	C(22)-C(23)-C(34)-O(22)	-24(4)
C(30)-C(24)-C(25)-C(26)	-3(4)	C(30)-C(23)-C(34)-O(22)	159(2)
C(24)-C(25)-C(26)-C(27)	3(4)	C(34)-O(22)-C(35)-C(36)	177(3)
C(24)-C(25)-C(26)-S(2)	-174(2)	C(71)-P(2)-C(37)-P(1)	165(1)
Au(2)-S(2)-C(26)-C(25)	-14(2)	C(61)-P(2)-C(37)-P(1)	-80(1)
Au(2)-S(2)-C(26)-C(27)	168(1)	Au(2)-P(2)-C(37)-P(1)	41(1)
C(25)-C(26)-C(27)-C(28)	2(4)	C(51)-P(1)-C(37)-P(2)	-118(1)
S(2)-C(26)-C(27)-C(28)	179(2)	C(41)-P(1)-C(37)-P(2)	128(1)
C(26)-C(27)-C(28)-C(29)	0(4)	Au(1)-P(1)-C(37)-P(2)	9(1)
C(27)-C(28)-C(29)-C(21)	-178(2)	C(51)-P(1)-C(41)-C(42)	-53(2)
C(27)-C(28)-C(29)-C(30)	-8(3)	C(37)-P(1)-C(41)-C(42)	60(2)
C(22)-C(21)-C(29)-C(28)	175(2)	Au(1)-P(1)-C(41)-C(42)	-179(1)
C(31)-C(21)-C(29)-C(28)	-9(4)	C(51)-P(1)-C(41)-C(46)	-175(1)
C(22)-C(21)-C(29)-C(30)	3(2)	C(37)-P(1)-C(41)-C(46)	-62(2)
C(31)-C(21)-C(29)-C(30)	180(2)	Au(1)-P(1)-C(41)-C(46)	59(1)
C(25)-C(24)-C(30)-C(23)	-179(2)	C(46)-C(41)-C(42)-C(43)	-62(2)
C(25)-C(24)-C(30)-C(29)	-6(4)	P(1)-C(41)-C(42)-C(43)	175(2)
C(22)-C(23)-C(30)-C(24)	174(2)	C(41)-C(42)-C(43)-C(44)	60(3)
C(34)-C(23)-C(30)-C(24)	-8(4)	C(42)-C(43)-C(44)-C(45)	-56(3)
C(22)-C(23)-C(30)-C(29)	-1(3)	C(43)-C(44)-C(45)-C(46)	55(3)
C(34)-C(23)-C(30)-C(29)	177(2)	C(42)-C(41)-C(46)-C(45)	56(2)
C(28)-C(29)-C(30)-C(24)	12(3)	P(1)-C(41)-C(46)-C(45)	-178(1)
C(21)-C(29)-C(30)-C(24)	-176(2)	C(44)-C(45)-C(46)-C(41)	-56(2)
C(28)-C(29)-C(30)-C(23)	-173(2)	C(41)-P(1)-C(51)-C(56)	-59(2)
C(21)-C(29)-C(30)-C(23)	-1(2)	C(37)-P(1)-C(51)-C(56)	-173(1)
C(32)-O(21)-C(31)-O(23)	10(5)	Au(1)-P(1)-C(51)-C(56)	63(1)
C(32)-O(21)-C(31)-C(21)	-171(3)	C(41)-P(1)-C(51)-C(52)	177(1)
C(22)-C(21)-C(31)-O(23)	177(3)	C(37)-P(1)-C(51)-C(52)	63(2)
C(29)-C(21)-C(31)-O(23)	1(5)	Au(1)-P(1)-C(51)-C(52)	-61(2)
C(22)-C(21)-C(31)-O(21)	-2(4)	C(56)-C(51)-C(52)-C(53)	56(2)
C(29)-C(21)-C(31)-O(21)	-178(2)	P(1)-C(51)-C(52)-C(53)	180(1)
C(31)-O(21)-C(32)-C(33)	-155(5)	C(51)-C(52)-C(53)-C(54)	-56(2)
C(35)-O(22)-C(34)-O(24)	1(4)	C(52)-C(53)-C(54)-C(55)	56(3)

C(53)-C(54)-C(55)-C(56)	-53(3)	C(62)-C(61)-C(66)-C(65)	-60(2)
C(52)-C(51)-C(56)-C(55)	-54(2)	P(2)-C(61)-C(66)-C(65)	171(2)
P(1)-C(51)-C(56)-C(55)	-180(2)	C(37)-P(2)-C(71)-C(72)	-68(2)
C(54)-C(55)-C(56)-C(51)	52(3)	C(61)-P(2)-C(71)-C(72)	-179(2)
C(37)-P(2)-C(61)-C(62)	157(2)	Au(2)-P(2)-C(71)-C(72)	57(2)
C(71)-P(2)-C(61)-C(62)	-93(2)	C(37)-P(2)-C(71)-C(76)	170(1)
Au(2)-P(2)-C(61)-C(62)	33(2)	C(61)-P(2)-C(71)-C(76)	59(2)
C(37)-P(2)-C(61)-C(66)	-74(2)	Au(2)-P(2)-C(71)-C(76)	-65(2)
C(71)-P(2)-C(61)-C(66)	36(2)	C(76)-C(71)-C(72)-C(73)	-56(3)
Au(2)-P(2)-C(61)-C(66)	162(1)	P(2)-C(71)-C(72)-C(73)	-175(2)
C(66)-C(61)-C(62)-C(63)	57(2)	C(71)-C(72)-C(73)-C(74)	54(3)
P(2)-C(61)-C(62)-C(63)	-173(1)	C(72)-C(73)-C(74)-C(75)	-58(2)
C(61)-C(62)-C(63)-C(64)	-56(2)	C(73)-C(74)-C(75)-C(76)	62(2)
C(62)-C(63)-C(64)-C(65)	58(2)	C(72)-C(71)-C(76)-C(75)	57(2)
C(63)-C(64)-C(65)-C(66)	-58(2)	P(2)-C(71)-C(76)-C(75)	175(1)
C(64)-C(65)-C(66)-C(61)	58(2)	C(74)-C(75)-C(76)-C(71)	-61(2)